ANALYSIS OF SIDE-SCAN SONAR, BATHYMETRIC, SUBBOTTOM, AND SEDIMENT DATA FROM THE UPPER HUDSON RIVER BETWEEN BAKERS FALLS AND LOCK 5

SEPTEMBER, 1993

Hudson River PCB Reassessment RI/FS
EPA Work Assignment 013-2N84
EPA Contract No. 68-S9-2001

for

TAMS Consultants, Inc.
TAMS Subcontract No. 5213-01

by

Roger D. Flood

Associate Professor
Marine Sciences Research Center
State University of New York
Stony Brook, New York 11794-5000

ANALYSIS OF SIDE-SCAN SONAR, BATHYMETRIC, SUBBOTTOM, AND SEDIMENT DATA FROM THE UPPER HUDSON RIVER BETWEEN BAKERS FALLS AND LOCK 5

Roger D. Flood, Associate Professor
Marine Sciences Research Center
State University of New York
Stony Brook, New York 11794-5000

Abstract

Geophysical investigations utilizing dual-frequency side-scan sonar, subbottom profiling and river bathymetry have been undertaken in the Upper Hudson River to characterize river bed morphology and sediment distribution patterns. Such information is needed to better understand the distribution of PCBs in these sediments and to characterize the potential for resuspension. Our studies have resulted in a series of 38 side-scan sonar mosaics at a scale of 1 inch = 200 feet using the 500 kHz sonar data. These and other images, including 100 kHz sonar mosaics, are also provided in digital form. Sediment samples were collected at a number of locations within the sonar survey. The combined analysis of sonar data and sediment data suggests that the value of the 500 kHz digital image is related to the mean sediment size with coarser sediments being more reflective than finer sediments. This relationship, sediment samples, sonar images, and subbottom profile data were used to determine sediment distribution patterns within the section of the river studied. Some of the river bed is underlain by silts and clays of glacial age. These sediments appear to be susceptible to erosion where exposed, and, in some areas, to deformation. Other portions of the river are characterized by outcropping rocky units that have been partially removed to form the Champlain Canal. Analysis of the sonar images suggests that several irregularly lineated areas of the river bed outside of the dredged channel may have undergone erosion. Some of these eroded areas may be glacial silts and clays while other areas are more recently deposited sediment. Fine-grained sediments appear to have accumulated in portions of the river where average velocities drop because of larger cross-section. Rock outcrops also help to localize finer sediment deposition. The combined analysis of river flow patterns and sonar reflectivity may help to identify areas of the river where high PCB levels exist and where these deposits may be susceptible to erosion.

List of Figures

List of Tables

Introduction

A detailed knowledge of the nature of the bed of the Hudson River is essential to our understanding of the distribution of sediment in the river and the processes that have been important in the erosion, transportation and deposition of those sediments. Such an understanding of river bed morphology is particularly important in the portion of the Hudson River downstream from Bakers Falls and Fort Edward, sites where PCBs are known to have entered into the river through discharges from capacitor manufacturing facilities operated by General Electric, Inc. (TAMS, 1991).

NYS DEC, based on sediment samples collected in 1977 and 1978, defined 40 areas (termed "hot spots") with elevated PCB levels (Figure 1). Twenty of these hot spots lie within the portion of the Hudson River from Fort Edward to the Thompson Island Dam (the Thompson Island Pool), seven are in the portion of the Hudson River between the Thompson Island Dam and the dam at Fort Miller, eight are between the dam at Fort Miller and Champlain Canal Lock 5, with the remaining five hot spots farther down-river in the general vicinity of Champlain Canal Locks 2 through 4.

More recent sediment and contaminant sampling was done in 1984 in the Thompson Island Pool where Brown et al. (1988) also identified regions where sediment PCB levels are elevated. However, the boundaries of these areas do not precisely correspond to the hot spots identified by NYS DEC. These and earlier sediment samples demonstrated that the sedimentation and contaminant distribution patterns can be quite complex often varying on a scale of less than 125 ft (TAMS, 1991). High-flow events also continue to occur (including possible sediment-transporting events in 1979 and 1983), and thus the location and concept of "hot spots" as defined by NYS DEC appears to be an oversimplification of the PCB distribution patterns (TAMS, 1991).

Studies to date have demonstrated the complexity of sediment and contaminant distribution patterns in this portion of the Hudson River. An understanding of sedimentation patterns here is made somewhat more difficult because of the rivers recent history. The Hudson River between Fort Edward and Schylerville (except for the region between the dams at Thompson Island and Fort Miller where the river is bypassed by a land cut) is part of the Champlain Canal that links the tidal Hudson River and the Erie Canal with Lake Champlain. This canal was dredged prior to about 1917 to provide a channel with a width of 200 feet and a depth of 12 feet. Dredging has continued in portions of the river to counteract sedimentation, including that associated with river floods in 1974 and 1976 (Sanders, 1989).

The effect of high river flows in 1974 and 1976 on sedimentation and contaminant distribution in the Hudson River was enhanced due to the removal of a high dam at Fort Edward in 1973. This dam was removed because of the danger of collapse due to its age and condition. While the dam was in existence, sediment and wood debris (wood chips and sawn lumber from upriver sawmill operations) accumulated behind it. The GE capacitor plants at Fort Edward and Bakers Falls were also upstream of the dam, and some portion of the PCBs that came from those plants was trapped associated with the sediments and wood debris that settled behind the dam. Following dam removal in 1973, sediment trapped behind the dam and their associated PCBs

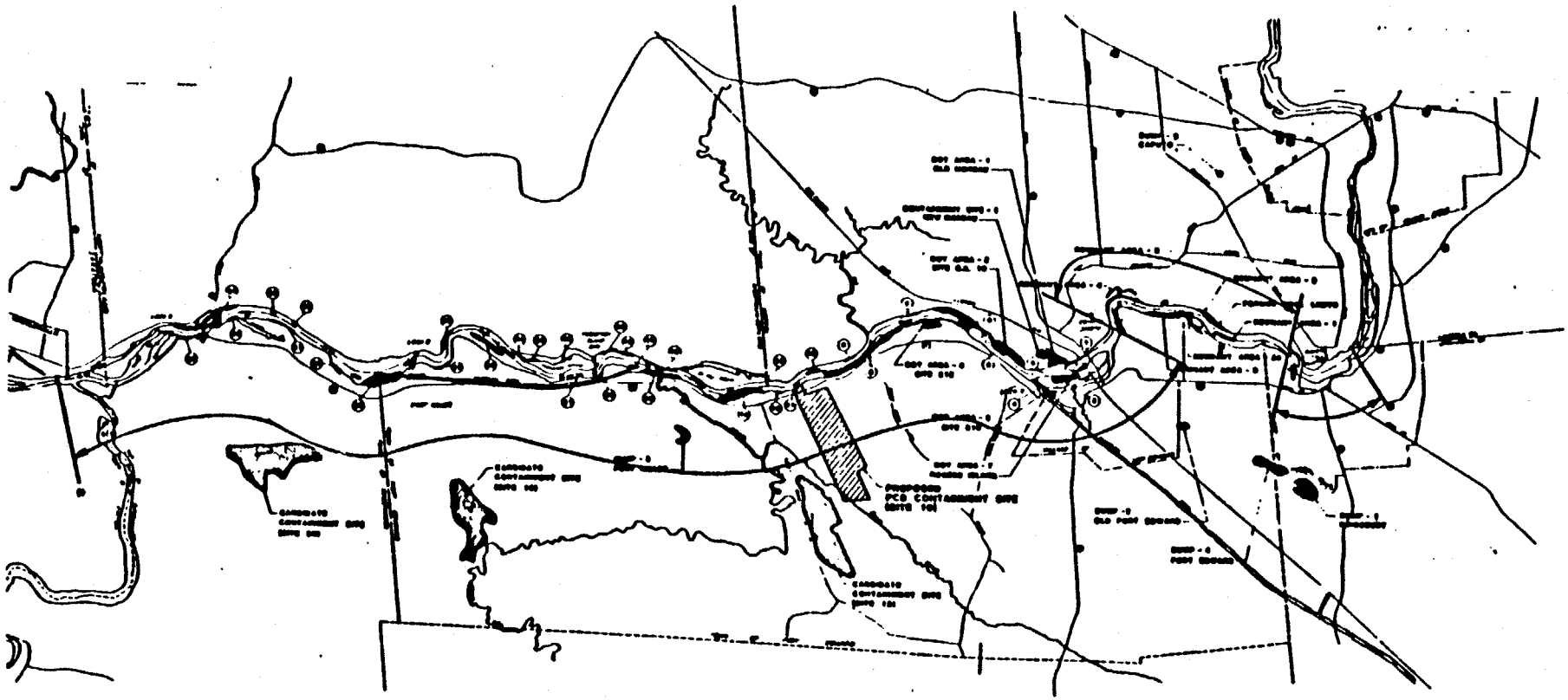

Figure 1. Map of the upper Hudson River between Bakers Falls in Hudson Falls, NY, and Lock 5 north of Schylerville, NY. The locations of the Remnant Deposits and hot spots 1 through 35 are shown. The marked sections of the river were surveyed in this study.

were exposed above the new river level and began to be eroded. Indeed, peak down-river PCB concentrations occur in sediments at this time (Bopp et al, 1985). The exposed material that was trapped behind the Fort Edward dam is known as the remnant deposits (Figure 1). High river discharges in 1974 and 1976 eroded portions of the unstable remnant deposits and carried that material downstream. This material clogged much of the river near Fort Edward, and dredging operations were required to clear the waterfront there (Sanders, 1989). These flood events may be identified in sediment cores as one or two wood-chip layers. The remnant deposits were capped by 1991 by General Electric to prevent further erosion and downstream transport (TAMS, 1991). However, the northern-most portion of remnant deposit 1 in the center of the river and the northern portion of remnant deposit 2 on the western side remain uncapped.

In order to better understand the distribution of sediments within the river, geophysical investigations utilizing side-scan sonar, bathymetry, subbottom profiles, and supplemented with limited sediment sampling, were undertaken in the portion of the Hudson River between Bakers Falls in Hudson Falls, New York, and Lock 5 immediately north of Schylerville, New York. This 13 mile section of the river was chosen for study because it includes the remnant deposits and 35 of the 40 original PCB hot spots. Also, we wanted to determine the distribution of sediment behind the dam at Bakers Falls.

Studies of sites on land can utilize airborne and satellite imagery, supported by field observations, to characterize the environment and to reveal the details of sediment distribution. However, these techniques cannot be used underwater because of reduced visibility. Mapping underwater with side-scan sonar permits a view of the river bottom somewhat equivalent to an aerial photograph. These data, especially when combined with bathymetry, sediment samples, and subbottom profiles, provide valuable insights into sedimentation patterns and some of the factors that control sedimentation processes. Side-scan sonar is being used to study sedimentation patterns in many environments in all water depths. Quantitative analysis of sonar data is important in several of these studies (Chavez, 1986; Reed and Hussong, 1989; Malinverno et al., 1990; Gardner et al., 1991; Sun, 1993). During our study, the side-scan sonar data were digitally compiled and analyzed to provide images of the river bed based on the reflectivity of sound. These images provide detailed information about the bottom morphology of the river, the distribution of sediment within the river, and the processes responsible for those distribution patterns.

Data Collected

Survey equipment used included a Klein Model 595 dual-frequency side-scan sonar (operating at 100 kHz and 500 kHz), an Innerspace 488 208 kHz narrow-beam (8°) echo-sounder with digital output, and a Raytheon RTT-1000 7 kHz subbottom profiler. The survey vessels and all field equipment was provided by and operated by Ocean Surveys, Inc. (OSI), Old Saybrook, CT. All ship tracks were navigated using a Hydro I IMC laser based range/angle system with a nominal accuracy of about 3 feet ($\pm$ 1 m) with fixes obtained every 0.7 seconds. Navigation is referenced to the New York State Plane Coordinate System (1927), and elevations are referenced to the North American Vertical Datum (1929). Navigation information (including position, water depth, and ship heading from a fluxgate compass) were logged on computer. The

side-scan sonar data was tape recorded using a TEAC 8-channel instrumentation recorder that digitally records 16-bit signal levels at 12,000 samples per second for each channel. Following field operations, OSI provided computer files of navigation and bathymetric data as well as analog 7 kHz subbottom profiler records, analog side-scan sonar records, and the recorded sonar data tapes. The side-scan sonar, bathymetric, and subbottom profiling data were collected during December 14-16, 1991, during April 10-26, 1992, and on June 4, 1992. Geophysical data was collected along tracks spaced 40 m (132 ft) apart in the along-river direction and 150 m (492 ft) in the across-track direction. All geophysical data (sonar, subbottom and bathymetry) was collected along all survey tracks.

A side-scan sonar operates by transmitting a sound beam, narrow in the fore-aft direction, to either side of the towed sonar fish, and recording the strength of the returned echo (Figure 2). The intensity of the sonar return is related to several factors, including the grain size of the sediment, small-scale topography of the river bed, the slope of bottom, and perhaps near-surface layering within the sediments. Instrumental factors such as the angular strength of the sound beam, also affect the returned signal levels. As the sonar is towed, a swath of the river bed to either side of the vessel is imaged. As multiple ship tracks are collected, a picture of the river bed is built up. The wavelength of 500 kHz sound in water is 0.3 cm, the wavelength of 100 kHz sound is 1.5 cm. The 500 kHz images often provide a higher-resolution image of the river bottom because of the shorter wavelength. We expected that the relative strength of the 100 kHz and 500 kHz images would differ as river properties change because of the difference in the sound wavelength.

The side-scan sonar was operated on a swath width of 37.5 m/side (123 ft) for a total width of 75 m (246 ft) mapped along each ship track. However, because of the shallow water depth (which can limit the range of the sonar data), adjacent sonar tracks running parallel to the river were placed 40 m apart resulting in considerable overlap of sonar data from adjacent tracks. Preliminary studies in May, 1991, suggested that this was an optimal design for a sonar survey in this setting (Flood, 1991). The sonar images were created using along-track data only to provide a consistent orientation for viewing the bottom. The side-scan sonar data was replayed and digitized by computer in the lab to provide digital sonar data suitable for constructing sonar mosaics of the river bottom. The digitizing process and steps used to construct the digital images and to analyze the sonar data are describe in a later section.

The 7 kHz profiler was used along all tracks (along-river and across-river) to obtain an indication of shallow sediment layering. Sound at 7 kHz can penetrate into sediments and reflect off layers in the sediments. Sound can penetrate farther into the sediment when the grain size is small than when grain size is large. The resulting 7 kHz profile can show layering within the sediments, and can in some instances can be used to study sediment type. The minimum layer thickness that could be observed was about 0.3 m (1 ft). Near-surface layers (subbottom depth less than about 2 ft) were particularly difficult to resolve due to interference with sound scattering of the sediment surface. Sound penetration is also limited by the presence of coarse sediments, gas in sediments, and possibly by layers of wood chips.

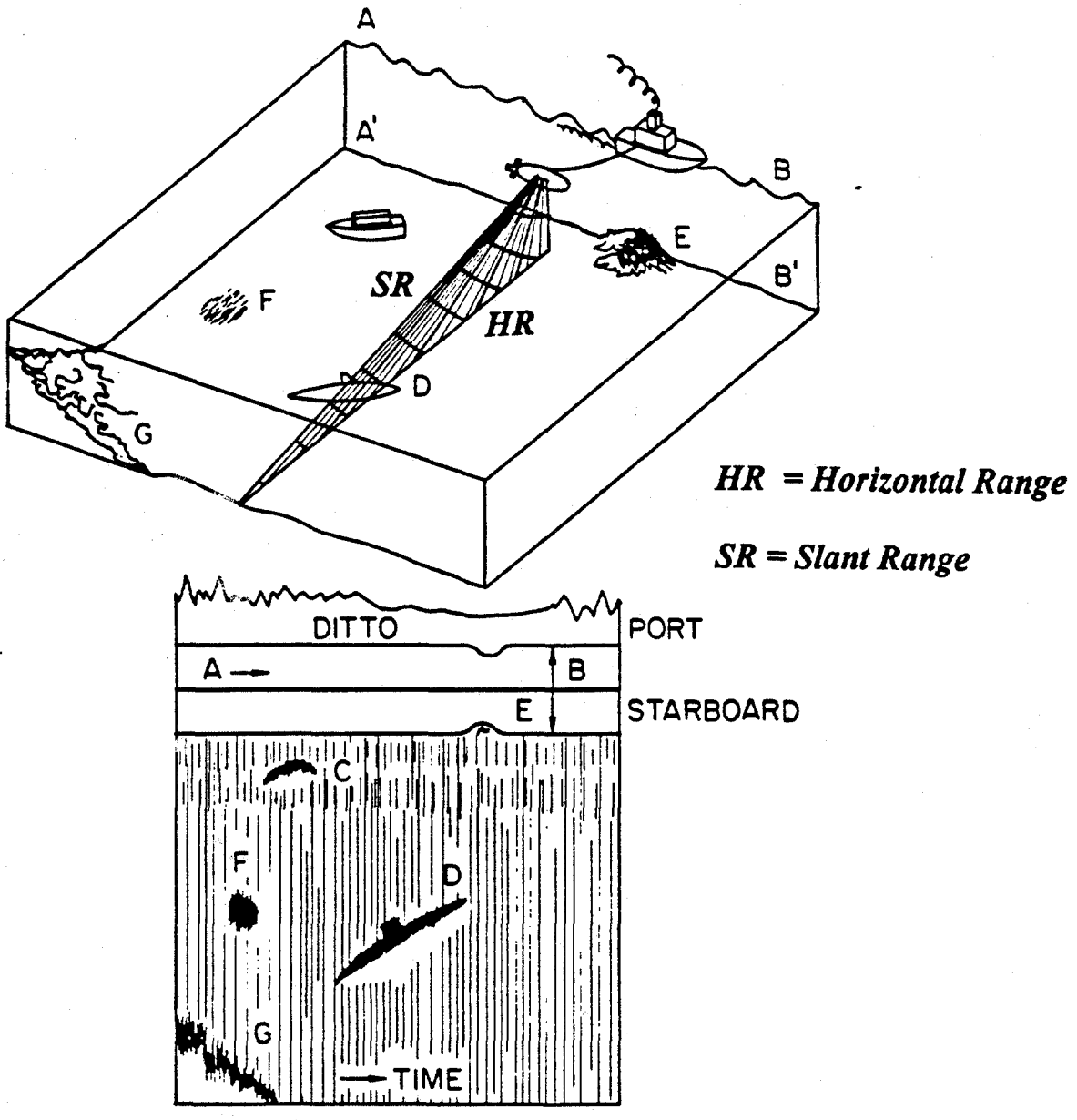

Figure 2. Sketch showing the operation of a side-scan sonar system, a similar sonar beam, narrow in the fore-aft direction, is transmitted from the other side of the sonar fish. Upper: equipment used in the field, lower: hypothetical sonar record for sea bed in upper sketch. For a dual-frequency sonar system, side-scan sonar records at two frequencies are collected simultaneously. SR = slant range, the direct distance from the sonar fish to a sonar target. HR = horizontal range, the horizontal component of the slant range. (after Edgerton, 1986).

Sediment samples were collected from May 25 to June 6, 1992 at about 178 sites selected on the basis of sonar images to allow the sonar patterns to be related to sediment character. The locations of all sediment samples were determined to within ± 3 ft. Samples were collected utilizing a push corer or a grab sampler. The push corer was attempted first. If a push core was collected, a second core was also collected for X-radiography to determine sediment structures. The first of the two cores was extruded, described, and sampled for grain size. If no sample was recovered with the core, the grab sampler was used. Grab samples were described and sampled for grain size. Grain size analyses were performed using both ATSM methodology and the Malvern laser technique.

Side-Scan Sonar Images

Side-Scan Sonar Processing

A number of steps were followed to produce digital side-scan sonar maps from the sonar data. The tape-recorded sonar data were replayed in the laboratory and digitized to an 8-bit image (signal values ranging from 0 to 255) utilizing a PC-compatible computer. At a swath width of 37.5 m/side, the side-scan sonar pings at a rate of about 19 times each second. This corresponded to an along-track spacing between sonar pings of about 0.35 ft (0.11 m) at a boat speed of 4 knots, varying from about 0.1 ft to 1 ft as survey boat speed varied. The side-scan sonar data was digitized at a rate of 11,905 samples/second corresponding to an across-track sample spacing of 0.13 feet (0.04 m).

A number of steps were taken to create the sonar mosaics. The position of the sonar fish was determined from navigation data provided by OSI, and was merged with each sonar file. This navigation data includes position, direction of boat travel (course), direction in which boat is pointed (heading), fish depth, and fish height above the bottom. There is an overall time uncertainty of about 1 second in aligning the sonar data with the navigation. This results in an uncertainty of up to about 7 feet (2.1 m) in distance, which is about the same as the navigational uncertainty (± 3 ft). The merged sonar files were smoothed and decimated (or subsampled) with a median filter to produce a record where along-track and across-track data points were spaced about 0.8 feet (0.24 m) apart. Using a median filter reduces the noise in the image and improves image quality. Both these steps are important for creating the best sonar image at a resolution of 1 ft (0.3 m) per image pixel. An additional processing step (termed "destriping") was applied to the 500 kHz sonar data to remove acoustic interference from the 200 kHz echosounder and the 7 kHz subbottom profiler. This interference did not occur on the 100 kHz sonar data.

The intensity of the sound return on the sonar record depends on the gain settings in the sonar electronics and the pattern of sound transmitted by the sonar fish as well as on the character of the bottom. Corrections need to be applied to the sonar data to compensate for changes in the sonar record that are due to the gain settings and beam pattern. These corrections, termed "shading" corrections, are necessary to create a sonar image that can be easily viewed. Shading corrections are essentially made by normalizing each sonar data value to an average sonar value for that fish height and slant range.

The first step in determining shading corrections was to average together all of the decimated, destriped survey data for each pair of fish elevation and slant range. This array of average values at each fish elevation and slant range was modified to produce the shading correction factors. Since the deeper-water portions of the survey are predominantly rocky while the shallower-water portions of the survey have more uniformly distributed bottom types, the calculated average values in deeper water (deeper than about 15 ft) were reduced slightly to be more similar to the average values of records in shallower water . The average value array was also smoothed to provide a more uniform array. These steps were needed so that the shading corrections did not remove geological features from the sonar image. For example, if a certain water depth is dominated by rock or highly reflective sediment, then the average reflectivity of this depth interval will be large. If the sonar data were normalized with this large average value, the highly reflective sediment surface would be reduced to the average value of the entire sonar image, and the reflective nature of this depth interval would be lost. By reducing the average value in depth ranges where high-reflectivity sediments are more common and by smoothing the average-value array, much of the original information on river bottom character is retained in the sonar images.

Different shading corrections were necessitated for different portions of the survey because of changes in gain or other instrumental settings. All of the 500 kHz and 100 kHz sonar data south of Fort Edward was processed with a consistent shading correction with a minor correction made for a gain change that occurred in the 100 kHz port channel part way through the survey. Because a consistent shading correction is applied throughout this range, these sonar data can be directly inter-compared. Different shading corrections were needed for data collected in both the remnant area and in the pool behind Baker's Falls. Thus the digital values of sonar images in those two areas cannot be compared to each or to the data below Fort Edward.

Digital side-scan sonar mosaics were produced at the Lamont-Doherty Earth Observatory, Palisades, NY, in collaboration with Dr. W.B.F. Ryan. The mosaics were created by plotting the sonar data (processed using the approach described above) in its proper position on a base map. This position was determined from fish position, fish orientation (based on boat heading or course), and fish elevation above the bottom. Fish elevation was used to correct slant range (travel time direct from fish to sonar target) to horizontal range (horizontal component of travel time from fish to sonar target) assuming a flat bottom. Where two tracks covered a given part of the river bed, only the sonar record from the closer track was plotted.

A total of 40 map areas 2000 feet on a side were defined covering the river from the pool behind Bakers Falls to Lock 5 north of Schylerville (Figure 3; Table 1). Side-scan sonar data were collected in 37 of the 40 map areas; no sonar data were collected in map areas 37 or 38 in the northern portion of the remnant areas or in map area 39 in the rapids south of the dam at Bakers Falls. Sonar mosaics utilizing the 500 kHz sonar data were created for each of these 37 map areas (map areas 1 to 36 and map area 40). Sonar mosaics were also created using the 100 kHz data for map areas 1 to 33. 100 kHz mosaics were not created for the Remnant Area (100 kHz data is poor due to air bubbles in the water) and in Bakers Falls (primarily rock outcrops well resolved with the 500 kHz data). Full-scale plots on paper were made of the 500 kHz images

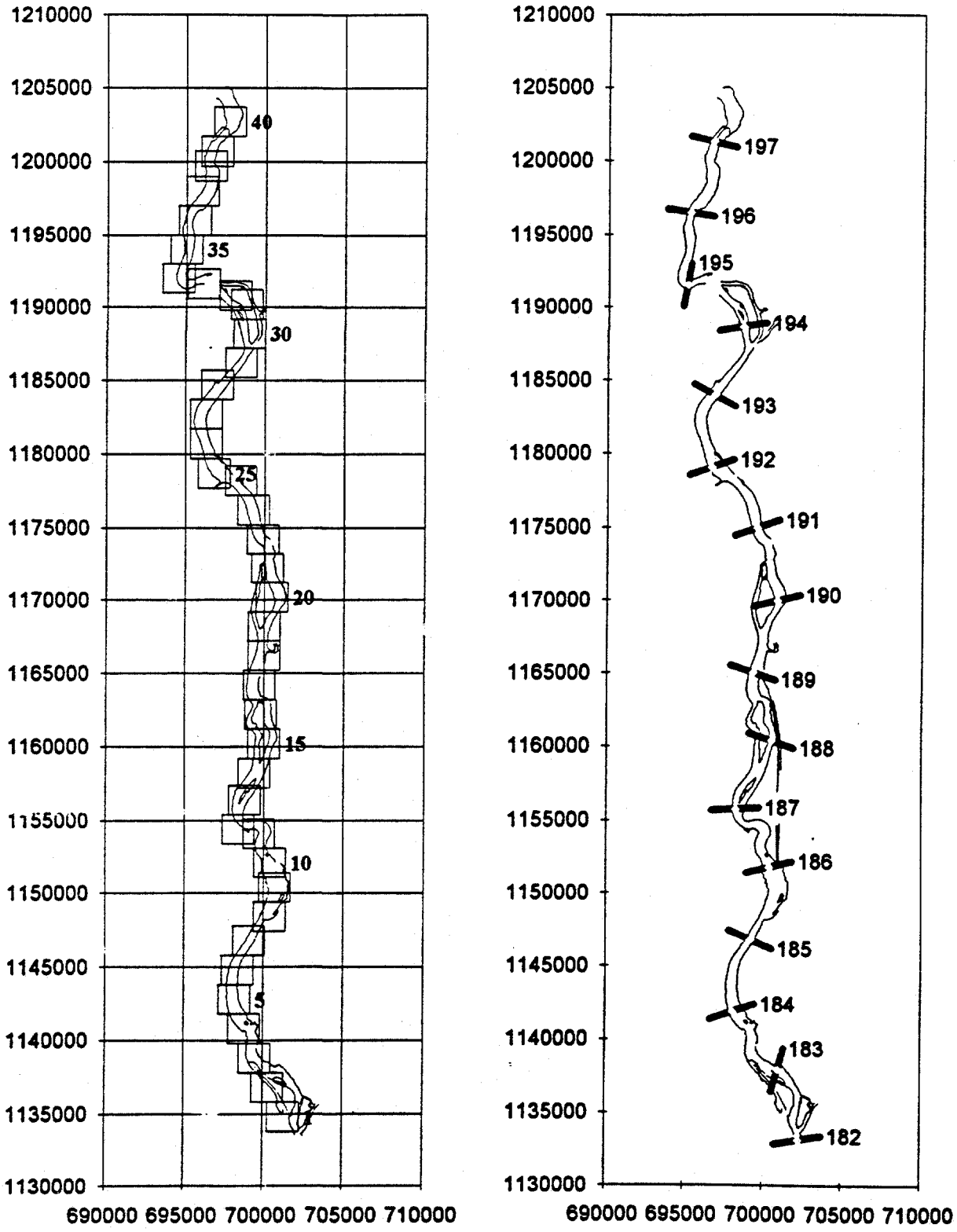

ıre 3. Left: locations of sonar map areas. Map area 1 is at the southern end of the section surveyed, map ıs at the northern end, each map area is 2000 ft by 2000 ft. Precise boundaries of the map areas are given in able 1. Right: map of the portion of the Hudson River surveyed along with river mile.

Table 1

Side-Scan Sonar Map Areas -- Bakers Falls to Lock 5

(note: maps are 2000 feet on each side)

Map Number	Map Boundaries south	north	east	west
1	1,133,800	1,135,800	700,300	702,300
2	1,135,800	1,137,800	699,500	701,500
3	1,137,800	1,139,800	698,500	700,500
4	1,139,800	1,141,800	697,800	699,800
5	1,141,800	1,143,800	697,200	699,200
6	1,143,800	1,145,800	697,400	699,400
7	1,145,800	1,147,800	698,100	700,100
8	1,147,400	1,149,400	699,400	701,400
9	1,149,400	1,151,400	699,700	701,700
10	1,151,100	1,153,100	699,400	701,400
11	1,153,100	1,155,100	698,700	700,700
12	1,153,400	1,155,400	697,400	699,400
13	1,155,400	1,157,400	697,800	699,800
14	1,157,200	1,159,200	698,400	700,400
15	1,159,200	1,161,200	699,000	701,000
16	1,161,200	1,163,200	698,800	700,800
17	1,163,200	1,165,200	698,700	700,700
18	1,165,200	1,167,200	699,000	701,000
19	1,167,200	1,169,200	699,000	701,000
20	1,169,200	1,171,200	699,500	701,500
21	1,171,200	1,173,200	699,200	701,200
22	1,173,200	1,175,200	698,900	700,900
23	1,175,200	1,177,200	698,300	700,300
24	1,177,200	1,179,200	697,500	699,500
25	1,177,700	1,179,700	695,800	697,800
26	1,179,700	1,181,700	695,300	697,300
27	1,181,700	1,183,700	695,300	697,300
28	1,183,700	1,185,700	696,000	698,000
29	1,185,200	1,187,200	697,500	699,500
30	1,187,200	1,189,200	698,000	700,000
31	1,189,200	1,191,200	697,800	699,800
32	1,189,900	1,191,900	697,100	699,100
33	1,190,600	1,192,600	695,100	697,100
34	1,191,000	1,193,000	693,500	695,500
35	1,193,000	1,195,000	694,000	696,000
36	1,195,000	1,197,000	694,500	696,500
37	1,197,000	1,199,000	695,000	697,000
38	1,198,700	1,200,700	695,500	697,500
39	1,199,700	1,201,700	695,900	697,900
40	1,201,700	1,203,700	696,700	698,700

only (Appendix A). All images (including the 500 kHz mosaics) are provided as digital files that can be viewed by computer (Appendix B).

The primary sonar mosaics are 2000 points on a side with each data point (or pixel) representing 1 square foot on the river bed. These images were printed at a scale of 1 inch = 100 ft (a natural scale of 1:1200) at a size of 20 inches on a side (Appendix A). Sonar signal levels range from a value, or digital number (DN) of 1 (black) to 254 (white). Reflective portions of the image have a high signal level and are light or white in color and non-reflective portions of the image have a low signal level and are dark or black in color. Areas of the sonar map with no sonar data (e.g., the area outside of the river) have a DN of 0, and the 500 ft grid lines and text superimposed on the image have a DN of 255. These images exist as digital as well as paper images. The 2000 by 2000 pixel images have a size of 4,000,800 bytes; a 800 byte header (used by the Sun computer system that created the raster images) followed by a 4,000,000 byte image.

Other sonar images were derived from these primary 2000 point by 2000 point digital images. A suite of images covering the same map areas but reduced in size (decimated) to 400 points by 400 points (pixel size 5 feet) was created for use in image calibration and analysis by reducing each group of 5 by 5 pixels to one pixel. Three images were created for each frequency and each map area where both 500 kHz and 100 kHz data are available (map areas 1 to 33). One image is the median value of each pixel group, a second image is the mean value of each pixel group, and a third image is the standard deviation of each pixel group. Scale lines and labels were removed from the decimated image by not considering values of 255 when reducing the image. Background values of 0 were also not used in decimating the image. The median value image preserves much of the pattern of the original image. The mean value image is similar to the median value image, although the image appears more smoothed. The standard deviation image shows high values where there is small-scale variability in the targets. These decimated images are provided in digital form only (Appendix B).

The six reduced images for each area (two frequencies, three maps per frequency) were subjected to principal component analysis (Richards, 1986) to determine the groupings of these image data that best represent the variability observed throughout the survey area. This analysis suggested three combinations of the sonar images that together account for 99.1% of the data variance (Table 2). Component 1 represents most of the variance (89.1%). This component consists primarily of the average of the median and mean images for both the 100 kHz and 500 kHz data. Component 2 represents 6.8% of the variance observed, and consists primarily of the difference between the 100 kHz and 500 kHz images. Component 3 represents 3.2% of the variance observed, and consists primarily of the standard deviation images for both the 100 kHz and 500 kHz data. These three components can be combined into a false-color image by assigning one of the three image colors (red, green, and blue respectively) to each of the components. False-color images made up of the component images combined to make an 8-bit color composite image, are provided in digital form only (Table 2; Appendix B).

Information Extraction from Side-Scan Sonar Data

There is a need to understand how the sonar data relates to river bed characteristics, including sediment size and other variables. As noted previously, the intensity of the sonar return can depend on many instrumental and environmental factors. Previous processing steps were described that reduced the effect of many instrumental artifacts in order to provide a sonar image that can be used to describe the river bed in a qualitative fashion. Environmental factors that may effect the sonar character include bottom type (sediment, rock outcrop, vegetation), sediment size (gravel, sand, silt, clay), small-scale roughness (ripples, lineations, rock layering or fracture pattern, mounds created by animals), sediment layering (buried but near-surface sand or gravel layers), larger discrete features (trees, large chunks of sawn wood, docks, other large debris, and shadows cast by those features), bottom slope (flat-lying, sloping away from sonar fish, sloping toward sonar fish), and the shoreline (rip-rap, marsh, sediment). The effects of some of these environmental factors on the sonar image is clear. For example, when the bottom slopes towards the sonar fish, signal strengths are enhanced whereas when the bottom slopes away from the sonar fish signal strengths are reduced and there may even be large regions in shadow. However, the importance of other environmental factors, such as grain size, in affecting signal strength needs to be established.

The reduced images (400 pixels x 400 pixels) and the surficial grain size measurements made on samples recovered during confirmatory sampling were used to study the relationships between image digital value (DN) and sediment grain size for both the 100 kHz and 500 kHz images. A total of 155 stations with grain size data were used in this analysis. The other stations occupied were in the remnant area and at Bakers Falls where the sonar image was not quantified. Grain size analysis techniques are discussed in a later section.

The DNs of the sonar images were determined in areas centered on the sample locations. Image values were read from a 10-ft diameter area (500 kHz median image) and a 50 ft diameter area (all images) centered on each sample site. This process resulted in a file that includes sample position, ID, grain size parameters, and mean values and standard deviations of the decimated median, mean and standard deviation images for the 500 kHz and 100 kHz images.

We next needed to determine whether the sonar image in the vicinity of each sample is uniform. If the image near a sample site is contaminated with artifacts such as reflective shore lines, regions of large shadows, or discontinuities in the image between adjacent sonar tracks caused primarily by bottom slope, then the DN of the image will be related to factors other than the bottom sediment characteristics. The 500 kHz median image was visually examined in the vicinity of each core site to determine if any artifacts were present. On the basis of visual analysis, 96 of the original 155 grain size analysis used were classified as being in uniform areas of the sonar mosaic.

A methodology was developed to allow the uniformity of the image in the vicinity of a sample site to be assessed from the 500 kHz median image parameters alone. First, the difference between the mean values of the 10 ft and 50 ft diameter circles was calculated. For a non-uniform image, the mean value will change as the diameter of the circle changes due to the changing

nature of the image near the sample site. Samples where this difference is greater than 30 were not used in the calibration. Samples where the standard deviation of the 50 ft circle is greater than 25 were also excluded. A large standard deviation suggests a non-uniform image, perhaps indicating shadows and local topography. The ratio between the standard deviation and the mean value of the 50 ft circle was calculated, and the sample excluded if the ratio is greater than 0.4. A larger ratio may indicate a bimodal distribution of image values and thus a non-uniform image. The sample was also excluded if the standard deviation to mean ratio increased by more than 0.3 from the 10 ft to the 50 ft circle. An increasing ratio suggests a change in image characteristics, and thus a non-uniform image near the core site.

Through the application of these rules, 113 of the original 155 grain size analyses were considered acceptable (Table 3). The results of this process agrees well with the results of the visual analysis; 86% of the samples were classified similarly in the two processes. Two of the 96 samples accepted by application of these rules had been excluded on the basis of the earlier visual examination, and 17 of the 59 samples excluded during the visual examination were accepted using these rules. Most of these newly accepted samples occurred in regions where visual analysis suggests that regional bottom slope altered the sonar return, although no discontinuities were present within the 50 ft circle. Additional information about the sample site (for example, bottom slope) would be required to identify these samples. Using these additional samples in the calibration process is acceptable at this stage because changing bottom slope is one of the major unquantified effects on the sonar record. Our calibration data set should include this unquantified effect.

The subset of 113 grain size analyses and DNs where the sonar mosaic is uniform were analyzed through linear regression to determine possible relationships between grain size parameters and image values (Table 4; Figures 4-8). In describing the relationships observed, we use "positive correlation" to mean that image value increases as grain size increases. However, since grain size is measured on a phi scale (size [mm] = $2^{[-phi]}$), larger grain sizes have a smaller phi value. Thus the slope of a correlation curve between phi size and DN will be negative for a positive correlation between DN and grain size. See the section on grain size for a further discussion of grain size parameters.

500 kHz Images

The best correlation between grain size parameters and image values is between mean grain size and the 500 kHz median and mean image DNs ($r^2 \sim 0.55$; Table 4; Figures 4, 5 and 6). Similar correlations are observed the six calculated percentiles (d(15) to d(90)) and for % mud ($r^2 \sim 0.49$ to 0.54). There is a poor correlation between image DN and % gravel or % sand ($r^2 \sim$ 0.16 to 0.22). This is in part due to the non-linear relationship between grain size expressed as % gravel or % sand and the actual sediment size. For example, in a sample with 50% sand, there could be 50% gravel, 50% mud, or 25% gravel and 25% mud. Since each of these sediments would have a different mean grain size, we would expect a different image DN in each case although % sand remains constant. In general, the 500 kHz standard deviation image correlates with grain size parameters less well than the median or mean images ($r^2 \sim 0.25$ to 0.34) with the best correlations with % mud, d(85), d(70), d(90) and mean size.

CC-060	700059	1154865	0.676	2.361	2.630	3.219	4.417	5.554	7.2	78.6	14.2	2.574	1.871
CG-061	699730	1154990	0.927	1.860	2.129	2.655	3.181	3.695	0.0	93.6	6.4	2.079	1.127
CG-062	699734	1154984	-1.749	-0.625	-0.303	1.108	2.340	2.996	19.3	76.7	4.1	0.096	2.044
CC-063	700008	1154864	0.629	1.989	2.261	2.992	4.391	5.613	8.5	76.9	14.6	2.427	1.881
CG-068	698179	1155651	-0.229	1.064	1.397	2.012	2.808	3.506	6.3	86.7	7.0	1.326	1.518
CG-069	698307	1155645	-0.156	0.761	1.070	1.552	2.029	2.293	3.6	95.4	1.2	0.981	1.093
CG-070	698359	1155647	-0.186	0.747	1.031	1.508	2.031	2.319	5.7	92.4	1.9	0.959	1.108
CG-072	698545	1155625	-0.312	0.466	0.721	1.315	2.012	2.496	4.3	92.1	3.8	0.807	1.162
CC-074	698627	1156199	4.073	5.352	5.767	6.680	7.513	7.914	0.0	22.6	77.4	5.784	1.720
CG-076	699140	1156933	-1.848	-0.670	-0.227	0.905	1.728	2.332	26.3	69.4	4.3	-0.116	1.788
CG-077	699217	1156896	-2.187	-1.423	-0.933	0.804	2.203	3.563	47.0	45.8	7.1	-0.306	2.195
CC-078	699292	1156842	1.821	2.635	3.163	4.486	6.241	6.874	0.0	70.2	29.8	3.741	2.210
CC-080	698874	1157789	2.013	2.423	2.575	2.855	3.215	3.445	0.0	96.0	4.0	2.601	0.601
CG-081	698945	1157727	-2.238	-0.638	0.472	1.561	2.418	2.890	31.6	64.6	4.1	0.217	2.328
CG-082	699096	1157638	-0.174	0.793	1.078	1.553	1.936	2.175	3.8	95.3	1.0	0.946	1.055
CG-083	699183	1157563	-1.416	-0.064	0.576	1.735	2.573	3.112	16.5	79.1	4.7	0.578	1.994
CC-084	699213	1157551	2.593	3.616	4.025	5.153	6.508	7.028	0.0	60.0	40.0	4.375	1.958
CC-086	699503	1158679	1.882	3.020	3.433	4.414	5.616	6.136	0.0	66.7	33.3	3.644	1.868
CC-088	699704	1158595	0.754	1.738	2.016	2.750	4.674	5.774	2.4	82.0	15.6	2.481	1.960
CG-089	699773	1158576	-0.706	0.173	0.458	1.088	1.605	1.954	9.2	89.2	1.7	0.452	1.156
CG-090	699988	1158518	-2.495	-1.589	-1.026	0.914	3.052	4.093	44.0	47.1	9.1	-0.156	2.773
CC-091	700102	1158495	3.125	4.672	5.252	6.347	7.147	7.575	0.0	37.4	62.6	5.174	2.011
CG-092	700312	1159849	-0.697	0.174	0.574	1.688	3.958	4.525	17.9	70.0	12.1	1.278	2.328
CC-093	700638	1161280	3.279	4.528	5.034	6.032	6.975	7.438	0.0	39.5	60.6	5.096	1.848
CG-109	697199	1191298	-0.733	-0.087	0.319	1.203	2.056	2.322	30.6	67.2	2.2	0.547	1.394
CG-111	697629	1190418	-1.916	-1.775	-1.719	-1.607	-1.522	-1.274	92.3	6.9	0.8	-1.719	0.197
CG-113	696923	1191044	1.324	2.156	2.528	3.603	5.159	5.926	0.0	80.1	19.9	3.004	1.918
CG-114	697107	1191149	-1.881	-1.683	-1.604	-0.838	1.291	1.849	72.8	26.3	0.9	-0.731	1.586
CG-115	697862	1191635	-1.875	-1.667	-1.583	-0.241	1.178	1.579	68.4	30.9	0.7	-0.760	1.527
CG-116	698509	1191543	-1.860	-1.628	-1.535	0.061	1.358	1.723	65.5	34.2	0.4	-0.679	1.609
CG-118	698933	1191306	2.412	3.776	4.204	5.260	6.428	6.821	0.0	56.8	43.2	4.348	2.008
CG-121	697871	1191599	-1.867	-1.646	-1.557	-0.573	0.985	1.467	70.8	28.5	0.7	-0.813	1.426
CC-122	700061	1166660	3.521	4.811	5.249	6.210	7.088	7.518	0.0	33.5	66.5	5.286	1.783
CG-124	699704	1166357	0.475	1.909	2.314	3.250	4.688	5.401	3.9	79.7	16.4	2.492	2.106
CC-125	699778	1166354	-1.764	-1.012	-0.321	1.629	2.979	3.750	47.6	45.4	7.1	0.298	2.371
CC-126	699802	1166350	-1.101	0.233	0.804	2.171	3.337	4.106	24.6	67.1	8.3	1.014	2.219
CG-127	699936	1166309	4.554	5.818	6.257	7.121	7.938	8.288	0.0	14.2	85.8	6.250	1.692
CC-128	700004	1166253	4.582	5.884	6.341	7.223	8.013	8.356	0.0	13.8	86.2	6.312	1.716
CC-129	700071	1166288	3.968	5.229	5.690	6.697	7.527	7.943	0.0	25.7	74.3	5.728	1.779
CG-132	700856	1151041	2.505	3.546	3.976	5.240	6.552	6.990	0.0	59.6	40.4	4.345	2.024
CC-133	701200	1150993	2.146	3.022	3.316	4.272	5.508	6.203	0.0	70.3	29.7	3.656	1.681
CC-134	701419	1150533	0.756	2.735	3.233	4.288	5.874	6.578	4.7	67.8	27.5	3.288	2.559
CC-135	701490	1150530	-0.490	0.680	0.885	1.403	1.865	2.055	14.9	84.5	0.6	0.753	1.177
CC-136	701551	1150661	3.333	4.492	4.958	5.885	6.842	7.261	0.0	40.2	59.8	5.044	1.755
CC-137	701353	1149844	2.084	4.376	4.906	5.898	6.851	7.268	0.0	42.5	57.5	4.614	2.384
CC-138	700724	1149656	2.164	3.218	3.485	4.629	6.298	6.838	0.0	68.7	31.3	3.982	2.067
CG-138	700724	1149656	1.276	2.302	2.638	3.390	4.515	5.227	0.0	84.9	15.1	2.809	1.620
CG-139	700336	1149201	0.557	0.968	1.184	1.675	2.291	2.723	0.0	96.3	3.7	1.344	0.867
CG-140	700749	1149181	0.725	1.569	1.933	3.617	5.585	6.315	0.0	76.6	23.4	2.748	2.430
CG-141	700538	1150585	-1.727	-0.594	0.078	1.136	2.065	2.568	40.5	56.0	3.5	0.139	1.896
CG-142	700715	1150625	6.572	7.470	7.741	8.320	8.972	9.263	0.0	0.0	100.0	7.762	1.200

316683

CC-144	700607	1148400		4.231	5.356	5.770	6.662	7.439	7.843	0.0	20.4	79.7	5.813	1.604
CC-145	700605	1148350		3.693	5.068	5.537	6.596	7.446	7.858	0.0	29.2	70.8	5.559	1.876
CG-147	701079	1151486		3.102	4.403	4.995	6.223	7.185	7.641	0.0	41.8	58.2	5.094	2.041
CC-149	701244	1151458		2.482	4.056	4.575	5.734	6.872	7.356	0.0	48.7	51.3	4.643	2.195
CC-157	699484	1140639		3.667	4.989	5.425	6.411	7.201	7.627	0.0	30.3	69.7	5.431	1.767
CG-158	699500	1139840		3.056	3.692	3.992	5.311	6.486	6.811	0.0	58.3	41.7	4.511	1.715
CG-161	699270	1138485		4.019	5.052	5.413	6.266	7.050	7.477	0.0	26.8	73.2	5.494	1.515
CG-162	699061	1139253		-1.915	-1.774	-1.718	-1.605	-1.520	-1.269	93.7	5.2	1.2	-1.718	0.198
CG-163	699049	1139791		2.554	3.841	4.371	5.650	6.788	7.234	0.0	52.2	47.8	4.571	2.117
CG-164	699135	1139787		2.892	4.631	5.087	5.987	6.910	7.337	0.0	36.3	63.7	4.963	2.009
CC-168	698774	1141901		2.292	3.164	3.453	4.981	6.503	6.980	0.0	65.5	34.5	4.082	2.106
CG-168	698774	1141901		2.929	4.386	4.971	6.265	7.232	7.662	0.0	42.6	57.4	5.044	2.152
CC-169	698398	1142789		3.716	5.227	5.673	6.624	7.473	7.879	0.0	26.7	73.3	5.621	1.879
CC-170	698346	1141173		4.173	5.529	5.934	6.826	7.654	7.993	0.0	19.9	80.1	5.920	1.740
CC-171	698582	1141764		2.726	4.086	4.750	6.063	7.093	7.572	0.0	46.8	53.2	4.856	2.183
CG-172	698266	1141660		-1.539	0.265	0.897	2.213	3.332	4.072	28.3	63.2	8.5	0.897	2.436
CC-174	698391	1144125		4.156	5.240	5.606	6.481	7.236	7.643	0.0	22.2	77.8	5.666	1.540
CC-178	698405	1145865		3.322	4.226	4.615	5.729	6.911	7.445	0.0	47.7	52.3	4.949	1.795

Surface Sample Location			Image Data (50 foot diameter around sample)								
			500 kHz Sonar Mosaic			100 kHz Sonar Mosaic			Composite Image Mosaic		
Sample ID	Easting	Northing	Median	Mean	Std. Dev.	Median	Mean	Std. Dev.	comp. #1	comp. #2	comp. #3
CC-002	701261	1170250	22.1	22.4	5.9	24.7	25.8	9.7	42.5	46.5	92.1
CC-003	701126	1170277	36.9	38.0	11.2	45.5	50.0	22.6	82.3	54.5	114.6
CC-004	701016	1170270	45.1	46.3	11.8	38.2	46.8	24.8	87.2	55.3	90.1
CC-006	700836	1170223	66.5	67.3	13.0	77.5	79.4	23.6	143.0	36.6	129.2
CG-007	700790	1170206	78.8	79.6	15.4	66.5	68.5	21.5	146.8	34.4	84.8
CG-008	700792	1170180	72.8	73.6	13.8	65.5	68.0	23.1	139.5	36.8	94.0
CG-009	700765	1170179	63.2	64.1	11.5	62.5	64.5	20.9	125.3	36.9	103.5
CG-009	700765	1170179	63.2	64.1	11.5	62.5	64.5	20.9	125.3	36.9	103.5
CC-010	700727	1170160	78.3	79.0	14.9	64.6	66.0	19.6	143.9	32.6	81.1
CG-012	700910	1169812	49.0	49.5	10.0	55.9	58.0	20.8	103.2	43.1	114.1
CG-013	700939	1169699	41.5	42.0	8.8	46.0	48.3	18.4	85.5	44.9	106.1
CC-014	701018	1169849	24.0	24.5	6.0	17.5	18.9	8.6	38.2	46.4	73.8
CC-016	700939	1169699	41.5	42.0	8.8	46.0	48.3	18.4	85.5	44.9	106.1
CC-018	700907	1171071	32.8	33.0	6.2	36.7	38.1	12.5	65.7	42.0	100.2
CC-019	700759	1171025	47.4	47.8	11.5	45.7	47.3	15.3	91.4	42.8	93.8
CG-020	700650	1171026	72.2	73.7	16.0	81.6	82.8	21.8	153.3	35.2	125.9
CG-021	700598	1171000	77.1	78.0	14.1	87.8	89.6	24.4	164.3	31.5	132.6
CG-022	700530	1170987	73.2	74.1	15.6	50.0	52.5	18.7	125.7	38.5	59.9
CG-023	700455	1170964	83.5	84.2	14.7	75.8	77.8	19.9	160.0	27.7	96.4
CG-027	700463	1172092	40.9	41.7	9.1	48.9	51.5	16.6	87.6	43.2	112.8
CG-028	700459	1172410	63.2	65.7	19.5	84.9	87.9	28.9	149.3	50.3	149.1
CG-030	699989	1167113	44.3	46.5	15.4	56.6	59.3	22.1	100.9	53.7	121.6
CG-031	699599	1166395	38.9	40.2	12.0	34.4	37.7	15.9	73.3	50.7	85.4
CC-033	699642	1166380	54.7	55.2	10.6	54.8	56.6	17.3	107.9	38.0	101.3
CG-033	699642	1166380	54.7	55.2	10.6	54.8	56.6	17.3	107.9	38.0	101.3
CC-034	697029	1178979	54.3	58.3	21.3	59.3	67.6	34.4	120.7	68.2	115.4
CC-035	696957	1178954	57.3	59.7	19.6	49.1	52.8	18.1	109.2	50.9	83.3
CG-035	696957	1178954	57.3	59.7	19.6	49.1	52.8	18.1	109.2	50.9	83.3
CG-037	696868	1178951	82.3	82.9	18.3	47.8	49.2	15.1	132.9	34.8	37.8
CG-038	696889	1178934	71.2	72.3	16.0	37.3	40.0	13.8	111.6	38.1	35.7
CG-039	696740	1178920	85.3	86.1	15.9	86.1	88.1	25.0	172.3	31.0	115.4
CG-040	696763	1178897	86.7	87.8	17.1	84.5	87.7	26.8	173.5	34.1	110.7
CG-044	696250	1183000	81.4	83.5	25.2	70.2	76.9	33.8	159.3	57.5	91.7
CG-045	696244	1182988	82.7	84.7	25.3	69.7	75.4	31.9	159.5	55.4	87.2
CG-046	696187	1183045	70.1	73.0	19.6	70.9	74.7	26.3	144.5	47.9	108.6
CG-047	696188	1183031	70.8	73.9	20.4	68.5	72.5	27.0	143.6	50.0	102.4
CG-048	696140	1183089	69.9	71.1	17.9	92.7	94.5	27.1	161.9	41.5	154.1
CG-049	696047	1183168	51.4	52.8	15.5	38.6	43.1	17.7	92.4	50.2	73.9
CC-051	695927	1183286	41.2	41.7	12.1	51.5	55.3	23.5	92.1	53.1	119.7
CC-052	695885	1183350	46.7	50.1	18.3	62.9	67.2	28.3	112.0	61.0	131.7
CG-054	698987	1187207	67.9	69.3	13.4	75.7	77.3	25.5	143.4	38.6	122.7
CC-056	700281	1154713	55.6	56.7	13.0	48.4	52.2	19.3	105.2	44.2	87.7
CC-057	700267	1154678	39.2	39.8	9.8	37.6	40.0	15.4	75.2	46.3	91.7
CC-059	699955	1154893	64.0	65.4	17.4	40.1	42.8	18.5	107.2	47.2	53.8

316685

CC-060	700059	1154865	56.2	59.1	20.4	53.5	55.4	23.3	112.3	56.5	92.9
CG-061	699730	1154990	75.4	78.8	22.2	54.1	58.1	20.4	135.3	47.1	62.9
CG-062	699734	1154984	75.2	78.6	21.4	46.8	51.3	18.9	128.2	46.3	48.4
CC-063	700008	1154864	59.9	61.6	17.6	29.0	31.2	14.7	92.2	48.3	36.1
CG-068	698179	1155651	68.4	69.7	18.0	33.0	34.6	14.3	104.7	43.5	29.7
CG-069	698307	1155645	74.2	74.8	14.6	42.2	43.8	15.4	118.5	35.1	40.9
CG-070	698359	1155647	50.2	51.0	13.3	22.4	23.7	6.7	72.7	41.0	38.1
CG-072	698545	1155625	74.7	76.2	19.1	34.4	37.4	15.6	114.0	43.1	23.4
CC-074	698627	1156199	38.7	39.4	8.3	43.6	44.3	11.2	78.6	39.1	102.8
CG-076	699140	1156933	79.5	81.5	18.9	58.0	61.2	19.0	141.4	38.4	65.1
CG-077	699217	1156896	86.2	87.8	19.6	71.2	72.2	17.6	159.3	31.9	79.0
CC-078	699292	1156842	72.3	75.0	26.4	70.5	74.2	30.7	148.2	60.3	103.1
CC-080	698874	1157789	35.7	36.9	10.2	23.3	24.9	10.3	57.8	46.9	65.4
CG-081	698945	1157727	75.9	76.8	14.4	88.1	90.2	25.3	163.5	33.3	135.6
CG-082	699096	1157638	63.2	65.8	20.7	26.9	29.8	14.4	95.2	51.1	25.3
CG-083	699183	1157563	77.8	79.8	25.4	93.3	101.1	42.8	177.8	62.9	148.7
CC-084	699213	1157551	59.5	61.5	19.4	51.2	55.3	21.3	113.9	52.4	85.3
CC-086	699503	1158679	30.1	30.9	6.9	15.1	17.1	9.7	43.5	46.2	59.1
CC-088	699704	1158595	51.6	55.1	18.3	29.7	32.3	14.4	84.8	52.7	50.1
CG-089	699773	1158576	80.8	82.5	22.8	45.6	49.2	20.5	132.5	47.4	37.1
CG-090	699988	1158518	75.6	76.2	14.7	57.2	59.6	17.2	134.2	33.0	70.8
CC-091	700102	1158495	66.2	67.4	17.0	54.8	56.3	19.0	122.3	42.8	79.9
CG-092	700312	1159849	77.1	78.1	14.9	80.6	82.8	22.1	157.8	32.0	117.4
CC-093	700638	1161280	56.7	57.3	13.6	32.4	35.4	13.9	90.6	42.9	51.0
CG-109	697199	1191298	96.6	98.6	27.6	78.1	79.3	19.4	179.0	37.9	74.2
CG-111	697629	1190418	87.8	89.3	21.5	107.9	109.6	26.2	196.0	33.7	154.4
CG-113	696923	1191044	71.4	73.1	22.3	67.8	67.7	17.7	140.0	43.3	94.5
CG-114	697107	1191149	61.8	64.7	21.1	36.0	37.9	14.7	101.6	50.5	45.3
CG-115	697862	1191635	61.5	63.9	17.0	45.0	46.4	11.6	107.8	40.2	64.9
CG-116	698509	1191543	77.7	79.1	19.2	95.1	95.5	25.1	172.1	37.2	143.9
CG-118	698933	1191306	79.8	80.8	22.3	73.6	75.1	21.7	155.4	41.9	95.6
CG-121	697871	1191599	90.3	91.4	16.9	78.6	79.0	18.9	169.7	25.8	88.1
CC-122	700061	1166660	20.2	20.5	4.0	25.2	26.7	5.5	40.2	40.8	96.5
CG-124	699704	1166357	71.3	72.0	12.7	45.7	47.5	14.5	118.1	32.3	53.5
CC-125	699778	1166354	59.6	60.6	13.4	55.8	58.6	20.9	116.0	42.6	95.7
CC-126	699802	1166350	53.4	54.4	13.3	39.5	42.1	17.6	93.9	46.0	71.3
CG-127	699936	1166309	20.4	20.8	6.1	29.7	33.5	15.9	47.3	52.4	109.2
CC-128	700004	1166253	14.7	15.1	3.5	24.8	26.2	7.3	33.9	44.6	105.0
CC-129	700071	1166288	31.0	31.6	10.4	40.1	42.6	17.5	68.9	52.5	110.8
CG-132	700856	1151041	28.3	28.3	5.2	28.0	29.7	10.3	52.4	42.6	89.8
CC-133	701200	1150993	45.5	49.4	17.9	35.5	45.8	33.8	89.7	72.6	83.6
CC-134	701419	1150533	25.6	25.3	4.1	35.9	38.7	10.7	56.8	40.9	112.5
CC-135	701490	1150530	99.4	99.6	19.3	57.6	57.6	14.6	160.0	25.3	28.3
CC-136	701551	1150661	31.5	32.0	7.1	27.2	29.7	9.2	56.0	42.7	82.5
CC-137	701353	1149844	62.2	63.5	18.8	52.0	53.9	19.7	115.9	48.4	80.7
CC-138	700724	1149656	48.4	49.5	14.7	30.9	35.9	17.3	81.9	52.0	63.8
CG-138	700724	1149656	48.4	49.5	14.7	30.9	35.9	17.3	81.9	52.0	63.8
CG-139	700336	1149201	64.3	65.4	16.7	32.2	35.7	14.1	99.9	43.7	37.3
CG-140	700749	1149181	75.9	77.0	22.4	61.6	66.8	27.4	142.9	52.1	81.8
CG-141	700538	1150585	81.4	82.3	17.9	60.6	62.3	18.5	144.3	35.1	66.8
CG-142	700715	1150625	26.9	27.4	4.9	28.9	30.1	10.1	51.7	42.4	93.2

CC-144	700607	1148400		33.0	33.6	6.5		13.0	15.1	8.3		44.5	43.5	50.0
CC-145	700605	1148350		40.4	44.9	15.2		19.9	25.8	17.7		65.6	59.4	52.2
CG-147	701079	1151486		39.0	39.7	8.9		19.0	20.1	5.7		56.2	40.1	50.4
CC-149	701244	1151458		32.6	32.9	9.1		19.7	20.4	3.1		49.0	40.7	61.8
CC-157	699484	1140639		28.8	28.9	4.3		15.5	18.3	10.2		42.1	43.9	64.3
CG-158	699500	1139840		60.4	64.8	27.2		54.8	65.3	38.4		126.1	78.2	97.1
CG-161	699270	1138485		39.4	40.4	12.4		42.3	46.1	23.6		82.2	56.5	103.0
CG-162	699061	1139253		55.2	58.1	17.9		42.8	45.0	18.4		100.5	51.4	72.2
CG-163	699049	1139791		41.0	43.7	14.4		35.0	40.3	24.7		79.5	61.2	85.0
CG-164	699135	1139787		35.5	36.2	9.8		36.5	39.0	13.7		70.0	46.8	95.2
CC-168	698774	1141901		36.0	36.6	8.8		20.1	22.3	11.2		55.2	46.4	59.8
CG-168	698774	1141901		36.0	36.6	8.8		20.1	22.3	11.2		55.2	46.4	59.8
CC-169	698398	1142789		24.9	26.0	7.4		26.4	28.4	8.8		48.1	46.1	90.8
CC-170	698346	1141173		28.0	28.4	5.7		20.9	22.6	10.1		45.9	44.8	75.1
CC-171	698582	1141764		48.3	50.0	13.1		34.9	37.6	17.5		84.5	49.0	69.9
CG-172	698266	1141660		74.7	76.5	23.6		70.3	74.3	30.5		149.8	55.3	100.3
CC-174	698391	1144125		37.5	38.6	11.0		50.0	57.6	29.2		89.3	59.4	127.3
CC-178	698405	1145865		16.2	16.4	3.5		19.7	21.0	7.1		30.7	44.8	92.1

Table 4

Results of Linear Regression Study -- Grain Size Parameter vs. Image DN

DN = (grain size parameter) * (slope) + (intercept)

Reduced 500 kHz Images

	median			mean			std. dev.		
Grain Size Parameter	slope	intercept	r-square	slope	intercept	r-square	slope	intercept	r-square
d(15)	-6.420	62.129	0.536	-6.496	63.531	0.533	-1.280	15.734	0.258
d(40)	-5.929	68.470	0.507	-6.020	69.989	0.508	-1.261	17.156	0.278
d(50)	-5.810	70.864	0.494	-5.909	72.442	0.496	-1.274	17.757	0.288
d(70)	-6.125	78.342	0.515	-6.236	80.072	0.519	-1.373	19.503	0.314
d(85)	-6.185	85.040	0.536	-6.292	86.869	0.539	-1.369	20.928	0.319
d(90)	-6.113	87.815	0.529	-6.215	89.671	0.531	-1.343	21.486	0.309
% gravel	0.419	50.544	0.217	0.426	51.788	0.217	0.077	13.514	0.090
% sand	0.330	37.933	0.158	0.337	38.904	0.160	0.092	9.403	0.150
% mud	-0.524	71.683	0.522	-0.533	73.282	0.525	-0.121	18.106	0.336
mean	-6.475	73.679	0.551	-6.575	75.278	0.551	-1.382	18.277	0.304
std. dev.	-1.902	60.228	0.003	-2.210	62.140	0.004	-1.506	17.461	0.023

Reduced 100 kHz Images

	median			mean			std. dev.		
	slope	intercept	r-square	slope	intercept	r-square	slope	intercept	r-square
d(15)	-5.423	53.875	0.346	-5.338	56.637	0.332	-1.019	19.579	0.104
d(40)	-4.946	59.108	0.319	-4.879	61.810	0.308	-0.936	20.576	0.098
d(50)	-4.671	60.673	0.289	-4.608	63.357	0.278	-0.883	20.869	0.088
d(70)	-4.474	65.092	0.249	-4.411	67.708	0.239	-0.853	21.732	0.077
d(85)	-4.344	69.191	0.239	-4.280	71.732	0.230	-0.839	22.561	0.076
d(90)	-4.291	71.128	0.236	-4.224	73.619	0.226	-0.817	22.875	0.073
% gravel	0.500	41.955	0.279	0.482	45.057	0.257	0.065	17.760	0.041
% sand	0.028	47.674	0.001	0.042	49.714	0.002	0.047	16.053	0.025
% mud	-0.346	59.172	0.206	-0.345	61.975	0.202	-0.078	20.948	0.089
mean	-5.068	62.577	0.305	-4.994	65.218	0.293	-0.962	21.240	0.094
std. dev.	5.671	38.670	0.025	5.545	41.741	0.023	0.876	17.076	0.005

Composite Image

	component 1(red)			component 2 (green)			component 3 (blue)		
	slope	intercept	r-square	slope	intercept	r-square	slope	intercept	r-square
d(15)	-12.348	117.469	0.494	-0.302	86.289	0.001	1.555	43.825	0.148
d(40)	-11.377	129.612	0.466	-0.125	86.281	0.000	1.319	42.521	0.118
d(50)	-10.998	133.836	0.441	0.265	85.384	0.000	1.235	42.130	0.105
d(70)	-11.188	146.555	0.429	1.240	81.647	0.010	1.234	40.780	0.098
d(85)	-11.131	158.031	0.433	1.609	78.652	0.016	1.252	39.404	0.103
d(90)	-10.992	162.976	0.427	1.595	77.905	0.016	1.264	38.709	0.106
% gravel	0.932	93.355	0.267	0.311	81.491	0.054	-0.144	47.253	0.121
% sand	0.422	82.999	0.065	-0.497	114.257	0.163	0.007	44.728	0.000
% mud	-0.927	133.525	0.407	0.178	80.928	0.027	0.088	42.628	0.069
mean	-12.117	138.796	0.481	0.571	84.532	0.002	1.417	41.425	0.124
std. dev.	2.653	102.020	0.001	15.626	56.836	0.094	-1.575	48.089	0.010

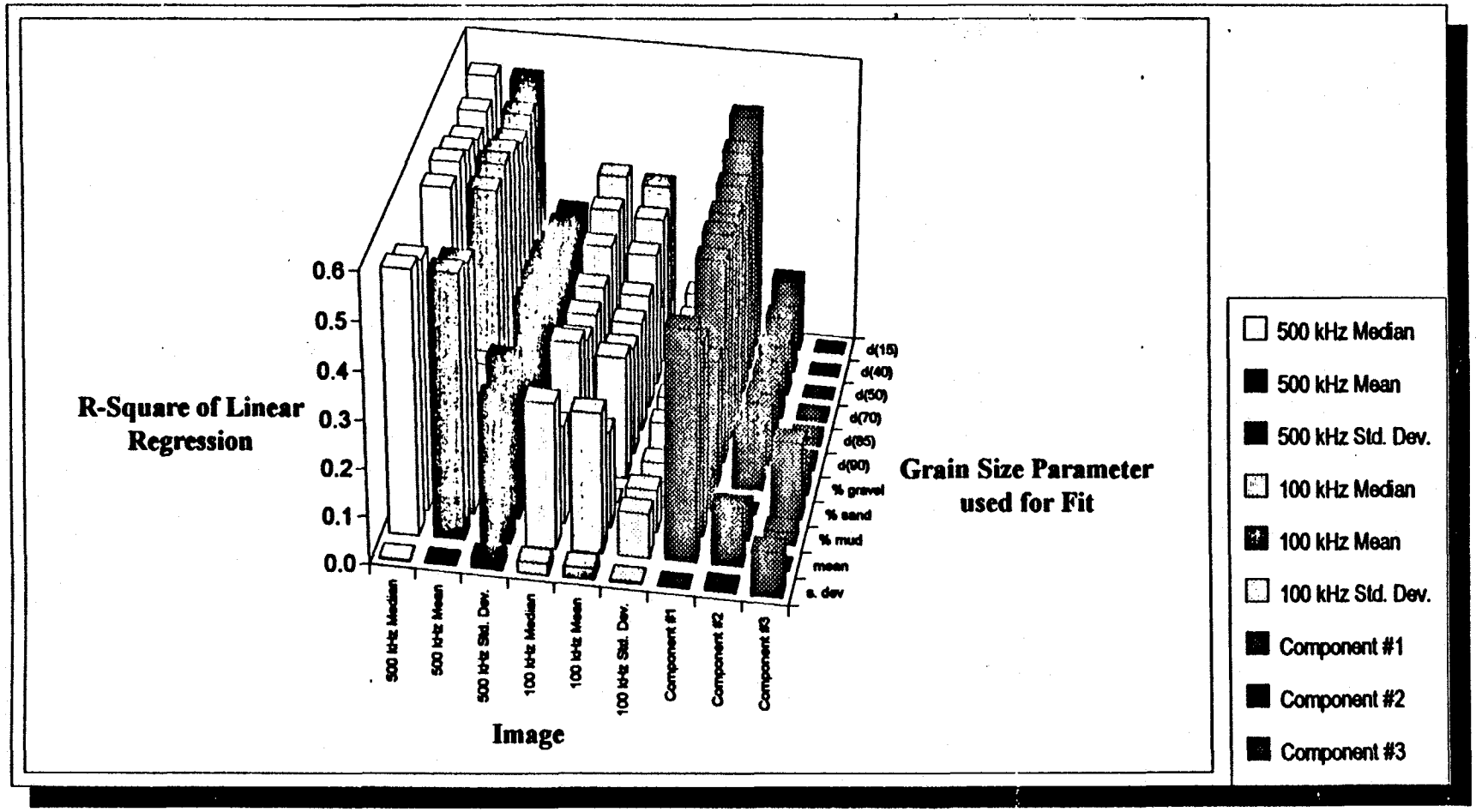

Figure 4. Three-dimensional plot of the correlation coefficient (r^2) of the linear regression of DN as a function of grain size parameter for different combinations of image and grain size parameter.

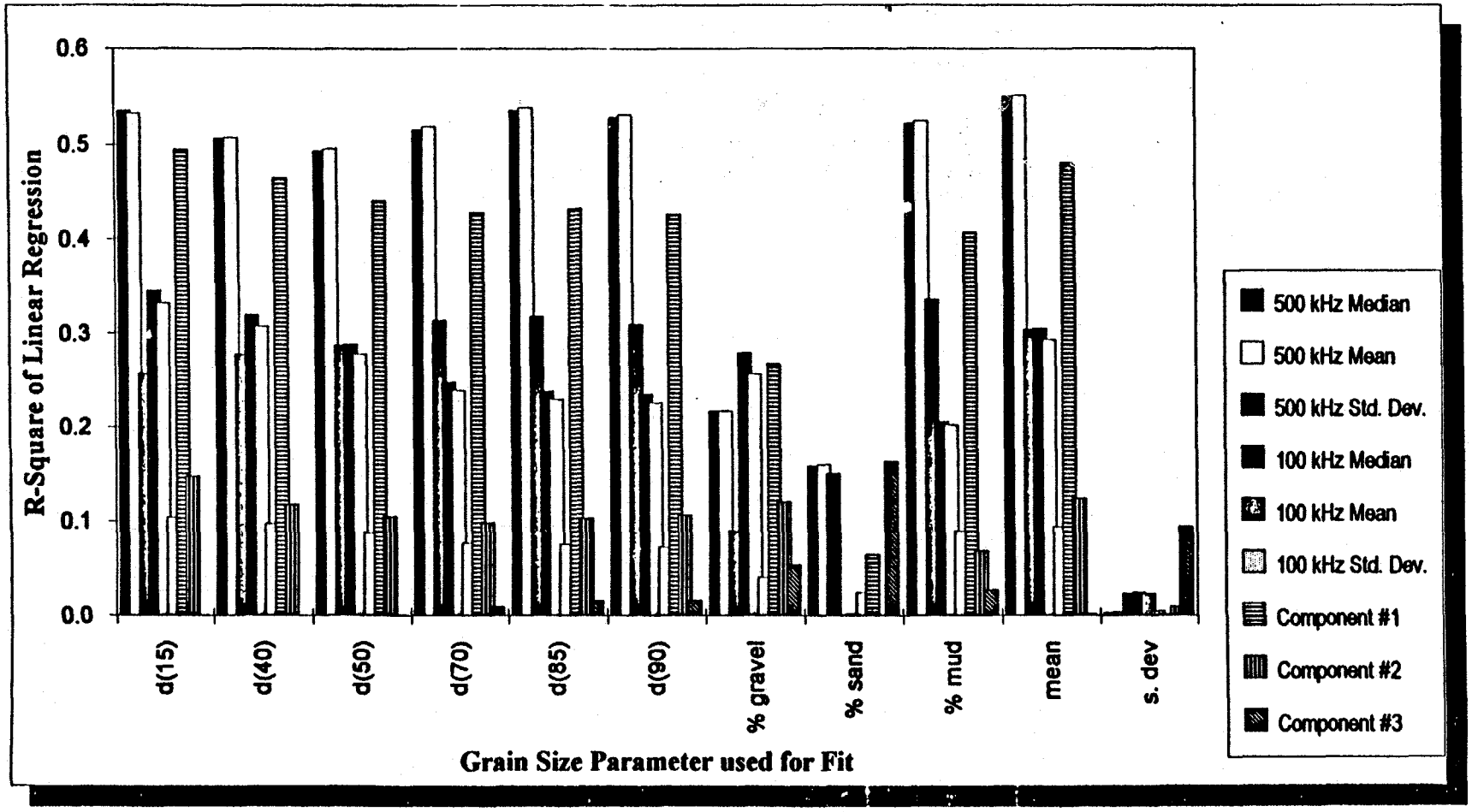

Figure 5. Two-dimensional plot of the correlation coefficient (r^2) of the linear regression of DN as a function of grain size parameter for different combinations of image and grain size parameter.

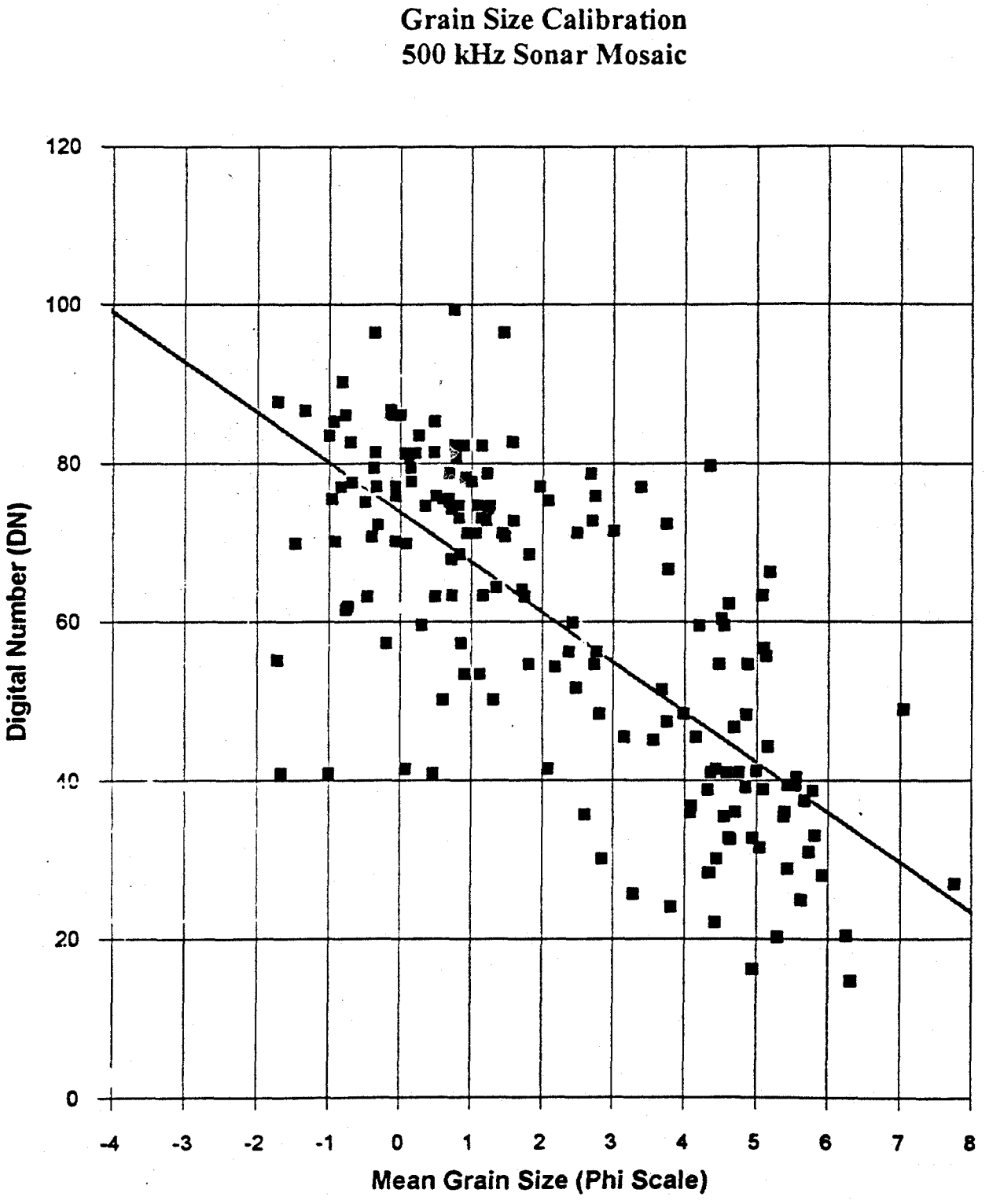

Figure 6. Scatter plot of 500 kHz median image DN vs. mean grain size for samples where the median image is uniform within 50 ft of the sample point. The least-square regression line (Table 4) is shown.

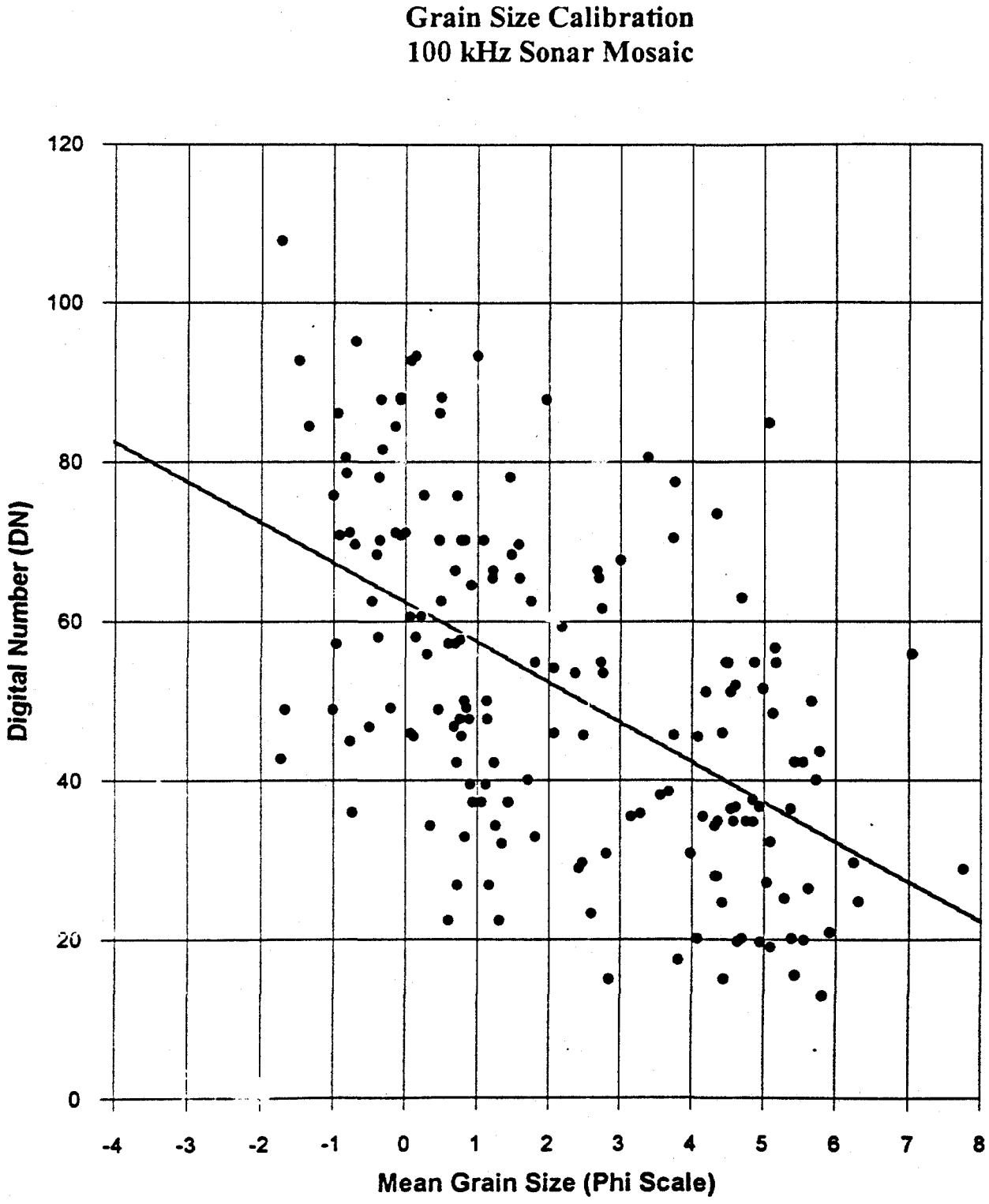

Figure 7. Scatter plot of 100 kHz median image DN vs. mean grain size for samples where the 500 kHz median image is uniform within 50 ft of the sample point. The least-square regression line (Table 4) is shown.

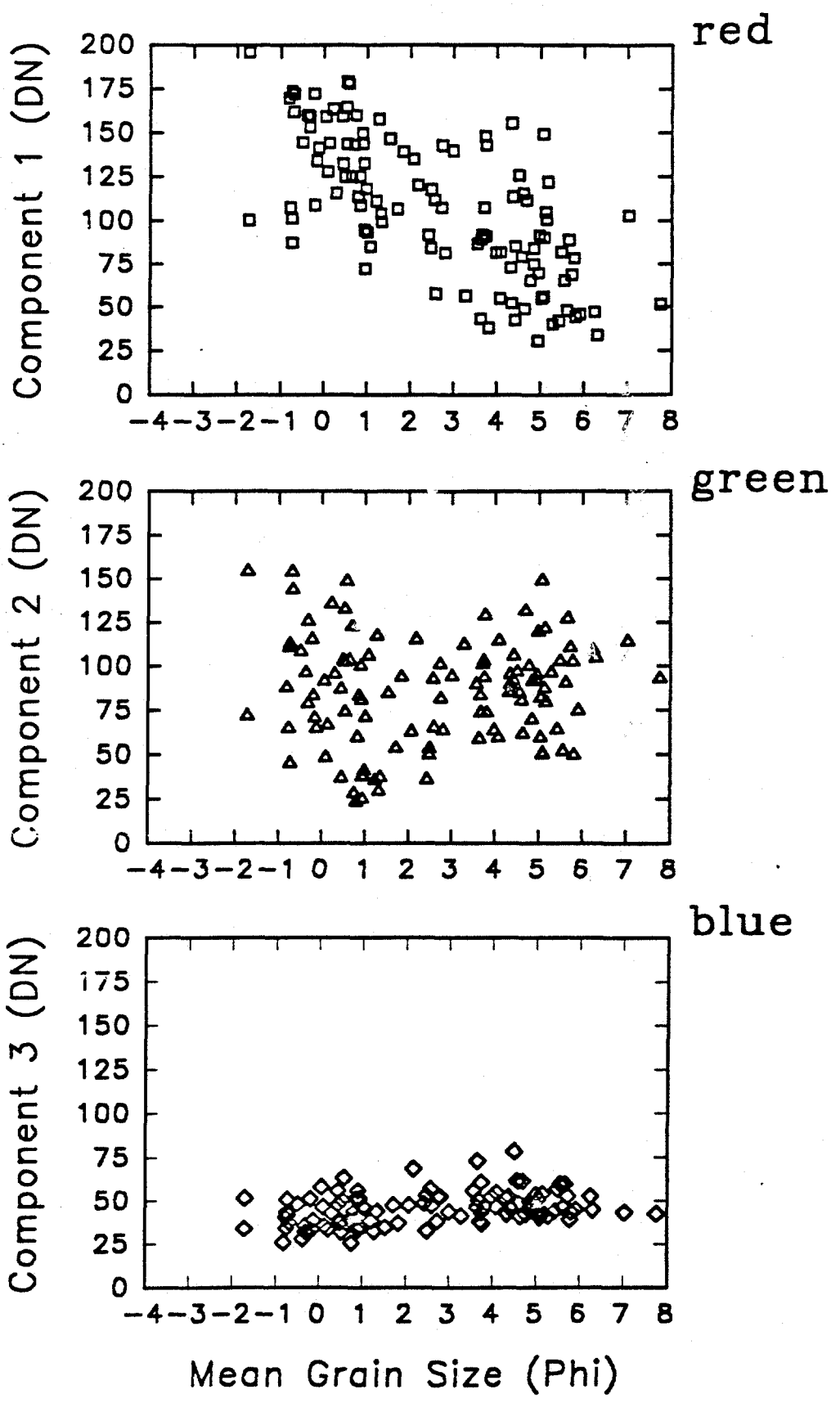

Figure 8. Scatter plots of the three major principal components that result from principal component analysis of the sonar records versus mean sediment size. These three components are used to construct false-color composite images.

100 kHz Images

The correlations between grain size parameters and the 100 kHz images are not as good as for the 500 kHz images (Table 4; Figures 4, 5 and 7); the correlation with mean size has $r^2 \sim 0.30$. The best correlation is for DN and d(15) ($r^2 \sim 0.35$), with the r^2 decreasing to 0.24 for d(90). There is a poor correlation with % gravel ($r^2 \sim 0.26$), a poorer correlation with % mud ($r^2 \sim 0.20$) and no correlation with % sand ($r^2 \sim 0.001$). The 100 kHz standard deviation image does not correlate with any grain size parameter ($r^2 \sim 0.04$ to 0.10).

Composite Images

Component 1 shows a moderately good correlation with mean size ($r^2 \sim 0.48$; Table 4; Figure 8). Moderately good correlations are also observed between component 1 and the percentiles d(15) through d(90) ($r^2 \sim 0.50$ to 0.42) and % mud ($r^2 \sim 0.41$). Component 1 is essentially the weighted sum of 500 kHz and 100 kHz median and mean images (Table 2), so the correlation between DN and grain size parameters should be similar. Since the 100 kHz correlations with grain size are poorer than 500 kHz correlations, the component 1 relationship with grain size is poorer than is the 500 kHz relationship. However, component 1 does appear to increase as grain size increases as suggested by the best correlation being with d(15) ($r^2 \sim 0.49$), a measure of the coarsest portion of the sediment. Component 1 is displayed in red on the composite images.

Component 2 statistically correlates best, but poorly, with the standard deviation of the grain size measurement (Table 4). Visually there appears to be a slight trend to higher DN values with larger mean size (Figure 8), but too many points fall off a line for a statistical correlation. Component 2 is primarily the weighted difference between the 100 kHz and 500 kHz images (Table 2). Examination of entire image set shows that component 2 is large in areas where bubbles in the water column limit the distance that the 100 kHz sonar can travel and in some shallow water areas where shading corrections can be significant. Thus while component 2 is sometimes higher where there is coarse sediment, other effects are also important. Component 2 is displayed in green on the composite images.

Component 3 shows a poor statistical correlation with mean size and with the six calculated percentiles ($r^2 \sim 0.10$ to 0.15; Table 4; Figure 8) although a slight decrease in component 3 with increasing grain size is apparent. However, component 3 is low (< 78) at all sites were sediment was recovered. Reference to the images suggests that component 3 is higher in areas of rock outcrop and in some areas of lineated, sometimes finer-grained sedimentary relief than in areas of uniform sediment cover. This suggests that component 3 may provide an indicator of rock outcrops and sediment roughness due to sediment transport. Component 3 is primarily the weighted sum of the 100 kHz and 500 kHz standard deviation images, and thus is an indicator of bed variability on the scale of 1 to 5 ft. Component 3 is displayed in blue on the composite images.

In summary, the 500 kHz median or mean image DN is best correlated with mean grain size. In particular, low DN values (less than about 60) generally correspond to finer grain sizes (mean size less than about 4 phi) while higher DN values generally correspond to coarser sediments (coarse sand, gravel). For the purpose of characterizing the sonar images, sediment type is described as "finer" (DN < 60), or as "coarse" or "coarser" (DN > 60) depending on a qualitative assessment of the DN value of the image. The terms "coarse" and "coarser" are both used where there is more than one region of distinctive high reflectivity in close proximity.

Possible reasons for the scatter in the observed correlation between 500 kHz image parameters and mean grain size include the following: (1) The effects of bottom slope on image value are not included, and the bottom is not horizontal at all sample locations. (2) The sonar correction technique results in a different "calibration" for different water depths or slant ranges, and this effect is not quantified. (3) There is variability in the sediments at a scale smaller than sonar can resolve, and not enough sediment samples have been recovered to adequately characterize the bottom at the scale of the sonar record. (4) The sediment grain-size results have not been uniformly described in terms of grain size parameters because two different size analysis techniques were used. (5) Standard grain size parameters may not be appropriate measures of bottom roughness to use for comparison to the sonar values. (6) Small bubbles of gas attached to sediment particles could affect sonar reflectivity. (7) Biota (e.g., shells, marsh grass) also affects sonar reflectivity in some areas. (8) In some areas a fine sediment veneer may overlie coarser sediments, and this veneer has not been properly sampled. (9) Shallow sediment layering may affect sonar returns. (10) There may have been changes in bottom sediment characteristics between the time of the sonar survey and the time of sampling. However, in spite of these and other possible problems with the correlation between grain size and reflectivity, a reasonable relationship does emerge that can be used with some confidence to interpret the sonar image in terms of likely sediment character.

The observed relationship between higher 500 kHz DN and coarser sediments may occur because of the relationship between the sediment size and wavelength of the sonar signal. The wavelength of 500 kHz sound in water is about 3 mm. Gravel-sized sediment is coarser than -2 phi (4 mm). The increase in 500 kHz reflectivity as grain size increases may be because a larger fraction of the sediment is nearly the same size as or larger than the wavelength of the 500 kHz sound for coarser sediments. This may result in more scattering of the sonar energy in coarser sediments (including scattering back towards the sonar fish), and thus the appearance of a more reflective sediment surface on the sonar record. For finer sediment, the surface roughness will be less (especially in the absence of extensive bioturbation). Thus more of the sonar energy will be specularly reflected off the bottom and away from the sonar fish, resulting in a weaker sonar return.

The wavelength of 100 kHz sound in water is about 15 mm. Sediment with a diameter of 16 mm has a phi size of -4. On the basis of the above discussion of 500 kHz sonar reflectivity, we expect the 100 kHz image to be more sensitive to these very coarse sediments. Our analysis does suggest that the 100 kHz sonar image appears to be better correlated with coarser sediment than with finer sediments. This is indicated by the increase in r^2 with coarser percentiles (i.e., there is a somewhat better correlation with d(15) representing the size of the coarsest 15 percent of the

sample than with d(90) representing the finest 10 percent of the sample). This is consistent with an increase in backscatter as the sediment size approaches the wavelength of the sound. However, no sediment samples with a mean size of -4 phi were recovered. The different response of 100 kHz and 500 kHz sound to sediment size suggests that component 2 of the composite image (based on the differences between the 100 kHz and 500 kHz images) may also be in part related to sediment grain size, with the difference increasing for coarser sediments. However, this effect appears to be less important than the primarily instrumental factors discussed above.

Subbottom Profiles

Profile Classification

A 7 kHz subbottom profiler was utilized throughout the survey to show layering within the river bottom, sediment characteristics, and sediment thickness. Sediment layering was recorded on the same chart paper used for bathymetric profiles, but offset so that the surface of the 7 kHz profile started about 2 to 3 feet below the bottom return of the echosounder (Figure 9). This was done to insure that layering in the upper few feet would be observed if present.

While subbottom layers are observed in some portions of the river, no subbottom layers were recognized in other large sections of the river. The general lack of subbottom layers appears to be due to several factors. Much of the river bed is coarse sand, gravels and weathered rocks. Sound is easily scattered and rapidly attenuated in these units thus little sound energy penetrates into the bottom. In some areas of the river there are layers of sawn wood fragments within the upper one to two feet. These layers may effectively stop sound penetration due to the generally coarse size of the wood fragments, the possible irregular nature of the layer, and the possibility of gas included in the layer. Gas may also be present where there are rapidly deposited fine-grained sediments. The presence of any gas in the sediments dramatically increases sound attenuation. Also, in many shallow-water areas (less than about 4 feet) no bottom was observed on the 7 kHz profiler. This appears to be because of the adjustment of the profiler settings to optimize the record in the center of the river.

The subbottom profiles were analyzed in a systematic fashion to provide a uniform data base for use in characterizing the river-bed sediment. The subbottom records were analyzed at every navigation event (about 10 seconds apart in time, or about 20 to 50 ft, 6 to 15 m, apart in distance) and classified into one of eight categories. These data were entered into a computer file and a position was assigned to all places where the subbottom records were classified (Appendix B). The eight categories are as follows:

Category 1: A distinctive sediment layering pattern that usually consists of up to about 30 ft (9 m) of parallel-laminated sediment (Figure 9). Where cored, these sediments are varved gray silts and clays that were apparently deposited during glacial times in Glacial Lake Albany that covered much of the present-day Hudson River at that time (Cadwell and Dineen, 1987). This pattern can start and stop abruptly along track suggesting that some additional factor, for example, attenuation or scattering of sound by coarse sediments on the river bed, prevents sound from reaching the buried varved sediments.

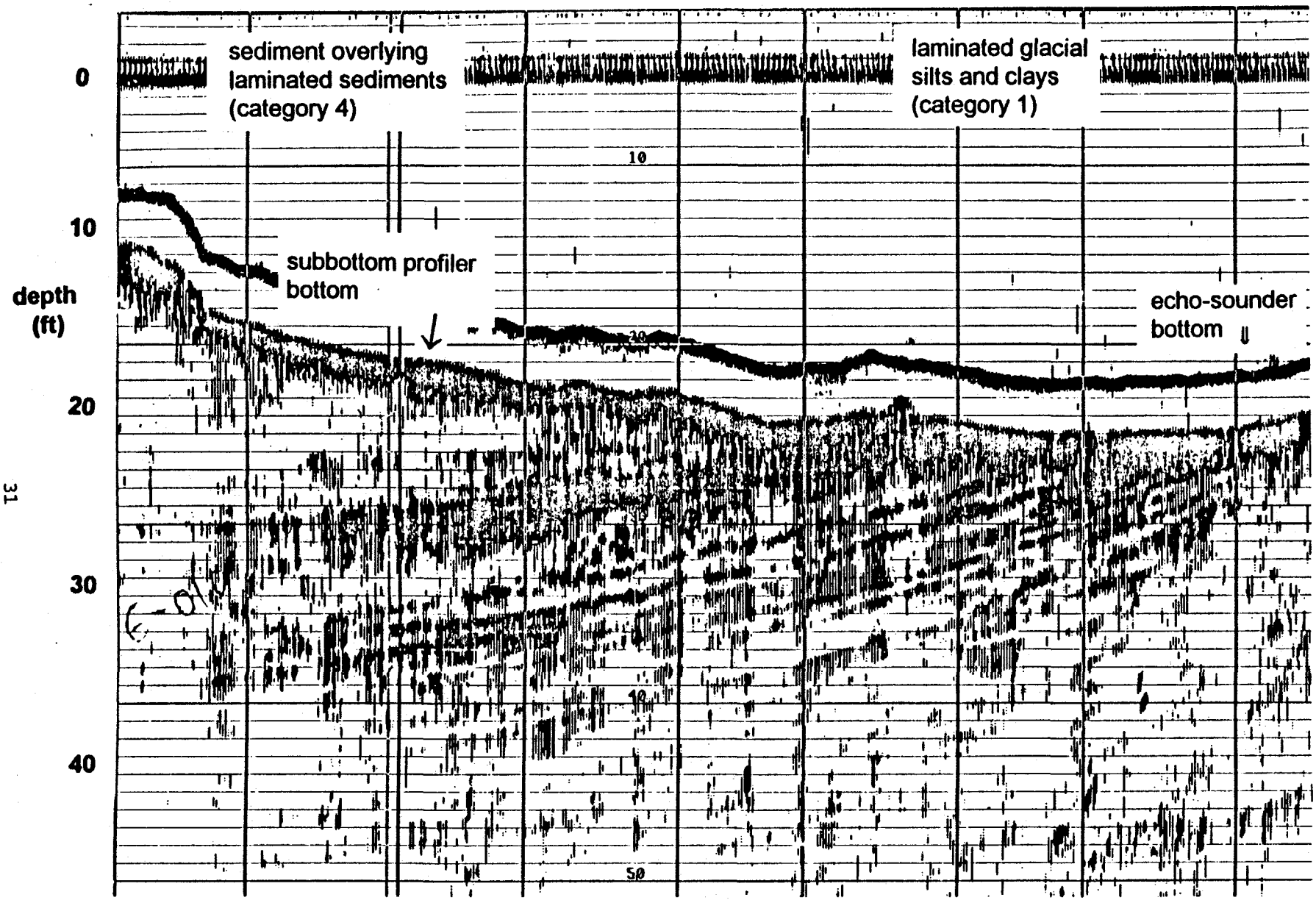

Figure 9. Subbottom profile at 7 kHz showing layered sediments (subbottom category 1) cropping out on the right-hand side of the profile. These sediments correspond to varved glacial clays. On the left-hand side of the profile, more-recent sediments have deposited on top of the varved glacial clays (subbottom category 4). Note that the surface of the subbottom record is offset from the 208 kHz echo-sounder river bottom. Profile from about river mile 190.0.

Category 2: Laminated sediments similar to category 1, but the sediments appear to overlay an older unit because a distinct, single reflector is observed beneath the laminated sediments (Figure 10). This deeper reflector could be older sediments, bedrock, or poorly resolved varved sediments.

Category 3: One clearly defined subbottom layer is observed, but there is no indication of deeper layering (Figure 11). Often these layers have a limited lateral extent. The depth to the reflector (in feet) was measured using water velocity for the sediments. These layers mostly represent deposition patterns within the Hudson River, although it is not always possible to determine whether these layers pre-date or post-date the formation of the Champlain Canal. In some limited areas this layering may actually be poorly displayed varved sediments.

Category 4: A clearly defined surface layer is observed (as in category 3), but this layer lies on laminated sediments (as in category 1; Figure 9). The thickness of the overlying layer was measured for this echo type.

Category 5: A clearly defined subbottom layer (as in category 3), but additional layers that do not resemble the laminated sediments were observed at depth (Figure 12). Only the thickness of the uppermost layer is measured.

Category 6: No clear subbottom echo was observed (Figure 13). This is the most common echo type.

Category 7: The record is too poor to interpret, in part because the sediment surface is not present on the subbottom record. This type of subbottom record occurs during operations in extremely shallow water.

Category 8: A single "subbottom layer" is observed, but this layer may be an artifact of profiling next to a steep channel wall. Thus the "subbottom layer" may actually be an echo from the river bed off to the side of the track and not a layer in the sediments. A depth to the "subbottom" echo was measured.

This subbottom data is plotted in color on seven maps, each covering an area 10,000 feet south-to-north and 8,000 feet east-to-west (Plates 1 to 7; Appendix C). Subbottom categories 1, 2 and 4 are plotted with similar colors because they both represent laminated sediments at or very near the surface. The size of the symbol for categories 3, 4 and 5 is related to the thickness of the uppermost layer. Categories 6 and 7 are plotted in large symbols before any other echo types are plotted, and categories 1, 2 and 8 are plotted with smaller symbols of constant size.

Distribution of Subbottom Echo Types

In describing the distribution of sonar images, subbottom echoes and sediments along the river, reference will be made to Northing and Easting for position in preference to river mile. This is because the survey data are directly referenced to Northing and Easting. For reference, Figure

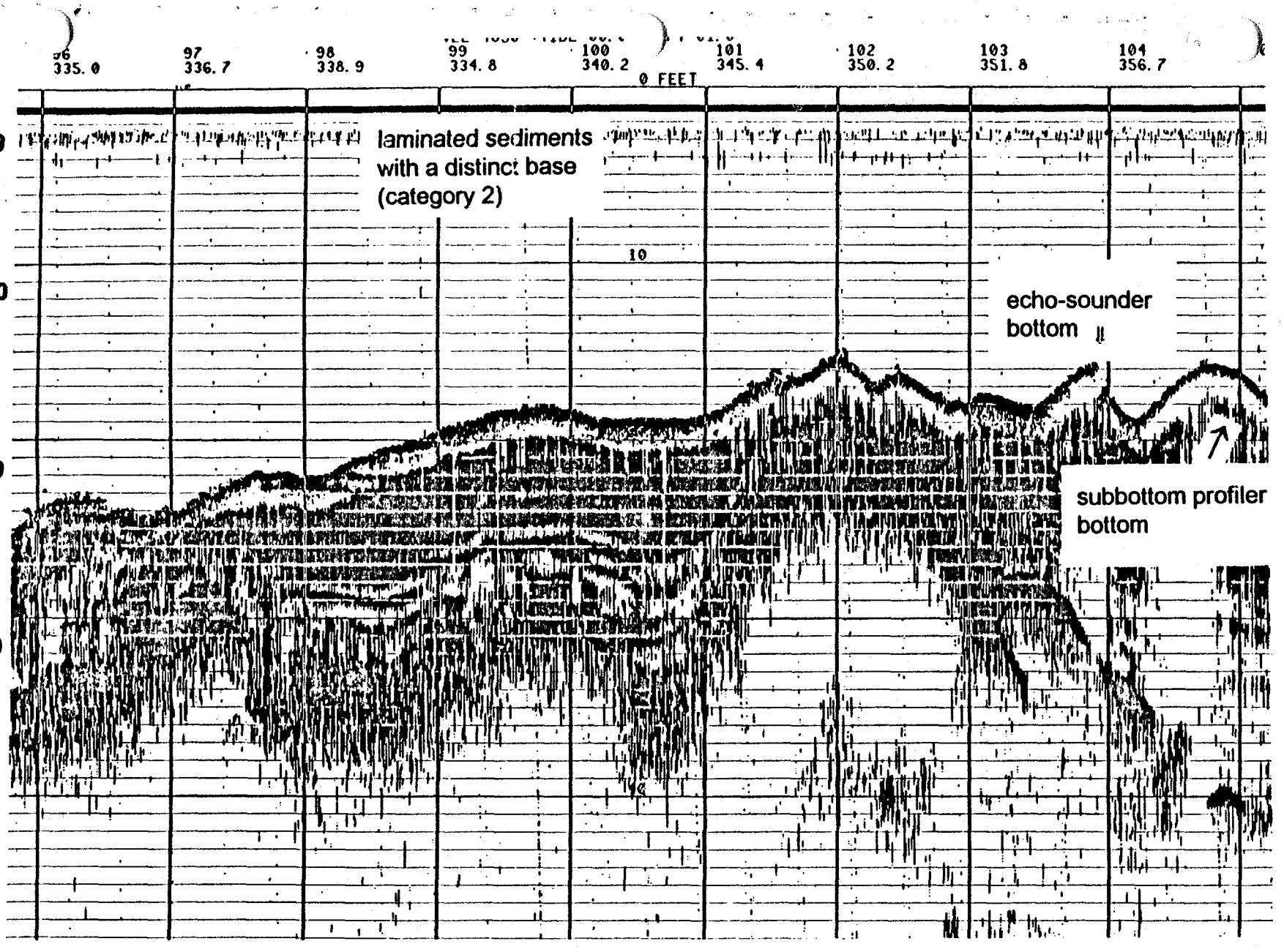

Figure 10. Subbottom profile at 7 kHz showing a distinctive sediment layering pattern such as in Figure 9, but overlying a distinct deeper layer which in this case appears to be bedrock (subbottom category 2). Profile from about river mile 186.9.

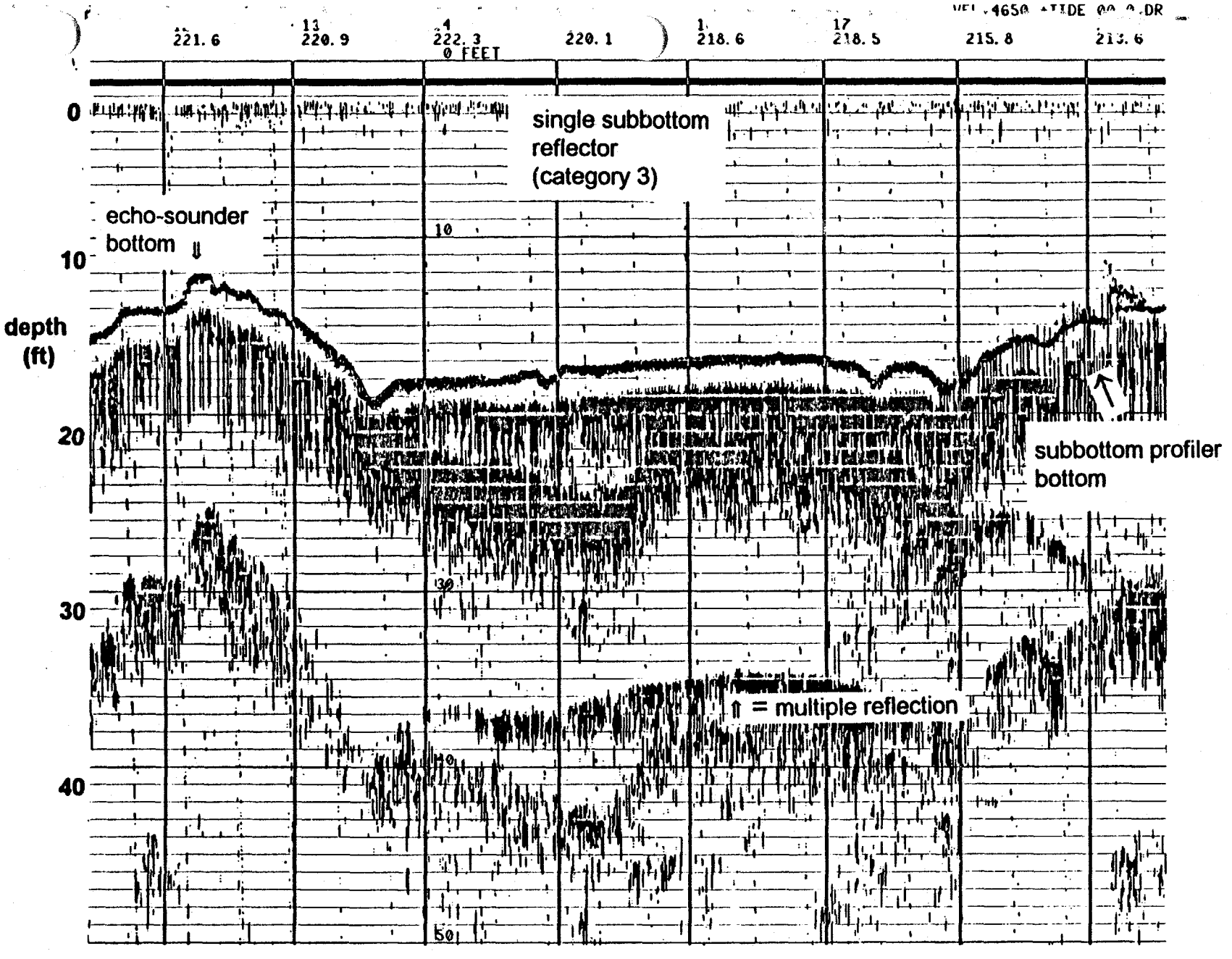

Figure 11. Subbottom profile at 7 kHz showing a single sediment layer in the center and left of the profile (subbottom category 3). The apparent deeper replication of the surface layering is a multiple reflection caused by sound bouncing of the sediment surface, the water surface, and the sediment surface again before being recorded. Profile from about river mile 187.8.

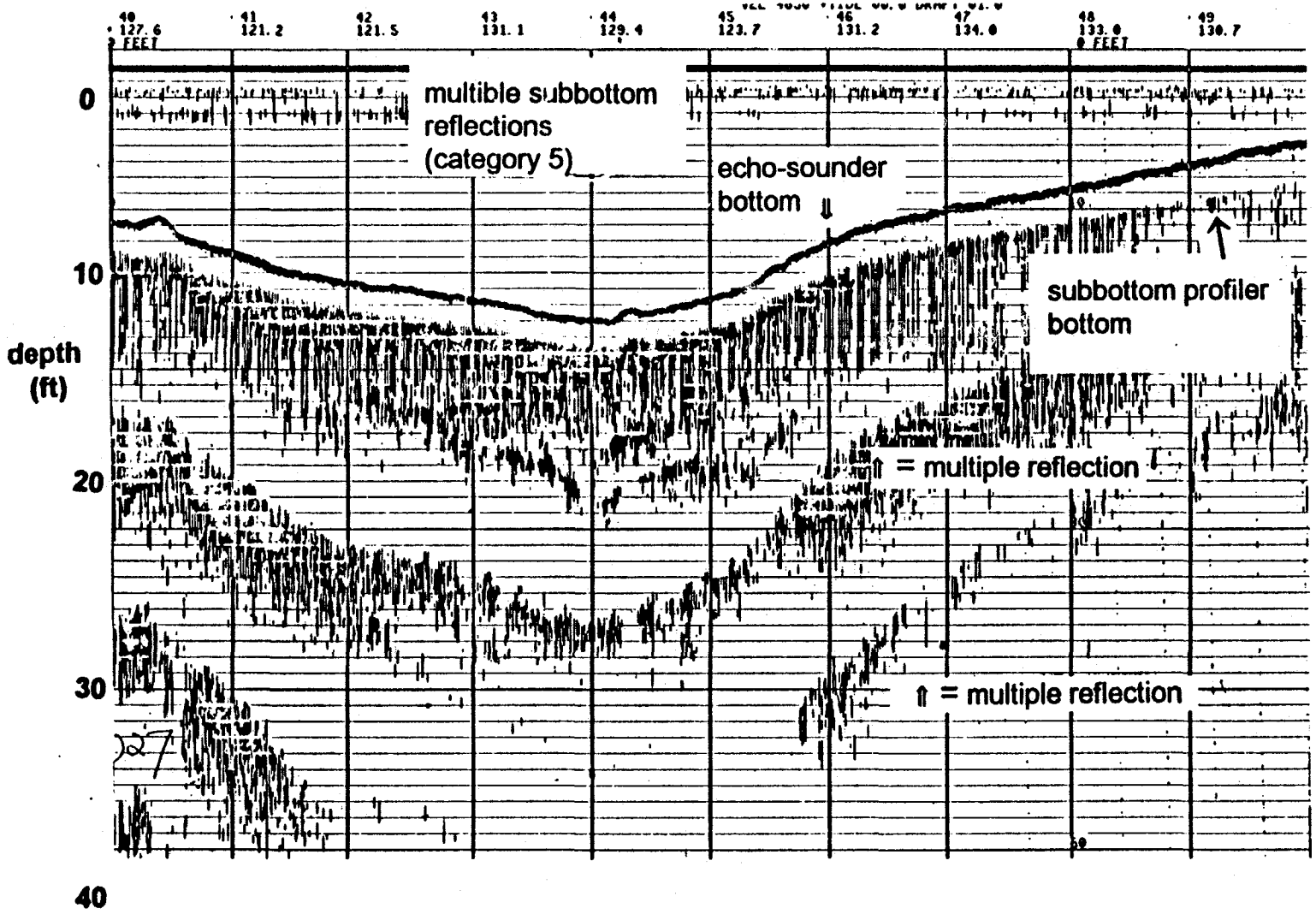

Figure 12. Subbottom profile at 7 kHz showing several subbottom layers (subbottom category 5) in the center of the profile. Two multiple reflections are observed here. Profile from about river mile 187.1

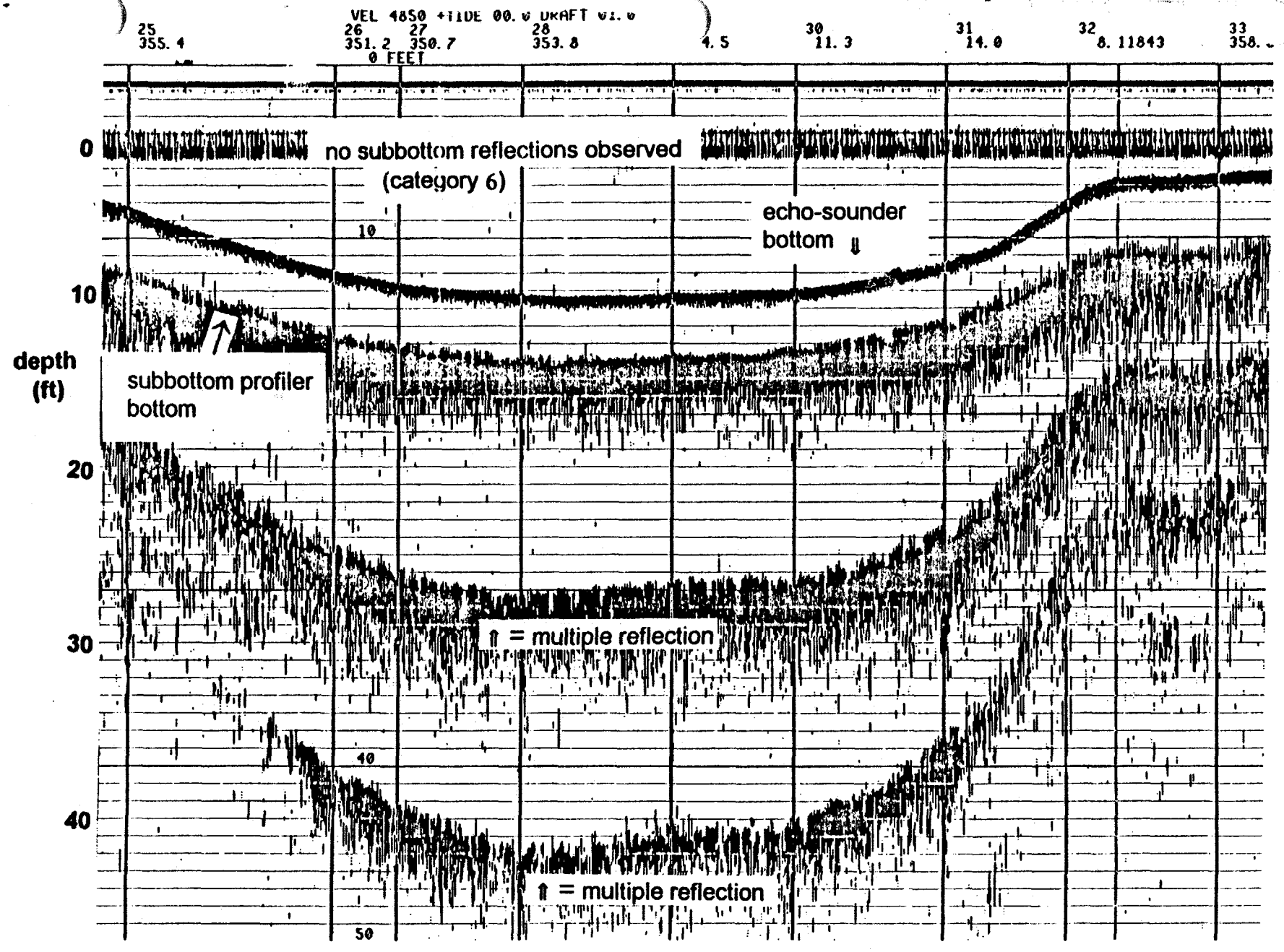

Figure 13. Subbottom profile at 7 kHz showing no subbottom layering (subbottom category 6). Several well-developed multiples are recorded. Profile from about river mile 190.2.

3 shows river mile for the portion of the river surveyed. These river miles appear similar to the river miles used by Zimmie (1985). Northing and Easting provide the definitive reference of location, river miles are given for reference only.

Laminated Sediments

Laminated profiles (categories 1, 2 and 4) are found in several areas of the river; often in the deepest portions of the river. Varved gray silts and clays have been recovered in most areas where these subbottom types are observed, suggesting that the laminated sediments on the subbottom profiles are indeed varved glacial silts and clays.

The northernmost occurrence of laminated sediments is on both sides of the southern end of Rogers Island and about 2000 feet down river near the channel axis to 1,185,800 (about river mile 193.5; Plate 6). Sediments in this area were sampled by Gahagan and Bryant Associates (1982), and they report sticky gray clay at many locations. Minor occurrences of laminated sediment are also noted near 1,184,600 and near 1,182,500 (about river miles 193.1 and 192.7). A second major zone of laminated sediments occurs near a Northing of 1,178,000 to 1,176,500 (about river mile 191.7 to 191.3) with occurrences of laminated sediments also near 1,178,600 (about river mile 191.4) upstream from this site and to 1,174,400 (about river mile 190.9) downstream of this site (Plate 5). Gahagan and Bryant Associates (1982) report sticky gray clay from many parts of this area, often overlain by a veneer of more recently deposited sediment. Figure 14 shows a subbottom profile from the eastern side of the river near 1,176,300 (about river mile 191.2). The left side of this profile shows category 1 laminated sediments that terminate abruptly, probably due to the presence of coarse sediments overlying the gray silts and clays. The mounds on the right side of the profile appear to be dredge deposits as a horizontal reflector passes beneath the mounds.

A third major zone of laminated sediments occurs on the western side of the river from Northing 1,170,300 to 1,169,400 (about river mile 190; Plate 4). Subbottom profiles that these fine-grained glacial sediments have been deformed (Figure 15), perhaps by the combined effect of sediment loading on the river flanks and scour in the center of the river (see also Figure 9). Sediment cores from this area of the river show varved gray clays. The fourth major zone where laminated sediments are observed is at the outside (western) bank of the river at a bend from Northing 1,157,200 to 1,154,500 (about river mile 187.3 to 186.8; Plate 3). Side-scan sonar records show that the layered sediments crop out on the steep slope at the margin of the river, and that they have slumped at some places. Varved gray silts and clays are also recovered in this area. The fifth zone of laminated sediments is about 2000 ft downstream of the dam at Millers Falls at Northing 1,150,600 (about river mile 185.7; Plate 2). Gray silts and clays were recovered in this area.

The Surficial Geological Map of New York State (Cadwell and Dineen, 1987) describes these varved silts and clays as lacustrine silts and clays. They note (1) that the sediments are generally calcareous and (2) that there is potential land instability in these regions. Gray silts and clays may be presently exposed in the study area because of dredging operations or river erosion. These clays, while exposed at the sediment surface, are susceptible to erosion and, depending on

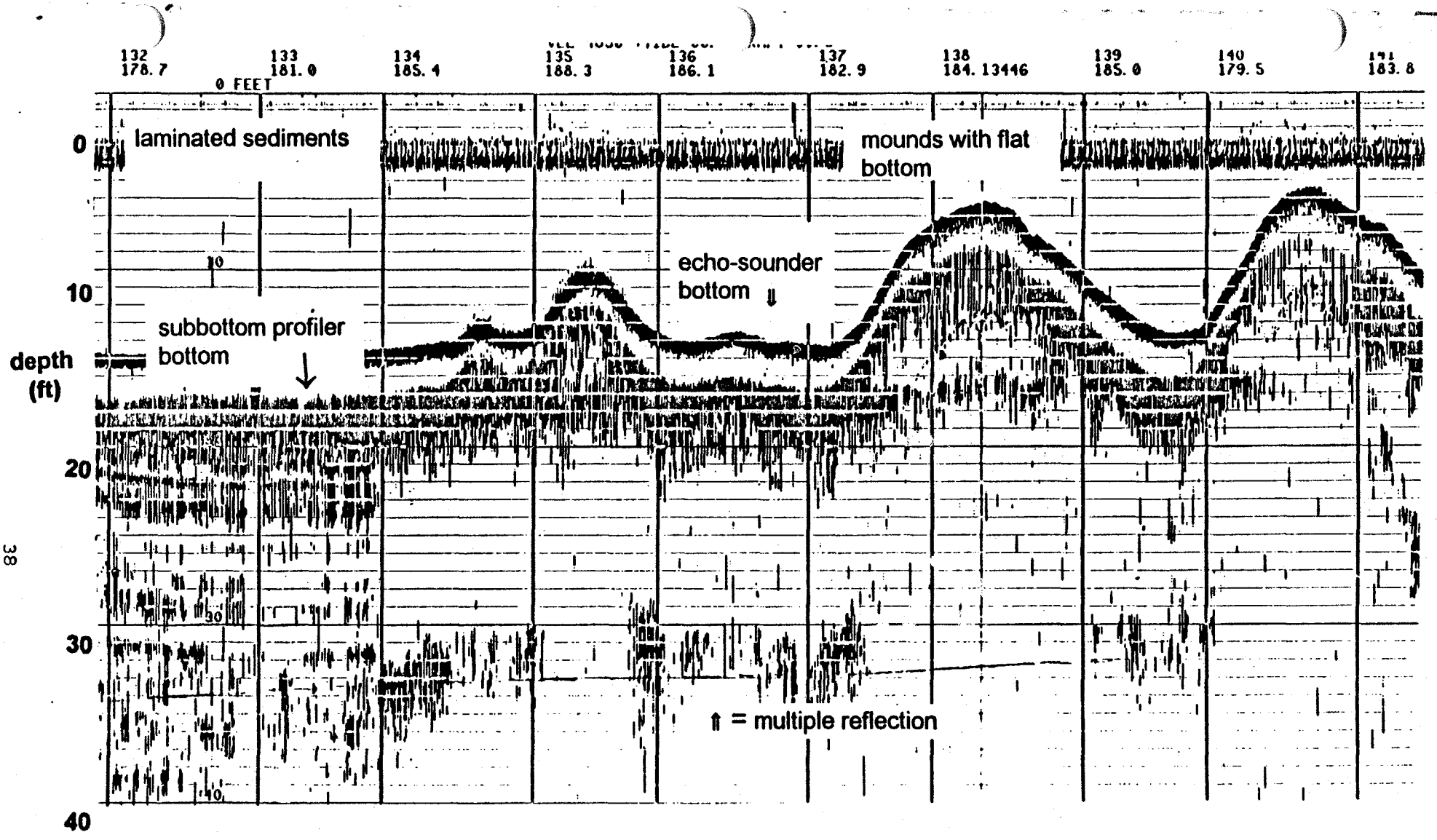

Figure 14. Subbottom profile showing laminated glacial clays (left; note abrupt termination along track) and mounds of dredge spoils (right) with underlying flat horizons. Profile from about river mile 191.2.

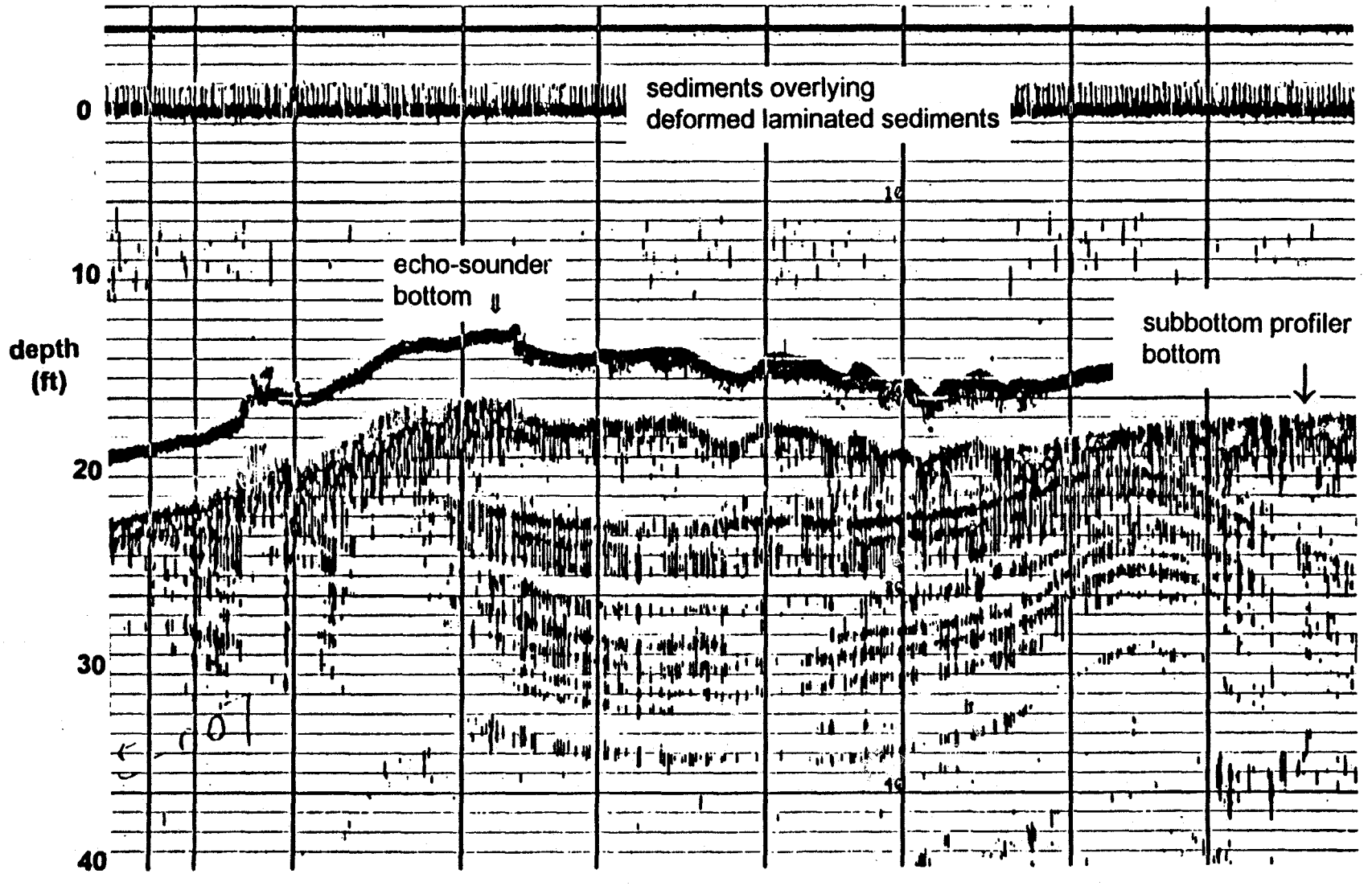

Figure 15. Subbottom profile showing deformed laminated glacial clays overlain by more recent sediments. These layers were originally horizontal, and their present curvature suggests deformation, perhaps related to differential loading related to sediment deposition at the river edge and sediment erosion or dredging in the center of the river. Profile from about river mile 190.0.

river chemistry, the calcareous component may dissolve. The apparent ability of the river to erode into glacial clays once the overlying sediments have been removed and the apparent deformation of the glacial clays associated with non-uniform loading by river sedimentation suggests that there may be adverse effects, such as increased bank slumping or increased suspended-sediment levels, if glacial silts and clays are exposed in large sections of the river. Many of the rivers that drain into the Hudson River in the study area also drain similar lacustrine silts and clays (Cadwell and Dineen, 1987).

Single Subbottom Layers

Discrete subbottoms (categories 3, 4 and 5) are observed in many portions of the river, but few systematic trends are observed. For the most part, single subbottom layers can only be followed for relatively short distances. In some areas these layers mark the boundary between sediment and rocks, with sediment filling depressions within rock outcrops (Figure 11). Such layers are generally less than about 5 feet deep and of limited horizontal extent. In other areas, discrete subbottoms mark areas where more recent sediments have accumulated over deeper strata such as the laminated glacial silts and clays (Figure 9). However, the underlying layers cannot be followed far underneath the more recent sediments. Discrete subbottoms also mark the bottom of some mounds of dumped dredged sediment (Figure 14) or sediment that has accumulated near such piles. The most extensive regions of relatively deep discrete subbottom horizons occur between the Thompson Island Dam and the Fort Miller Dam (Plate 3). Subbottom layers at depths of 10 to 25 feet are observed on both sides of the small island here (Galusha Island). Subbottom layers may be relatively common in this portion of the river because no dredging has occurred here.

Sediment Samples

Sediment samples were collected at a number of locations in order to relate the sonar image characteristics to specific sediment properties. In general, these samples were taken on transects across the river, although specific sonar targets were sampled on several occasions. Sediment grain sizes were determined for surficial sediments and for some deeper sediment samples using a Malvern Laser Particle Analyzer and standard ASTM procedures. The results of these grain size analyses have been provided to TAMS Consultants, Inc. by the contractors who did the analyses; however, identical measures of grain size were not reported by the two laboratories.

The ASTM grain size results provided include % gravel, % sand, % silt, % clay, and the percentile sizes d(15), d(40), d(50), d(70), d(85) and d(90). The percentile size d(XX) is the size which XX% is coarser than*, thus 15% of the sample is coarser that the size d(15). The laser size results provided include mean size, sorting, skewness, and the percentage of the sample in each 1/2 phi interval from -2 phi to > 10 phi. Mean size is the statistical mean of the sample, sorting is

* The ASTM results are actually reported as percentile sizes which XX% is finer than. We converted these to sizes which XX% is coarser than to be consistent with the terminology of Folk (1974). Thus the reported size d(60) is referred to here as d(40).

the standard deviation, and skewness is the third moment of the distribution. For this report we use the term standard deviation in preference to sorting.

These size data were converted to a consistent basis through the following steps. The laser interval size data was used to calculate % gravel, % sand, % silt, % clay, and the six percentiles reported in the ASTM results (d(15), d(40), d(50), d(70), d(85) and d(90)). For the ASTM and laser results, % silt and % clay were combined to give % mud because % clay is usually quite small. The percentiles were used to calculate similar grain size parameters for the two data sets following the graphical approach described by Folk (1974). Folk (1974) suggests that the plot of the cumulative grain-size distribution curve can be used to determine a "graphic mean" and "graphic standard deviation" as follows:

$$\text{graphic mean (Folk)} = \frac{d(16) + d(50) + d(84)}{3}$$

$$\text{graphic standard deviation (Folk)} = \frac{d(84) - d(16)}{2}$$

Dyer (1986) discusses the use of the graphic approach and notes that the quantities calculated by this method closely approximate the values that would be determined by calculating the moments of the distribution. The values of d(15) and d(85) were used instead of d(16) and d(84) because those parameters were not reported for the ASTM analysis. However, the effect of changing by one percentile should not be significant especially since the same percentiles are used throughout. Comparison between the calculated results and those provided for the ASTM analyses showed them to be quite similar. The relationships used in this study were thus:

$$\text{graphic mean (this study)} = \frac{d(15) + d(50) + d(85)}{3}$$

$$\text{graphic standard deviation (this study)} = \frac{d(85) - d(15)}{2}$$

These calculations provide a consistent set of grain size parameters including mean size, standard deviation, % gravel, % sand, % mud, and the percentiles d(15), d(40), d(50), d(70), d(85) and d(90). All sediment sizes are reported in phi units. In general, sediment samples analyzed by the laser technique appear finer than those analyzed by the ASTM technique. This may be due to the relatively small sample size provided for the laser analysis and the generally coarse nature of much of the sediment as well as to differences in the analysis technique, although sediments coarser than 0.064 mm (4 phi) were determined by sieve in both methods. For the purposes of this study, duplicate analyses were combined without any corrections to produce one surficial sediment size analysis per core or grab.

Grab samples were described and sampled for grain size. Duplicate sediment cores were collected when possible. One core was extruded on site, described and sampled for grain size. The second core was retained unopened and X-rayed to determine sediment structures. Unopened cores were X-rayed at the Lamont-Doherty Earth Observatory.

As noted previously, the strength of the 500 kHz sonar signal appears to be related to the mean grain size of the surficial sediments because the DN of the sonar image is higher where the sediment grain size is coarser (smaller phi values). In addition to their use for interpretation of the sonar image, these sediment samples also provide information on surficial sediment characteristics and on sediment layering.

Surface Sediment Composition

As noted by previous workers, surficial sediments vary considerably within this portion of the Hudson River. The coarse fraction of the sediments can be either fissile shale of gravel size, introduced from rock outcrops exposed on the bottom of the river, or rounded, light-colored pieces presumably derived from upriver sources. The fissile shale is especially common in the vicinity of rock outcrops. This coarse sediment mixes with finer sediments (especially sands from runoff upriver and from local sources) and wood chips to create the poorly sorted sediments observed. Also present in some portions is a white ash disposed of in the river.

Chunks of sawn wood and finer-sized wood chips from the sawing of logs are often found both at the surface and buried in river-bed sediments. Chunks of sawn wood, up to 15 to 20 cm in dimensions, are observed at the surface in the deeper water portions of the channel in many of the areas sampled during this project. This wood is entering the system either through (1) introduction north of Bakers Falls during high-flow events, (2) continued erosion of the remnant deposits, or (3) excavation of previously deposited sediments in portions of the river downstream from Fort Edward. Sonar data suggest that large wood debris is present in the river north of Bakers Falls. The remnant deposits have mostly been capped; however, remnant deposit 1 and the northern end of remnant deposit 2 are not capped and the northern end of remnant deposit 2 appears to be eroding. Sonar data suggest sawn lumber on the river bed immediately down river from the rapids at Fort Edward. These observations are consistent with an upriver source for wood today.

It is more difficult to determine sites that are serving as sources for chunks of sawn wood south of Rogers Island. While wood chunks are observed at the sediment surface in many samples, chips from sawing wood were identified at the surface in only a few locations. This may be because of lateral variability, or because the sediment samples which showed sawn wood chips were recovered downstream of areas where a wood chip layer is being eroded. Two instances of chips from sawing wood are (1) at the southern end of the remnant area (Sample CG-103) on the down-river side of a mound on the river bed, and (2) near Millers Falls (Sample CG-069) south of Galusha Island about river mile 186.9. Sources upstream of Bakers Falls, the uncapped portions of the remnant deposits, and the river-bed mounds (possibly remnant material) could provide the small chips at CG-103. Upstream erosion appears to be a likely source for the small chips at CG-069.

Buried wood chip/wood chunk layers were identified from many regions of the Hudson River sampled, especially from near the flanks of the river. These layers, identified from visual descriptions and from X-radiographs, are typically at subbottom depths of 10 to 30 cm, and are thought to date from river flooding and remnant deposit erosion in 1974 and 1976. In some areas, two woody layers appear to be present while in others there is only one. Occasionally more than two layers appear to be present.

Sediment Structures

X-radiographs of sediment cores provides valuable information on the nature of buried sediments, including whether or not the character of sediment changes with time, especially the character of deposition associated with historical flooding such as in 1974 and 1976. Sample location and a brief description are given in Table 5, and the X-rays are provided in Appendix D. In general, the number of X-rays that pass through a sediment core to expose the X-ray film is dependent on the bulk density of the material. Sediments with a high bulk density (sands, consolidated silty clays) are better attenuators of X-rays than are sediments of low bulk density (recently deposited muds and fine-grained sands). This can be used to provide a qualitative assessment of the downcore variations in sediment character with lighter X-radiographs suggesting denser material (coarser grain size or compacted gray clay) and darker X-radiographs suggesting less-dense material (finer-grained sediment and wood). X-radiographs also reveal bedding within the cores. Thus intervals of fine layering can be identified, as well as intervals that appear to be characterized by low-density woody material. Down-core changes in sediment type can be inferred from the X-radiographs in several areas. In particular, the surficial 3 to 7 cm of many cores downstream from Lock 8 appear to be coarser than the immediately underlying sediment. Also, in many instances, sediments associated with the woody layer appear to be coarser than those at the surface now. In some cores with low sedimentation rates, sandy layers that pre-date the wood-chip layer are also observed. Future detailed description and analysis of these and other sediments may provide additional information on present-day sedimentary processes, the distribution patterns of woody and other materials associated with flooding in 1974 and 1976, and how pre-1973 flow events affected sediment distribution.

Description of Sonar Images

The 500 kHz side-scan sonar mosaics demonstrate that sedimentation patterns in the river change significantly along the length of the river in the section studied. These images also demonstrate the importance of man's activity as well as natural sedimentation processes in controlling sediment distribution. The side-scan sonar mosaics were interpreted to provide the best estimate of bottom sediment character and to show the location of some of the major man-made features in the river. Where possible, results of subbottom profiling and confirmatory sampling are used to describe sedimentation processes. Interpretive maps made at a scale of 1 inch = 100 ft for map areas 1 to 36 and 40 are included in Appendix E. The following narration provides an overview of sediment distribution patterns and is designed to supplement the sonar mosaics and interpretive maps.

Table 5

nfirmatory Sampling				Description of X-Radiographs
dson River / TAMS				
(X-ray cores only)				
				Comments
Easting	Northing	Core ID	Core Length	
701310	1170315	CC-001-X	36	dk to 22 cm, dk chunk at 21 cm, lt to 34 cm
701261	1170250	CC-002-X	41	lt to 5 cm, dk to 22 cm, lt to 27 cm
701126	1170277	CC-003-X	51	lt to 8 cm, dk to 21 cm, lt to 33 cm, dk to 34 cm, lt to bottom
701016	1170270	CC-004-X	30	lt to 32 cm, dk chunk at 31 cm
700923	1170261	CC-005-X	15	lt to 9 cm
700836	1170223	CC-006-X	46	lt to 50 cm
700727	1170160	CC-010-X	10	lt to 7 cm
700652	1170133	CC-011-X	40	lt to 40 cm
700910	1169812	CC-012-X	15	lt to 12 cm
701018	1169849	CC-014-X	30	lt to 6 cm, dk to 15 cm, lt to 16 cm
701084	1169858	CC-015-X	10	dk to 10 cm
700939	1169699	CC-016-X	15	lt to 12 cm, dk chunk at 12-14 cm
701021	1171145	CC-017-X	30	dk to 11 cm, lt to 13 cm, dk to 18 cm, lt to 31 cm, dk chunk 26-28 cm
700907	1171071	CC-018-X	15	mod lt to 5 cm, lt to 9 cm, dk to 16 cm
700759	1171025	CC-019-X	15	lt to 7 cm, dk to 11 cm, lt to 15 cm
700375	1170935	CC-024-X	10	lt to 9 cm
700228	1171469	CC-025-X	13	lt to 22 cm, dk chunk at 17-19 cm
0235	1171410	CC-026-X	30	mod. lt to 20 cm with 2-5 cm lams, lt to 31 cm
699532	1166417	CC-032-X	10	lt to 2 cm
699642	1166380	CC-033-X	8	lt to 8 cm, lt chunks at 2 cm and 5 cm
697029	1178979	CC-034-X	6	lt to 7 cm
696927	1178955	CC-036-X	6	dk to 10 cm, mod. lt to 15 cm
696400	1182930	CC-043-X	18	lt to 20 cm with irreg. 1 cm lams.
696045	1183165	CC-050-X	5	lr to 4 cm
695927	1183286	CC-051-X	18	mod. lt to 15 cm, lt to 22 cm
695885	1183350	CC-052-X	35	lt to 25 cm, mod. lt to 30 cm, lt to 31 cm, mod. lt to 32 cm, lt to 40 cm,
ti1	ti1	CC-055-X	35	lt to 36 cm, many thin dk lams.
700281	1154713	CC-056-X	46	lt to 17 cm, dkr to 20 cm, lt with thin lams. to 32 cm
700267	1154678	CC-057-X	30	lt to 10 cm, dk to 12 cm, lt to 17 cm, dk to 20 cm, lt to 25 cm
699955	1154893	CC-059-X	30	lt to 21 cm, dk chunk 6-9 cm
700059	1154865	CC-060-X	15	lt to 7 cm, possible dk chunks throughout
698768	1154525	CC-065-X	10	dk to 10 cm with possible lt chunks
698384	1155313	CC-066-X	25	lt to 26 cm, dk intervals 9-10, 14-15, 18-20
698085	1155648	CC-067-X	41	lt to 36 cm
698456	1155941	CC-073-X	25	lt to 32 cm with some thin dk lams
698627	1156199	CC-074-X	19	dk to 10 cm, mod lt to 15 cm
699078	1156986	CC-075-X	22	dk to 24 cm, disturbed at bottom
699140	1156933	CC-076-X	6	lt to 6 cm
699292	1156842	CC-078-X	28	mod lt to 3 cm, lt to 30 cm, dk layers 11-12, 15-16 cm
698820	1157829	CC-079-X	24	mod lt to 15 cm, lt to 10 cm, mod lt 20-25 cm
698874	1157789	CC-080-X	19	lt to 21 cm, thin dk lams 7-8 cm
9213	1157551	CC-084-X	22	lt to 15 cm, dl to 20 cm, lt to 25 cm
9395	1158564	CC-085-X	11	lt to 14 cm
699503	1158679	CC-086-X	32	lt to 5 cm and 11-14, 17-20, 25-30, 35-40 cm; other units dk, dk chunks 9-11 cm
699704	1158595	CC-088-X	32	lt to 33 cm, mod dk layer 2-4 cm, dk chunks 16-18 cm, dl layer 20-20.5

316710

700102	1158495	CC-091-X	11		mod lt to 7 cm, lt to 12 cm
0638	1161280	CC-093-X	48		mod lt to 25 cm, dk to 37 cm, lt to 55
5200	1191369	CC-107-X	20		lt to 11 cm
694497	1192308	CC-108-X	10		lt to 6 cm
698464	1191443	CC-117-X	15		dk to 10 cm, mod lt to 12 cm, some dk pcs throughout
700061	1166660	CC-122-X	45		dk to 34 cm with some mod lt. lams, mod lt to 40 cm with dk lams, lt to 52 with dk chunk
699504	1166419	CC-123-X	10		mod lt to 11 cm, lt layer 7-9 cm
699778	1166354	CC-125-X	40		lt to 11 cm with few dk layers or chunks, lt to 49 cm
700004	1166253	CC-128-X	15		mod. lt to 16 cm
700071	1166288	CC-129-X	28		mod lt to 20 cm, lt to 31 cm with some dk lams
701200	1150993	CC-133-X	32		lt to 13 cm, mod lt to 32 cm, lt to 36 cm
701419	1150533	CC-134-X	32		lt to 20 cm with thin dk lams, lt 20-22 cm, dk to 34 cm, lt to 37 cm
701490	1150530	CC-135-X	40		lt to 10 cm, dk to 41 cm
701551	1150661	CC-136-X	38		dk to 5 cm, lt to 8 cm, dk to 40 cm with lt layers 15-16, 20, 22, 24 cm, lt to 28 cm
701353	1149844	CC-137-X	20		lt to 20 cm with dk layer 7-9 cm
700724	1149656	CC-138-X	20		mod lt to 5 cm with dk chunks, lt to 20 cm
700286	1150638	CC-143-X	16		lt to 18 cm
700607	1148400	CC-144-X	32		mod lt to 20 cm, lt to 23 cm, mod lt to 32 cm, lt to 35 cm
700605	1148350	CC-145-X	30		mod lt to 18 cm with dk layer or chunk at 15 cm, lt 18-20, mod lt to 32 cm
701101	1151451	CC-148-X	48		lt to 5 cm, mod lt to 17 w/ lt lams, lt to 30 mod dk to 52 w/ dk lams, dk chunk at 47 cm
701244	1151458	CC-149-X	36		mod lt to 7 cm, dk with lt lams to 23, mod lt with dk lams to 32, lt to 36 cm, dk to 37 cm
698442	1203152	CC-152-X	22		mod dk to 2 cm, lt to 25 cm with dk chunk at 10-14 cm
bfa	bfa	CC-154-X	25		lt to 8 cm, dk with possible chunks to 16 cm, lt to 20 cm, mod dk to 25 cm with lt areas
bfb	bfb	CC-155-X	10		lt to 13 cm
bfc	bfc	CC-156-X	10		lt to 12 cm
699484	1140639	CC-157-X	21		dk to 22 cm with mod dk lams at 15-17, 20-21 cm
281	1138279	CC-160-X	52		mod lt to 5 cm, lt to 19 cm with dk chunks at 18 cm, mod lt to 55 with 1-2 cm lt lams
9049	1139791	CC-163-X	17		mod lt to 7 cm, lt to 13 cm, mod lt to 16 cm
699028	1140460	CC-165-X	9		dk to 9 cm
699077	1141877	CC-166-X	50		dk to 52 cm, many thin dk lams 20-25, 28-29, 31, 40, 41 (diag?), 45, 48 cm
698774	1141901	CC-168-X	20		dk to 3 cm, lt to 6, dk to 16 cm with lam. at 10 cm, lt to 25 cm with dk interval 20-22 cm
698398	1142789	CC-169-X	50		mod lt to 18 cm, lt to 20 cm, dk to 38 cm, mod lt to 43 cm
698346	1141173	CC-170-X	13		lt to 15 cm with mod lt layer 9-12 cm
698582	1141764	CC-171-X	15		mod. lt to 14 cm, dk chunks 10-13 cm.
697736	1143748	CC-173-X	40		lt to 40 cm, dk chunks 35-40
698391	1144125	CC-174-X	40		dk to 35 cm with mod lt lams at 12, 17 cm, lt to 39 cm with dk chunk at 36
698412	1144943	CC-176-X	25		mod lt to 15 cm, dk layer 5-10 cm, lt to 21 cm
697950	1145012	CG-177-X	5		lt to 8 cm
698405	1145865	CC-178-X	52		lt to 52 cm with mod lt lams at 3, 9, 15-16, 28-30 cm
					lt = light unit on X-radiographs (less X-ray penetration into sediments)
					dk = darker unit on X-radiograph (more X-ray penetration into sediments)
					bfa = Bakers Falls pool, south of road bridge, west side
					bfb = Bakers Falls pool, south of road bridge, east side
					bfc = Bakers Falls pool, north of road bridge, west side
					ti1 -- near shore north of CC-051-X

316711

Bakers Falls (Map 40)

The river bed behind Bakers Falls is primarily composed of outcropping rock layers with a joint pattern tending generally east-northeast. There is some indication of coarser sediment along the margins of the pool as the rock outcrop patterns seem to be covered in those areas. To the south of the old bridge across Bakers Falls Pool, some sediment is observed along the base of the Bakers Falls dam, especially in the southeast corner. Sediment also appears to be present along the western side of the dam towards the entrance to the power plant. Visual inspection shows that there is sediment and sawn wood along the piers of the old bridge in the western portion of the area. No data was collected west of the island because of construction for a new bridge. Recovered sediment samples show mostly fine-medium sand with some wood and gravel.

Remnant Deposits (Maps 34 to 36)

No sonar data could be collected from the area of the remnant deposits in the vicinity of remnant areas 1, 2 or 3 because of air bubbles in the water due to the rapids south of Bakers Falls. No 100 kHz data could be collected in the remnant area because of air bubbles; 500 kHz data could be collected south of about 1,196,000. In most of this area, the bottom is characterized by outcropping rocks, perhaps covered with a thin coarse sediment veneer. A small creek enters into the western side of the remnant area near 1,194,000, transporting fine sand into the remnant area. Additional fine sand may enter the western side of the river through drainage across the capped remnant deposits. Five to six mounds are observed in the southern portion of the remnant deposits near 1,191,600 and 695,000 (about river mile 195.1). The largest mound is about 10 ft high, 50 ft wide and 150 ft long. It is visible from the surface, and is composed of sawn wood and sediment. It appears to be a portion of the remnant deposit. The other mounds identified are about 1/4 the size of the largest one, and are not visible from the surface. Sample CG-103, with chips from sawing wood, is located downstream from one of these mounds.

Rogers Island (Maps 33 to 30)

The river channels on the eastern and western sides of Rogers Island differ from each another. The northern part of the western channel downstream from the rapids at Fort Edward is characterized by outcropping rocks, a thin veneer of coarse sediment, and numerous pieces of lumber. Occasional sediment tails are observed downstream from obstacles suggesting active sediment transport. There are some areas of potentially finer sediment along the Rogers Island shore, but many trees are also present there. This general pattern extends to south of the railroad bridge, although the size of sediment pockets appears to get larger down-river. South of the railroad bridge sediments are more widespread and remain coarse. Some large targets (logs?) are also observed, and a scalloped pattern along the west shore of Rogers Island near the southern end may be due to dredging. Subbottom profiles show scattered laminated sediments, suggesting that some of this area is underlain by laminated glacial sediments.

The channel that runs to Fort Edward and then along the eastern side of Rogers Island has a different character. This area is sedimented, generally with coarser sediments, and some wood pieces. One exception is a zone of finer sediments directly opposite the dock in Fort Edward.

The area has a low reflectivity, and a core sample (CC-117) shows fine sediment with an organic odor suggestive of a high sedimentation rate. A possibly similar area is also present on the north end of Rogers Island.

The channel is quite narrow in the vicinity of the road and railroad bridges, but expands south of the railroad bridge. Finer sediments are present in the mouth of a creek on the east side near 1,189,500 and along the western edge opposite the creek. There is a scalloped nature to the western side of the creek from 1,190,000 to 1,189,250 that may have been caused by dredging. A water treatment plant outfall occurs near 1,189,200 on the eastern shore. Coarser sediments are expected in the center of the channel downstream of the outfall, with finer sediments near shore on the eastern side. Many trees are partially and fully submerged along both sides of the river. Subbottom profiles suggest that laminated glacial silts and clays crop out in places along the eastern shore.

Rogers Island to Snook Kill (Maps 29 to 25)

There is a change in sediment character at the south of Rogers Island; the image becomes more uniform with fewer large sonar targets present (e.g., trees and sawn wood). The channel floor is distinctly different from the flanks as it is smoother; however, reflectivity is about the same in both environments. Two mounds are present along the west side at about 1,186,530, and other mounds occur about 1,186,000 (at about river mile 193.5). These latter mounds appear to be associated with sheet piling that Sanders (1989) describes being driven in this area. The river is relatively deep in this area, and there are pronounced irregular lineations along the western side of the channel that may correspond to where subbottom profiles suggest gray clays crop out.

Two additional sets of mounds are found along the western portion of the channel, two 50 ft diameter mounds are found near 1,185,250 and 697,500 and an irregular 200 ft diameter mound is found near 1,185,000 and 697,350 (both about river mile 193.3). These mounds have the morphological character of dredge spoil deposits. Six small circular targets are resolved near the river edge at 1,185,000 and 697,250. These are marks left by test cylinders deployed in 1991 by GE to study biodegredation of PCBs (Harkness et al., 1993). The center of the channel in this area is characterized by coarse, lineated sediments. The eastern edge of the channel throughout this area is characterized by an irregularly lineated flank with finer sediments near the shoreline and many submerged trees. The irregularly lineated flank, which ends at about 1/2 way through the bend to the south, may correspond to an area where gray silts and clays are close to the surface.

Finer sediments appear to have been deposited along the western river bank in the area downstream from the dredge mounds. This is confirmed by several confirmatory samples taken nearshore which show silty sediments. A small creek enters the western side near 1,183,700 (about river mile 192.9). This creek may provide some of the fine sediment deposited in this area.

The western side (outside) of the prominent river bend near 1,182,000 (about river mile 192.6) is characterized by mounds of dredge spoils, many of which have sediment tails, and near-surface rocks that have been cut through to make the canal. Places with finer sediments appear to

exist within this complex zone. This pattern continues to about 1,180,400 at about river mile 192.3.

Nearly the entire river bed is coarse and lineated south of about 1,180,400. However, a small creek enters the eastern side about 1,180,600 and there is a less-reflective, finer-grained zone off the creek mouth. Dredge spoil mounds are observed on the eastern side near 1,179,200 (about river mile 192). Sediment samples in this area show fine sand and silt. There is a finer-grained patch on the western edge of the channel near 1,178,700 (with H_2S smell; about river mile 191.9). Patches of finer sediment also occur off a small creek at 1,178,500 and off Snook Kill at 1,178,200. The channel floor in this area has gravel with wood chunks. No data was collected behind the islands on the eastern side of the river.

Snook Kill to Thompson Island Dam (Maps 26 to 16)

A rocky area crosses the Hudson River immediately downstream from Snook Kill (about river mile 191.7). Downstream from this rocky area the river bed drops by about 10 ft and is an extensive region of fine-grained sediments. Subbottom profiles suggest that gray silts and clays crop out in the center of the channel, but that these sediments are covered by more recent sediments near the edges of the channel. Black Horse Creek enters on the east side at about 1,178,000 and may contribute some of the sediment deposited in this area. High reflectivity along the western side of the river here may be due to fill for the roadway which runs alongside the river. On the eastern side of the river near 1,176,000 (about river mile 191.2) are a number of large and small dredge-spoil mounds (Figure 14). These mounds appear to have been smoothed by river flow. The central area of the river is coarser and the flanks of the river is finer as the river approaches a rocky zone near 1,174,000 (about river mile 190.8). A small creek enters from the western side on the up-river side of this rocky area at 1,174,200 and may contribute some of the sediment that deposits upstream and downstream of the rocky area.

From 1,174,000 to 1,171,750 (to about river mile 190.3) the river bed is mostly rocky with some intervals of coarser and finer sediments. Many discontinuous subbottom reflections are observed in this section of the river. Numerous current-smoothed small dredge spoil mounds are observed at several locations along the eastern edge of the river.

The river widens at about 1,171,750 and an extensive area of finer sediment is found to the eastern side of the river extending south to about 1,169,750 (about river mile 189.7). Coarser sediment are found in the deeper part of the channel, but no wood chunks were recovered from the channel in this area. The central portion of the river is shallow and is lineated in an irregular fashion. This area appears to be somewhat eroded for the following reasons. (1) Cores from the finer sediments near the shore consistently show a wood-chip layer at a subbottom depth of 25-35 cm overlain by a finer sediment. In the lineated area samples suggest a sandy surface unit with possible wood chunks at several depths. (2) The side-scan sonar image appears to show tongues of finer-grained material being transported down-river across coarser-grained sediments at the southern edge of this zone. This may be finer-grained material being worked out of the sediments by river flow. (3) Wood chunks are found in the river channel south of this point off Moses Kill, but no wood chunks were found in the river channel in this area. It is possible that the wood

chunks observed to the south have been eroded out of the lineated deposit here, although similar lineated zones are also observed south of this site.

Subbottom profiles and sediment cores show that gray silts and clays crop out on the river bottom where the river narrows near 1,169,750. Much of the eastern side downstream from this section is rocky, with several deep depressions along the eastern side. Finer sediments are predicted along the western side of the river off Griffin Island, and a portion of this zone is irregularly lineated. Coarser sediments are present in the deeper channel. At about 1,168,000 (about river mile 189.6) the river widens and finer sediments are present on both the western and eastern flanks of the river.

The area on the eastern side of the river around Moses Kill is dominated by finer-grained sediments. Some of these sediments come from up-river, but some must come from the Moses Kill which has often been muddy when we have been in the field. Many of the other small creeks also appear to have been significant sources of finer-grained sediment to the Hudson River, especially during winter and spring rains. Sediment samples show fine-grained sediment off both shores with a zone of sand along the western slope and gravels with wood chunks in the deep channel. Subbottom profiles show many discontinuous reflectors in this area.

At 1,166,200 (about river mile 189.2) the sediment texture along the western wall begins to change, and a number of mound-like targets are observed. The Champlain Canal leaves the Hudson River at 1,165,400 as a land cut. The lineations in the deep channel go into the land cut. South of the zone where the canal leaves the river, the river-bed character changes dramatically. Numerous mounds are present, especially towards the western portion of the river. The eastern side is somewhat smoother, but sediments are still coarse. Finer sediments seem to occur along the western side of the abutment that leads into the canal, and in some places along the western side of the river. There are two small creeks that feed into the river along the western shore at 1,164,875 and at 1,163,750.

Marshes are present on both the western and eastern shore immediately upstream from the Thompson Island Dam. Rocks outcrop upstream from the dam north of Thompson Island.

Thompson Island Dam to Millers Falls Dam (Maps 16 to 10)

The river bed from the Thompson Island Dam to the Millers Falls Dam changes in character from its up-river to down-river ends. The river bed on either side of the northern end of Thompson Island has a rocky bed, but with sediments (both finer-grained and coarser-grained) accumulating between rock outcrops. The river gets quite deep to the west of Thompson Island (to 45 feet), perhaps because of river-bed erosion before the construction of the Thompson Island and Millers Falls dams. Towards the southern end of Thompson Island, the river bed becomes more sedimented in the eastern channel with coarse sediments, and there is a pronounced lineated zone that extends down-river to near the northern tip of Galusha Island. Finer sediments are observed near the eastern shore in a depression. The western channel is characterized by outcrops with sediment pools throughout. A ridge extends from the southern tip of Thompson Island (note shadows caused by sonar tracks over ridge near 1,158,700; about river mile 187.6). Sediments

associated with this ridge have a well-defined wood-chip layer. Channels apparently created by bed-load movement bound this ridge on either side, and the sediment ridge may be susceptible to erosion.

Sedimentation patterns are different to either side of Galusha Island (near river mile 187.3). On the western side, the river channel is relatively broad with a zone of irregularly lineated bed near the center of the channel. This lineated zone becomes less pronounced towards the south end of Galusha Island. Wood chunks are found in grab samples near Galusha Island. Along the western shore of the river, gray glacial silts and clays crop out on the river margin. These gray silts and clays extend around the western side of the broad river bend to 1,154,500 (about river mile 186.5). The deepest part of the river here is along the base of these laminated sediments. The eastern channel is narrower, with a somewhat smoother bed. A shallow area near the north end of this channel must deflect much of the river flow to the western side of the island. Towards the southern end of the eastern side, there is a pronounced region of less-reflective finer-grained sediment that was sampled. This appears to be the site of recent fine-grained sediment accumulation.

Sediments to the south of Galusha Island differ west to east because of up-river sedimentation processes. To the west (but east of the gray clays), three river-bed sediment samples (CG-068, CG-069 and CG-070) all have wood chunks and/or sawn wood chips at the surface suggesting upstream erosion of a wood-chip layer. To the east side of the river, two sediment samples (CG-071 and CG-072) have somewhat finer (but still coarse) sediments with no wood debris.

Sediment moving down-river as bedload appears to go along the eastern (inner) side of the river bed. The western side of this bend is relatively deep (up to 26 ft). Sediments moving down-river extend along the northern/eastern side of the river to about 1,154,500. Near the eastern end of this zone, the sediment extends to the south across the rocky river bed, in part localized by a channel that pre-dated the dam at Millers Falls. A small river which enters on the north/east side at about 1,154,700 may provide some of the sediment in this area.

Much of the river bed directly upriver from the Millers Falls dam is rocky with small sediment ponds. The dam at Millers Falls has been moved since the USGS topographic sheet was made, most likely associated with the building of the electric generating plant at Millers Falls.

Millers Falls Dam to Lock 5 (Maps 10 to 1)

The Champlain Canal rejoins the Hudson River at Millers Falls, and the river again becomes a dredged channel. The river bed is rocky on the western side immediately down-river from the rapids at Millers Falls, while finer-grained sediments (including gray silts and clays) are present in the deep, central portion of the river to 1,150,500 (about river mile 185.7). Some pockets of finer-grained sediments are also observed along the western shore near 1,150,500 and 1,150,000 in part related to sediment input from Pecks Creek. Finer-grained sediments are also present on the eastern side of the river, but sediments in this area have a somewhat variable surface texture. X-radiographs of samples from the eastern portion of the river here suggest that

the uppermost sediments are coarser than those at depth, and the variable surface texture may result from sedimentary processes related to that grain-size increase. The surface sediments may be coarser because of changes in flow pattern related to the construction or operation of the power plant at Millers Falls. These rougher, finer-grained eastern-shore sediments extend south to about 1,148,200 (about river mile 185.3). The eastern shore also has a number of mounds, probably sediments from dredging operations.

South of 1,150,500 (about river mile 185.7) the river bed becomes more reflective due to rock outcrops and coarse sediments although there is a somewhat finer (less coarse?) zone in the center of the channel immediately south of a 500 ft wide reflective zone. The river bed becomes rocky from about 1,148,300 to about 1,147,000 (about river miles 185.3 to 185.0) with a smaller patch about 1,146,500 (about river mile 184.9). A 25 ft deep, finer sediment area exists between the two rocky zones, and sediments become coarser towards the south. Coarse sediments occur in a zone through the center of the rocky/coarser zone.

South of 1,145,500 (about river mile 184.7) the river widens and river-bed sediments become generally less coarse. Finer sediments are observed along the river margins with coarser sediments in the center of the channel. There is a wide, shallower area of the finer sediment to the eastern side of the river to 1,141,500 (about river mile 183.9). There are patches of more reflective sediments, perhaps coarser sediments, in this area. Also, there are a number of cribs and dredge-spoil mounds in this area, many with sediment tails downstream. The western river bank is also finer, as shown by sediment samples, and the somewhat higher reflectivity in this area may also be due to bottom slope as sonar swaths that look upslope have a higher reflectivity than those that look downslope. Small creeks enter to both sides of the river in this area, and they may provide sediments to the river.

Rock outcrops are present to the western side starting at about 1,142,000 (about river mile 184.0). These rocks were truncated to dredge the canal, and finer-grained sediments appear to be trapped in depressions in the rocks. The river bed is rocky where the river narrows at 1,140,800 (about river mile 183.7) and US. Route 4 crosses by bridge. Some coarser sediments are observed around an island north of the bridge.

Finer-grained sediments, confirmed by sampling, are observed on both the west and east sides of the river immediately down-river from the constriction. Finer sediment continues on the western side to 1,139,250, and on the eastern side to about 1,139,800. Water is up to 35 ft deep 500 ft downstream of the bridge. Sonar records suggest that these sediments are coarse. Coarse sediments and some rocks are present in the center of the river downstream, with rocks more common towards the Lock 5 dam. A channel extends to a dock to the east side of Lock 5, and there are some cribs on the river bed near the dock, perhaps dating from the time when a mill or other water-powered plant was in this area.

The Champlain Canal passes to the west of the rocky area and dam, and the deeper river bed is characterized by coarser sediment. The reflective zone of coarser sediment ends at the southern end of the dam (at 1,133,600). South of this the canal sediment are still coarse in the central region (and finer at the edge), but less reflective than north of the dam. The canal

sediments becomes generally finer off a small creek near 1,137,500, and then coarser near 1,136,500. The entrance to Lock 5 is at 1,135,250 with the entrance to the old canal lock, perhaps filled with some dredged sediment, to the west of the present-day lock.

1984 PCB Measurements and Sediment Texture

The technique used to correlate sonar DN with grain size information can also be used to correlate the strength of the sonar image with other information. We have used this approach to determine whether or not relationships exist between PCB surficial concentration and sediment texture determined in 1984 in the Thompson Island Pool (Brown et al., 1988) with sonar properties. This is a reasonable task to undertake since one of our major interests is to understand PCB distribution patterns in the Hudson River.

During the 1984 study, sediment texture was classified into one of 20 different categories (Table 6). These terms were ranked in relative order of decreasing grain size and a number was assigned to each size category with larger numbers assigned to smaller grain sizes. This was done to simulate a phi size scale where smaller numbers correlate with larger grain sizes.

The rules described for the sonar-grain size calibrations were used to select stations where the sonar image is uniform. These rules resulted in 667 stations out of 1040 with uniform sonar images. Figure 16a is a scatter plot of 1984 sediment texture vs. 1991/1992 DN for the 500 kHz median image. Other sonar results are similar. Several descriptive sediment terms were widely used (e.g., gravel, fine-sand, coarse sand with wood chips), and there is a wide range in DN for these sediment textures. As noted previously, the use of overly general grain size terms may mask information about the mean grain size of a sediment. Also, these texture terms may not be uniformly applied and our assignment of a relative grain size to some texture classifications may be in error. There is a slight visual correlation between sediment texture as recorded by Brown et al. (1988) and image DN, with finer sediments having a slightly lower average DN than coarser sediments (Figure 16a). However, there are many instances where areas of gravel sediment in 1984 had low DNs in 1991/1992 and fine sediment in 1984 had high DNs in 1991/1992. This may suggest that the sediment texture has changed in some areas during last eight years between this sampling and the sonar study.

The plot of 500 kHz median image DN vs. surficial total PCB concentration in 1984 is shown in Figure 16b. There is no simple correlation between these variables. Total PCB concentrations greater than 200 ppm correspond to a DN range of 20 to 60. Based on the 1991/1992 grain size calibration, this corresponds mostly to regions of finer sediments. Many samples with a DN from 10 to 70 had PCB concentrations greater than 50 ppm, and few samples with a DN greater than 80 have PCB concentrations greater than 50 ppm. There are also many samples with DN in the range of 10 to 80 with PCB concentrations below about 25 ppm. If one assumes that surface sediment properties have not changed drastically since 1984, then one should look in areas where 1991/1992 DN values range from 10 to 70 to find elevated PCB levels.

Table 6

Classification of 1984 Sediment Type Categories

Category	Classification Number
GRAVEL*	1
CS-GR	2
GR-WC*	3
GR-MK	4
CL-GR	5
GR-CL	6
CS-SND*	7
CS-WC*	8
SC-WC	9
SC-SND	10
FC-WC	11
SAND	12
FS-GR	13
FS-WC*	14
FN-SND*	15
FS-CL	16
SILTWC	17
SILT	18
MUCK*	19
CLAY*	20

* category contains more than 5 samples with a uniform sonar image

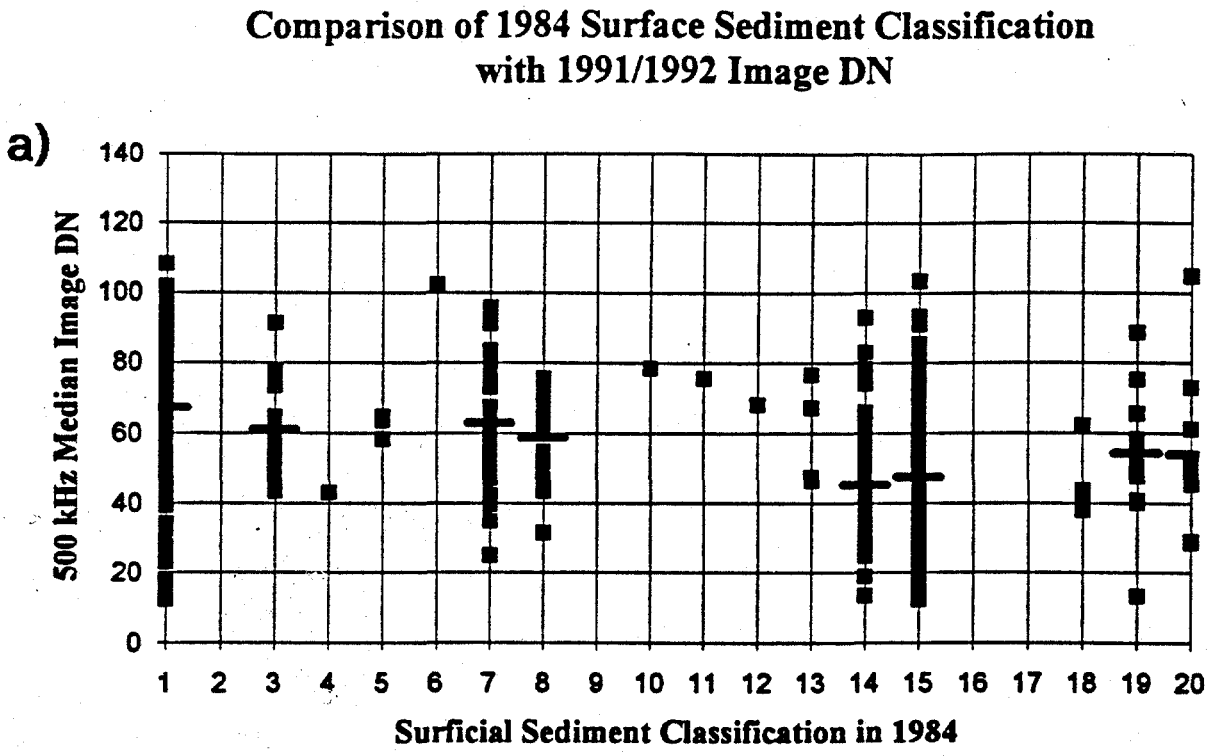

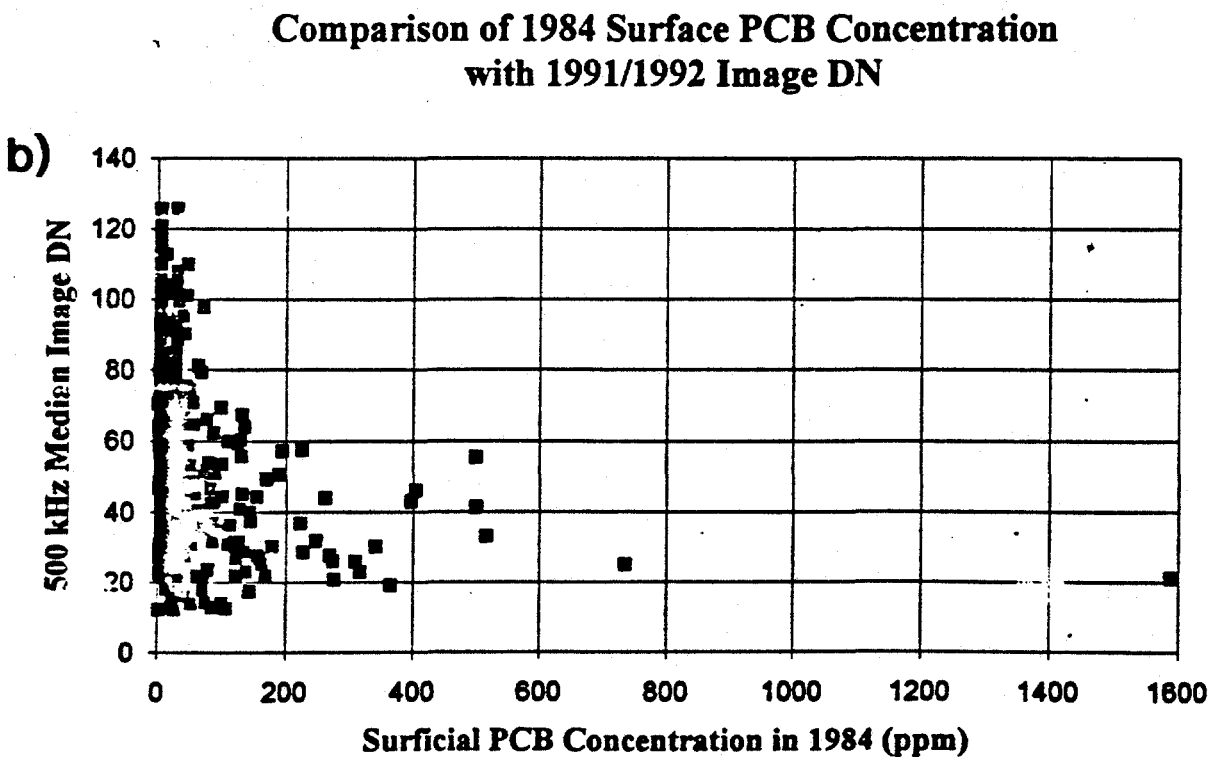

Figure 16. a) Sediment texture from 1984 samples (see Table 6 for sediment classification) versus DN of 1991/1992 500 kHz sonar image. Horizontal lines are shown for sediment classifications with more than 5 samples. b) Total PCB Inventory determined for sediment samples collected in 1984 versus DN of 1991/1992 500 kHz sonar image.

Sedimentation Patterns, Erosional Patterns and Contaminant Distributions

A number of factors appear to be important in determining sediment distribution, erosional patterns, and contaminant distributions within this portion of the Hudson River. A complete understanding of these issues is beyond the scope of this study. However, our analysis of side-scan sonar data, subbottom profiles and sediment samples suggests that general comments are warranted on several topics.

Damming, Dredging and Disposal

Man's activity (damming, dredging, and disposal) has influenced sediment distribution patterns in several ways. In addition to the role of up-river dams in flood control and the history of the Fort Edward Dam in supplying sediment to the river, dams have also affected sediment distribution patterns. Dams exist at Bakers Falls, Thompson Island, Fort Miller, and at Lock 5. Construction of dams initially deepens the river upstream from the dam, often resulting in enhanced sediment accumulation within that river reach. The present dam at Thompson Island appears to date from the enlargement of the Champlain Canal about 1917 while dams were built at earlier times at other sites. Recent reconstruction of the dam at Fort Miller, associated with the construction of an electrical generating plant, may have altered the flow rate upstream from tne dam, perhaps resulting in the apparent increase in sand observed downstream from Fort Miller. Increased flow speed upstream of Fort Miller may lead to an increased erosion potential in that area. Changes to any of the dams on the Hudson River may potentially alter flow patterns and the potential for sediment accumulation and/or resuspension.

Until about 1917 (and except for a short time from 1822 to 1828), the course of the Champlain Canal was separate from the Hudson River north of about where the U.S. Route 4 bridge crosses about river mile 183.8. Dredging of the river associated with the enlargement of the canal has had a significant impact on sedimentation processes, and a scalloped pattern at the edge of the dredged channel can often be discerned. Dredging can create places in which sediments can accumulate, especially along the corners at the bases of the channel walls. Dredging through rock outcrops can create a narrow channel where water travels quickly, while dredging in wider portions of the river can increase river cross-section and thus decrease mean flow velocity.

The changes in river geometry associated with the initial and maintenance dredging of the canal means that the river topography is not in equilibrium with its sediment load and thus an equilibrium river bed profile cannot be assumed. Even to the side of the dredged canal, insufficient sediment has accumulated during the last 70 years to counter changes in geometry due dredging. One possible exception is the section of the river between the south end of Thompson Island and the Fort Miller Dam. Much of this section may be closer to equilibrium because of the age of the Fort Miller Dam and the lack of dredging.

The disposal of dredged sediment in the river also can affect sedimentation patterns aside from the obvious addition of dredged sediment. The disposal of significant amounts of material can serve to reduce channel cross-section, leading to increased flow velocities. Also, materials

dredged after about 1946 could be contaminated with PCBs. More recent sediment accumulation can occur as tails behind the dredge mounds, although the volume of these sediment tails may be small. Disposal of dredged material can also create a confused sediment stratigraphy as a result of the initial deposit, reworking of the deposit by currents, and sedimentation around pre-existing dredge mound topography. Sediments can also accumulate along the wall at the edge of the dredged channel. In particular, a large mound apparently formed by disposal of dredged sediments exists immediately down-river from Lock 7 near where the GE test cylinders were located (Harkness et al., 1993). The confused sediment record that apparently exists in this area may be related to sedimentation patterns around pre-existing dredge-mound topography as well as to rapid accumulation because of the close proximity to the Fort Edward Dam.

Relationship between River Flow, Sedimentation and PCB Distribution Patterns

In the description of the sonar mosaics, it is often noted that finer-grained sediments are more common in parts of the river downstream from, and especially along the river margins of, areas where the river widens. However, the distribution of sediments is clearly more complex than this with sites of finer-grained accumulation often depending on local topography and local sediment input to the river. Detailed modeling of sedimentation and river flow will be required to predict in detail where finer-grained sediments, and the PCBs that are often associated with those sediments, accumulate throughout the system.

Although a detailed modeling program is beyond the scope of the present study, some insights can be gained into the distribution patterns of finer-grained sediments and associated PCBs through use of the flow modeling study conducted by Zimmie (1985) and past measurements of total PCB inventories.

Zimmie (1985) determined flow velocities for several river discharges at a number of cross-sections in the Thompson Island Pool. These cross-sections are spaced approximately 800-900 ft apart and are based on bathymetric studies undertaken in 1977 and updated in 1982. However, because of the precise positioning of these cross-sections, they do not adequately characterize the rapid along-changes in channel geometry observed on the sonar records. Our new bathymetric studies will provide a more recent series of more closely spaced cross-sections, along with more detailed information on bottom character and roughness, but these data have not yet been reduced to cross-sections or used in a flow model. Zimmie (1985) used the HEC-6 model to calculate river velocities for particular sections of the river. Figure 17a shows the maximum vertically-averaged velocity calculated in the channel for each cross-section and discharge considered showing that the there are reaches of higher and lower flow speed as cross-sectional area decreases and increases down-river. Vertically-averaged flow velocities were also calculated for the slower flows outside of the main channel, but these are not considered here. Analysis of the sonar maps shows that the intervals of higher flow speed generally correspond to narrow, often rocky portions of the river and the intervals of lower flow speed generally correspond to the wider, often finer-grained portions of the river.

Studies of PCB contamination in river-bed sediments also show variation in the amount of PCB in sediments down river (Brown et al., 1988). Figure 17b is a plot of the calculated PCB

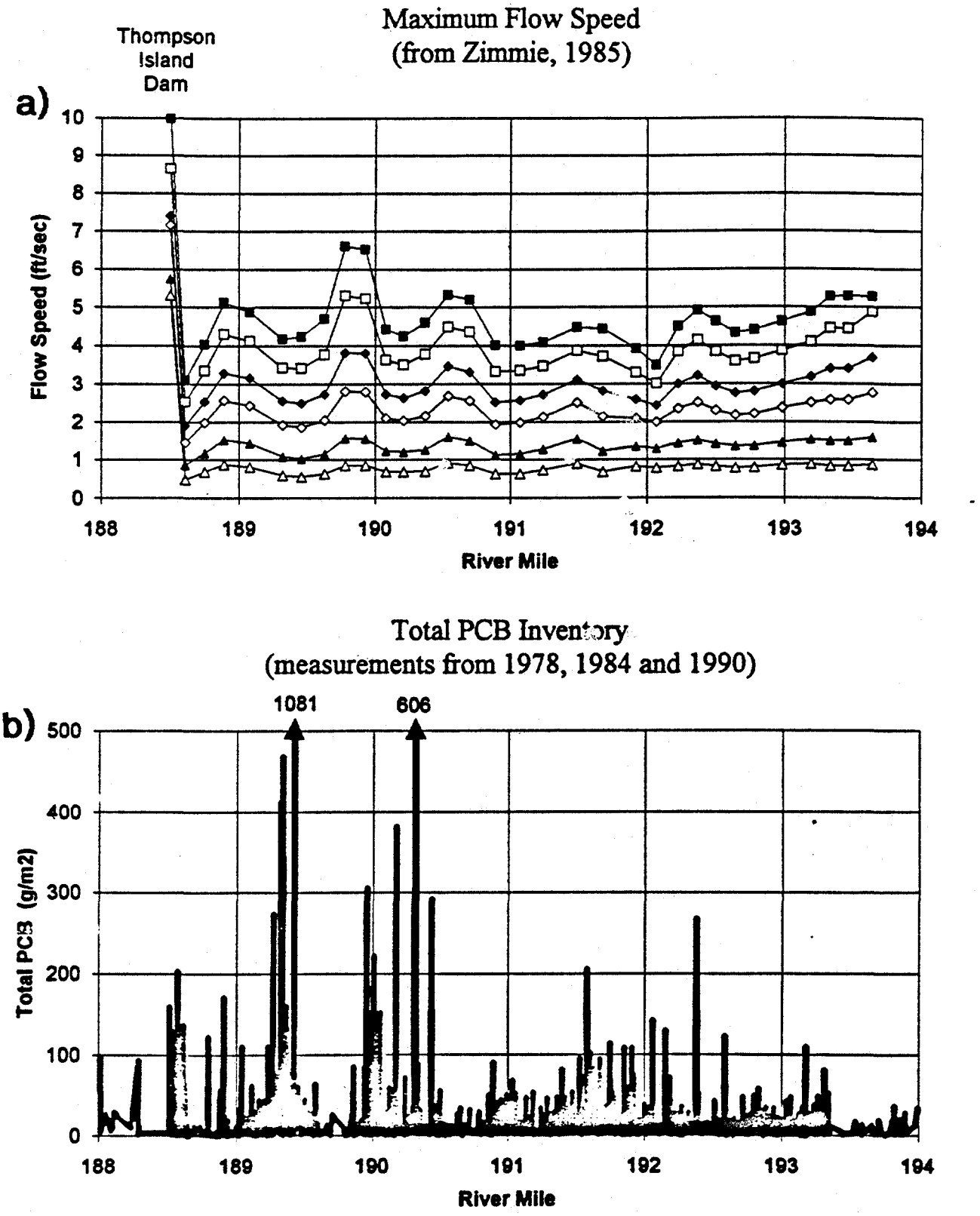

Figure 17. a) Maximum vertically-averaged flow speed determined by Zimmie (1985) for river cross-sections in the Thompson Island Pool. Different symbols represent different flow stages (■ 63,700 cfs, □ 46,600 cfs, ◆ 30,000 cfs, ◇ 20,000 cfs, ▲10,000 cfs, △ 5,000 cfs). b) Total PCB inventory for samples collected in 1978, 1984, and 1990. River mile calculated by reference to Northing only.

inventory for all samples collected from the Thompson Island Pool in 1978, 1984 and 1990 for which data is available. For this plot, river mile is calculated by reference to Northing only, thus there is some error where the river does not run north-south. There are high levels of total PCB inventories about river mile 190 to 190.5 (NYS DEC hot spots 12, 13, 14) and 189.25 to 189.5 (hot spots 15 and 16). These are both areas where maximum flow speed drops. Locally increased total PCB inventories also exist immediately above the Thompson Island Dam where the river widens (about river mile 188.5 to 188.7; hot spots 18, 19, 20). Marshes exists in this portion of the river because of the lower flows. Somewhat increased total PCB inventories are observed about river mile 191 (hot spots 9, 10, 11 and part of 8) and there is a diffuse peak about river mile 192 (hot spot 8) where the maximum average flow speed drops. Upriver from mile 192, total PCB inventories appear less well correlated with predicted river speed, possibly suggesting that some other mechanism, perhaps due to the close proximity of the site of the Fort Edward Dam, has been important in localizing PCB accumulation up-river from about mile 192.

Zimmie (1985) used the HEC-6 model to estimate the amount of erosion or deposition that might occur in the channel during different flow events. Zimmie (1985) suggests that the greatest potential for long-term erosion is in the high-velocity section of the river at about river mile 189.8. We note that this area of the river is characterized by rock outcrops on the eastern size but finer sediments (with irregular lineations in some places) are present on the western side. Presumably the finer sediments on the western side are most susceptible to erosion. Available PCB results suggest that in general sediments from this section of the river are not very contaminated (Figure 17b), thus the significance of erosion in this section of the river is unclear.

Zimmie (1985) suggests that sediment accumulation occurs about river mile 189.4 (near hot spots 15 and 16), a zone of relatively low average velocity just north of Moses Kill (Figure 17a). This area is characterized on sonar records by an extensive region of finer sediments along the eastern river bank, a smaller region of finer sediments along the western river bank, and coarser sediments in the channel. The finer sediments along the eastern river bank are deposited downstream of a zone of rock outcrops and where the river widens off Moses Kill. Irregular lineated patterns are observed near the channel both east and west of the channel suggesting that erosion may have occurred in some areas. However, the extensive region of finer-grained sediments on the eastern side may be less susceptible to erosion because of its location downstream from rock outcrops. However, finer-grained sediments that accumulate in other parts of the river here may be susceptible to erosion during high-flow events. Thus while some of the sediments in this area are high in PCBs, they may be in a stable setting.

The region of irregularly lineated sediments in the east-central part of the river about river mile 190 appears to correlate with a region of the river that Zimmie (1985) suggests is depositional during lower discharges (e.g., his Figure 3-11) but erosional during higher discharges (his Figure 3-9). This is in the vicinity of NYS DEC hot spot 14. Brown et al. (1988) suggested that hot spot 14 contains 33% of the total hot-spot PCB mass, thus understanding the stability of this deposit is important. Our studies show a cross-river variation in sediment character in this area. A large area of finer-grained sediments exists along the generally shallow eastern river bank while the western river is quite steep with only little finer-grained sediment. Channel sediments are coarser. The zone of irregularly lineated morphology lies in a shallow area east of the channel

and just east of the center of the river. The total PCB inventory data available for 1978, 1984 and 1990 suggests that the western margin of the river and the dredged channel have generally been characterized by lower inventories of PCB while the finer-grained sediment along the eastern and southeastern margin have been generally characterized by higher inventories of PCB. Sediments in the irregularly lineated zone have often had inventories of PCB intermediate between the eastern margin and the river channel. Lower PCB inventories in the irregularly lineated zone may indicate that sediment reworking by river flow has already removed some PCB from sediments here. The amount of PCB that can be introduced by future reworking at that site would then be limited. However, erosion closer to the eastern river bank would have the potential to resuspend larger quantities of PCB. A more complete understanding of flow velocity distribution and PCB contamination patterns will be required to better understand the potential stability of these and other deposits.

Irregularly Lineated Zones - Sites of Erosion?

An irregularly lineated sediment bed is noted in many parts of the river. As noted earlier, several lines of evidence suggest that these zones represent areas where the river bed has been eroded, although the timing and magnitude of the erosion is unclear. The irregular lineations themselves appear to be caused by scour patterns in the vicinity of materials on the river bed, perhaps materials exposed during erosion. A more regular pattern of lineations is often observed in the bottom of the channel. The erosional potential of these regularly spaced lineations is not clear, in part because of the tendency for this lineation pattern to occur in the dredged channel where sediments are often coarse. In contrast, the irregular lineations often occur in regions of finer-grained sediments and thus the potential for erosion in these areas appears to be larger.

In several of the irregularly lineated areas, subbottom profiles and sediment sampling demonstrate that lacustrine silts and clays are at or near the river bed. In those areas, the lineated zones may represent areas where lacustrine silts and clays are being, or have been, eroded. In other areas, especially near river mile 190 and in the portion of the river between the Thompson Island Dam and Millers Falls, the lineated zones occur in areas were lacustrine silts and clays are not near the river bed. In those areas, we suggest that modern river sediments are being, or have been, reworked by river flow.

Lacustrine Silts and Clays of Glacial Age

Lacustrine silts and clays are observed in many sections of the river, and may exist in other sections although they may be covered by more recent sediments. Many of the creeks and rivers that enter into this section of the Hudson River drain areas characterized by lacustrine clays and silts. The observed deformation of these sediments, combined with the suggestion of land instability by Cadwell and Dineen (1987), suggest that a geotechnical analysis of these sediments is needed to understand their stability should some of overburden be removed.

In discussing the sonar images, it is sometimes noted that the river bed deepens downstream of a rocky areas that may interrupt bed-load transport. Specific examples occur about river miles 191.7 (downstream from Snook Kill) and 185.8 (downstream from the Fort

Miller Dam). In both of these areas, lacustrine silts and clays were identified on the river bottom on the basis of subbottom profiles. The interruption of bed load transport in these areas may expose lacustrine silts and clays on the river bed, and these may be easily eroded, or dissolved, resulting in a deeper river here. These exposed lacustrine silts and clays will have a lower image DN because of the finer grain size; however, these sediments should not be contaminated.

The silts and clays resuspended from the river bottom or introduced from creeks that join the river may contribute significantly to the sediment load of the Hudson River. Since these sediments pre-date PCB contamination, their erosion will not introduce PCBs into the river system. In some areas these sediments appear to be covered by only a thin veneer of coarser, potentially contaminated sediments. If this thin veneer is removed there could be a change in the composition and character of suspended sediment with time. Deformation of these silts and clays may also expose them on the river bed.

Conclusions

Side-scan sonar maps of the Hudson River from Bakers Falls to Lock 5 were produced as a part of the Hudson River PCB Reassessment RI/FS. These sonar maps, along with interpretive diagrams, subbottom profiles, and sediment samples collected during this study provide important new insights both into the character of the Hudson River bed and the nature of the sedimentary processes active there. Such information is needed to ensure that any proposed solutions to the problem of PCB contamination in the Hudson River are discussed with a clear and accurate view of the river bed. Many specific comments and discussions on the images and their implications for sediment studies have been made in the text. However, a detailed, foot-by-foot analysis of sediment processes and river-bed contamination is beyond the scope of this study and will require integrated, computer-aided analysis of observational and modeling data. The project has provided image and subbottom data in a digital form (Appendix B) to allow its use in geographical information systems (GIS) that can combine the results of the numerous investigations that have been undertaken in this area.

Our side scan sonar maps and interpretation show:

1. The pool at Bakers Falls is primarily underlain by exposed rocks, although some sediment is observed near the base of the present dam and near the river edge. Much of the river bed in the remnant deposit area is rocky, although some sediments are found on the river bed. Several mounds are present on the river bed towards the southern end of the remnant area. These appear to be undredged remnant deposits.

2: South of Fort Edward, the sonar images can be quantified in terms of sediment grain size. Comparisons between sediment grain size analysis and the digital values of the 500 kHz sonar images (DN, digital number) suggest that, in areas where the sonar image is uniform, coarser sediments are more reflective (lighter) and finer sediments are less reflective (darker). Areas with DN less than 60 probably have mean grain sizes less than 4 phi (silts and clays), areas with DN greater than 60 probably have mean grain sizes in the sand and gravel size range (greater than 4 phi).

3. Evaluation of the sonar images and other data suggests that sediment distribution patterns are locally complex. Basement rocks, cut away to form the Champlain Canal, are exposed in some areas while lacustrine silts and clays of glacial age are exposed in other areas. Coarser-grained sediments are often observed in the channel while finer sediments are more common in shallow water. In some areas, an irregular lineation pattern is observed on the sonar records that suggests past river-bed erosion. Downriver of these areas of irregular lineations are apparently enhanced levels of wood chunks and wood chips in surface sediments. Also, mounds apparently created by disposal of dredged sediment in the river are observed in some areas.

4. Local sediment distribution patterns depend on river-bed geometry and down-river changes in sediment sources. Rock outcrops provide sheltered areas and/or limit bed load transport. The corners of dredged channels, depending on average flow velocity, provide sites where sediments can accumulate. Changing morphology of the river because of islands, entering creeks, geologic structures (e.g., rocky shorelines), and man-made structures (dredge mounds, cribs, canal structures, dams) change the cross-sectional area of the river and create areas of reduced flow where finer sediments tend to accumulate. Altering structures, especially dams, will affect up-river and down-river sedimentation and erosion patterns. Flow in the river is three-dimensional and some flow effects, such as the tendency for higher-flow speeds near the outside of river bends even when the dredged channel is in the inside of the bend, help to control sedimentation/erosion patterns.

5. The lacustrine silts and clays of glacial age that underlie several portions of the river, and also that are drained many of the creeks that drain directly into this portion of the river, affect river sedimentation in several ways. Where exposed, these sediments appear to have been eroded, increasing river cross-section and supplying uncontaminated fine-grained sediments to the flow. Deformed layering within these sediments is also observed. These deformed layers suggest that the stability of these sediments needs to be understood should large volumes of overlying sediments be removed.

6. Comparisons between along-river changes in flow velocity (Zimmie, 1985), sediment distribution patterns, and historical measurements of total PCB inventories provide insights into factors that control sites of sediment accumulation. In the Thompson Island Pool, finer-grained sediments and sediments with higher total PCB inventories are more common in areas where mean flows decrease because of increased river cross-section. In particular, the river near NYS DEC hot spots 15 and 16 (about river mile 189.4) and near hot spots 12, 13 and 14 (about river mile 190.1) has a generally lower average velocity because of increased cross-section. However, erosional patterns are observed in both these areas. Finer-grained sediments along the east side near river mile 189.4 appear to be shielded by rock outcrops, while those near the center of the river about mile 190.1 have experienced some erosion. The portion of the river near mile 189.9 where Zimmie (1985) suggests the maximum potential for long-term erosion is in part rocky, and PCB concentrations appear generally low suggesting that the potential for PCB resuspension is reduced here.

7. Detailed analysis of river flow needs to be undertaken using the new, more detailed river cross-sections in the Thompson Island Pool and in the other surveyed portions of the river to more clearly define areas where the most significant concentrations of PCBs may exist and where sediments are most susceptible to erosion. Precise sites of PCB accumulation and resuspension within those sections of the river will be controlled by the details of river-bed geometry and three-dimensional flow patterns within the river as well as changes in these flow patterns related to changes in river discharge. The sonar images will help to identify areas of finer-grained sediment accumulation and sites of past erosion.

Acknowledgements

Field and laboratory assistance for this project was provided by Jianguo Sun and Jang-Geun Park at MSRC. Dr. Barry Gordon did the analysis leading to Figure 16 while in a summer intern program at SUNY-Stony Brook. Dr. W.B.F. Ryan of the Lamont-Doherty Earth Observatory aided with the construction of the digital images, and Rusti Lotti, of the same institution , X-rayed the cores. The Research Foundation of the State University of New York, and especially Kathrine MacCormack, was invaluable in the prolonged contractual discussions. The work on which this publication is based was performed under Subcontract No. 5213-01 to TAMS Consultants, Inc. pursuant to EPA Contract No. 68-S9-2001.

References Cited

Bopp, R.F., Simpson, H.J. and Deck, B.L., 1985. Resease of polychlorinated biphenyls from contaminated Hudson River sediments. Final report NYS C00708 to NYS DEC, Albany, NY, Lamont-Doherty Geological Observatory of Columbia University, Palisades, NY.

Brown, M.P., Werner, M.B., Carusone, C.R. and Klein, M., 1988. Distribution of PCBs in the Thompson Island Pool of the Hudson River. Final report of the Hudson River Reclamation Demonstration Project Sediment Survey. New York State Department of Environmental Conservation, Albany, New York. 92 pp.

Cadwell, D.H. and Dineen, R.J., 1987. Surface Geological Map of New York State, Hudson-Mohawk Sheet. Map and Chart Series #40, New York State Museum Geological Survey, Albany, NY.

Chavez, P.S., 1986. Processing techniques for digital sonar images for GLORIA. Photogramm. Eng. Remote Sens., 52, 1133-1145.

Dyer, K.R., 1986. *Coastal and Estuarine Sediment Dynamics.* John Wiley and Sons, New York, 342pp.

Edgerton, H.E., 1986. *Sonar Images.* Prentice Hall, New Jersey, 296 pp.

Flood, R.D., 1991. Side-scan sonar and 200 kHz subbottom profiler demonstration, Thompson Island Pool -- May 4 and 10, 1991. In: TAMS Consultants, Inc., Phase 2A Sampling Plan - Review Copy. Hudson River PCB Reassessment RI/FS.

Folk, R.L., 1974. *Petrology of Sedimentary* Rocks. Hemphill Publishing Company, 1400 Wathen Ave, Austin, Texas, 78703, 182 pp.

Gahagan and Bryant Associates, Inc., 1982. Probing report - Thompson Island Pool; PCB hot spots - Hudson River; Fort Edward, New York. New York State Department of Environmental Conservation, Albany, NY.

Gardner, J.V., Field, M.E., Lee, H., Edwards, B.E., Masson, D.M., Kenyon, N. and Kidd, R.B., 1991. Ground-truthing 6.5 kHz side-scan sonography: What are we really imaging. J. Geophys. Res., 96, 5955-5974.

Harkness, M.R., McDermott, J.B., Abramowicz, D.A., Salvo, J.J., Flanagan, W.P., Stephens, M.L., Mondello, F.J., May, R.J., Lobos, J.H., Carroll, K.M., Brennan, M.J., Bracco, A.A., Fish, K.M., Warner, G.L., Wilson, P.R., Dietrich, D.K., Lin, D.T., Morgan, C.B., Gately, W.L., 1993. In situ stimulation of aerobic PCB biodegradation in Hudson River sediments, Science. 259, p. 503-507.

Malinverno, A., Edwards, H. and Ryan, W.B.F., 1990. Processing of SeaMARC swath sonar data. IEEE J. Oceanic. Eng., 15, 14-23.

Reed, T.B., IV, and Hussong, D., 1989. Digital image processing techniques for enhancement and classification of SeaMARC I side scan imagery. J. Geophys. Res., 94, 7469-7490.

Richards, J.A., 1986. *Remote Sensing Digital Image Analysis*. Springer-Verlag, New York, 281 pp.

Sanders, J.E., 1989. PCB-pollution problems in the Upper Hudson River: from environmental disaster to 'environmental gridlock.' Northeastern Env. Sci., 8(1), 1-86.

Sun, J., 1993. Digital processing of side-scan sonar images for geological interpretation. MS Thesis, Marine Environmental Science Program, Marine Sciences Research Center, State University of New York, Stony Brook. 85 pp.

TAMS, 1991. Phase 1 Report - Review Copy. Interim Characterization and Evaluation. Hudson River PCB Reassessment RI/FS. TAMS Consultants, Inc. for US EPA Region II, New York. 2 volumes.

Summary of Appendices

Appendix A:	500 kHz side-scan sonar mosaics at a scale of 1 inch = 200 feet for map areas 1 through 36 and 40.
Appendix B:	Summary of computer files produced for this study.
Appendix C:	Subbottom Profile Characterization Maps (Plates 1 - 7)
Appendix D:	X-radiographs
Appendix E:	Interpretive maps based on sonar mosaics

Appendix A

Full-Scale Plots of 500 kHz Side-Scan Sonar Mosaics

(scale 1 inch = 200 feet)

37 maps (map areas 1-36 and 40)

(previously provided to TAMS Consultants, Inc.)

Appendix B

Summary Listing of Computer Files

(Full listing of files and the files will be provided to TAMS Consultants, Inc. at a later date)

Appendix B: Summary of computer files produced for this study.

imageXX.sun	500 kHz primary mosaic image (black-white image with scale lines)
image1XX.sun	100 kHz primary mosaic image (black-white image with scale lines)
image5XX.rs1	500 kHz median image (black-white image with no scale lines)
image5XX.rs2	500 kHz reduced mean image (black-white image with no scale lines)
image5XX.rs3	500 kHz reduced standard deviation image (black-white image with no scale lines)
image1XX.rs1	100 kHz reduced median image (black-white image with no scale lines)
image1XX.rs2	100 kHz reduced mean image (black-white image with no scale lines)
image1XX.rs3	100 kHz reduced standard deviation image (black-white image with no scale lines)
image5XX.cmp	composite image (need comp3.pal with imdisp to correctly view file)
comp3.pal	palette file to use with composte images (sets color for each number in file
subchard.dat	subbottom classification data

Appendix C

Color Prints of Subbottom Profile Character

(Plates 1-7)

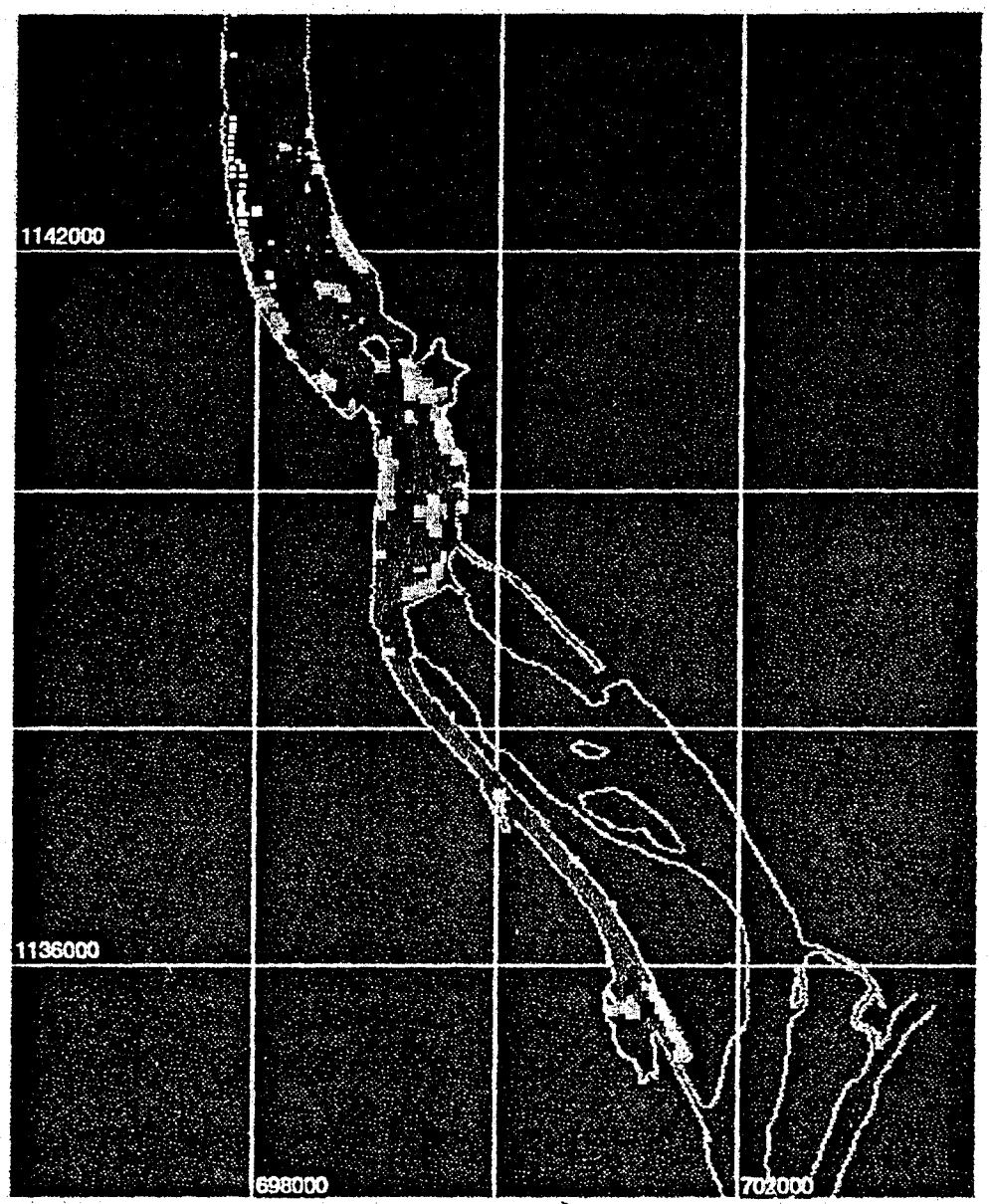

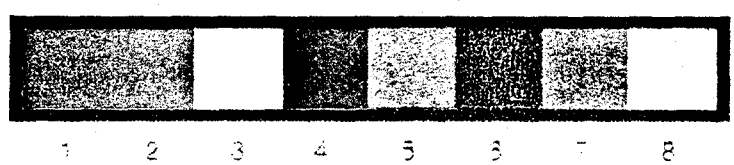

Plate 1. Classification of subbottom profiles in the Hudson River (Map sb-1).

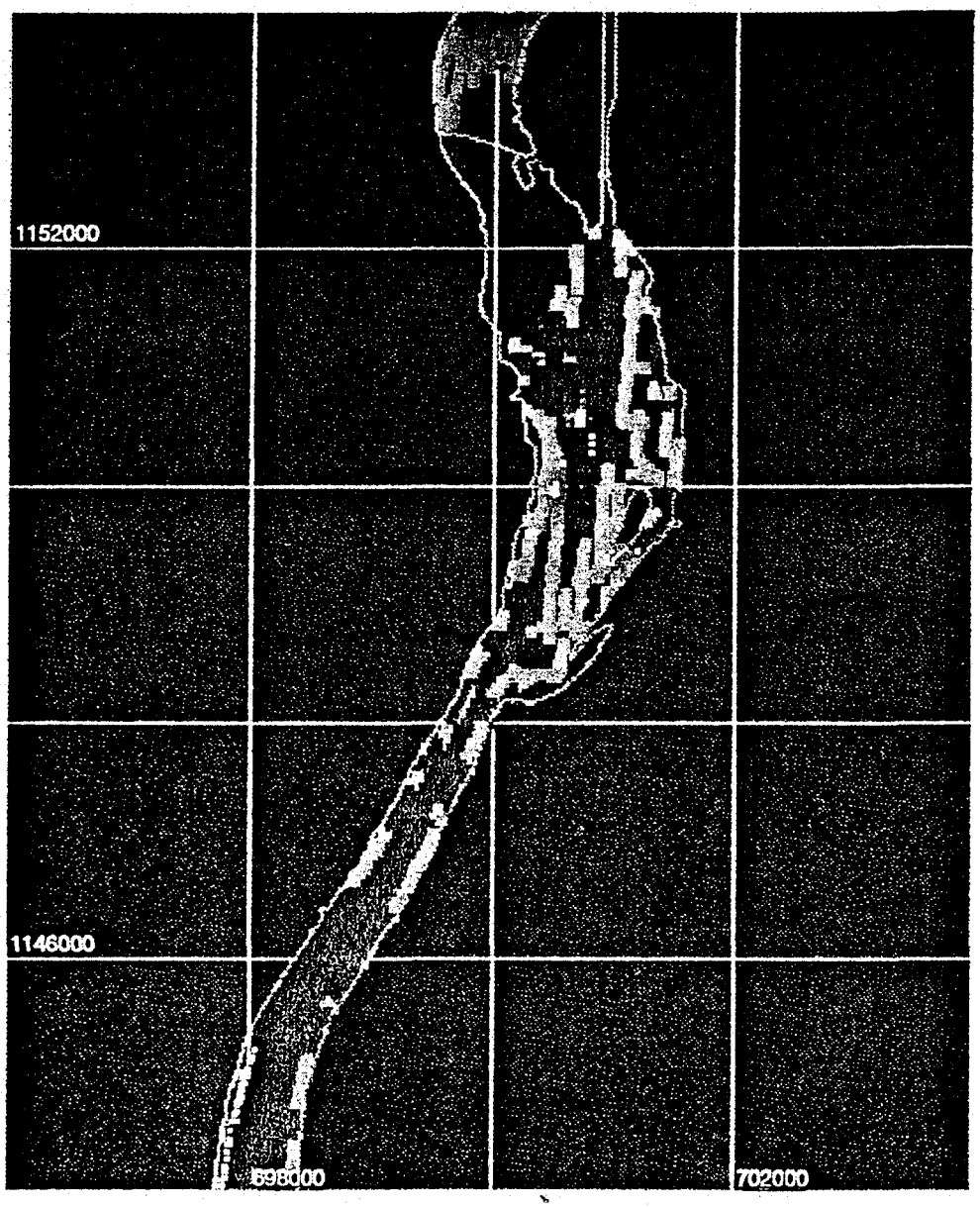

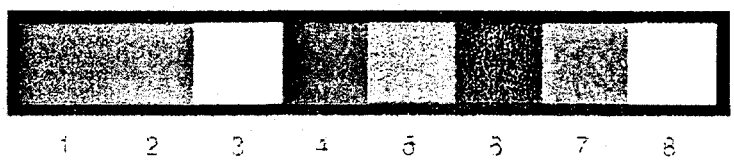

Plate 2. Classification of subbottom profiles in the Hudson River (Map sb-2).

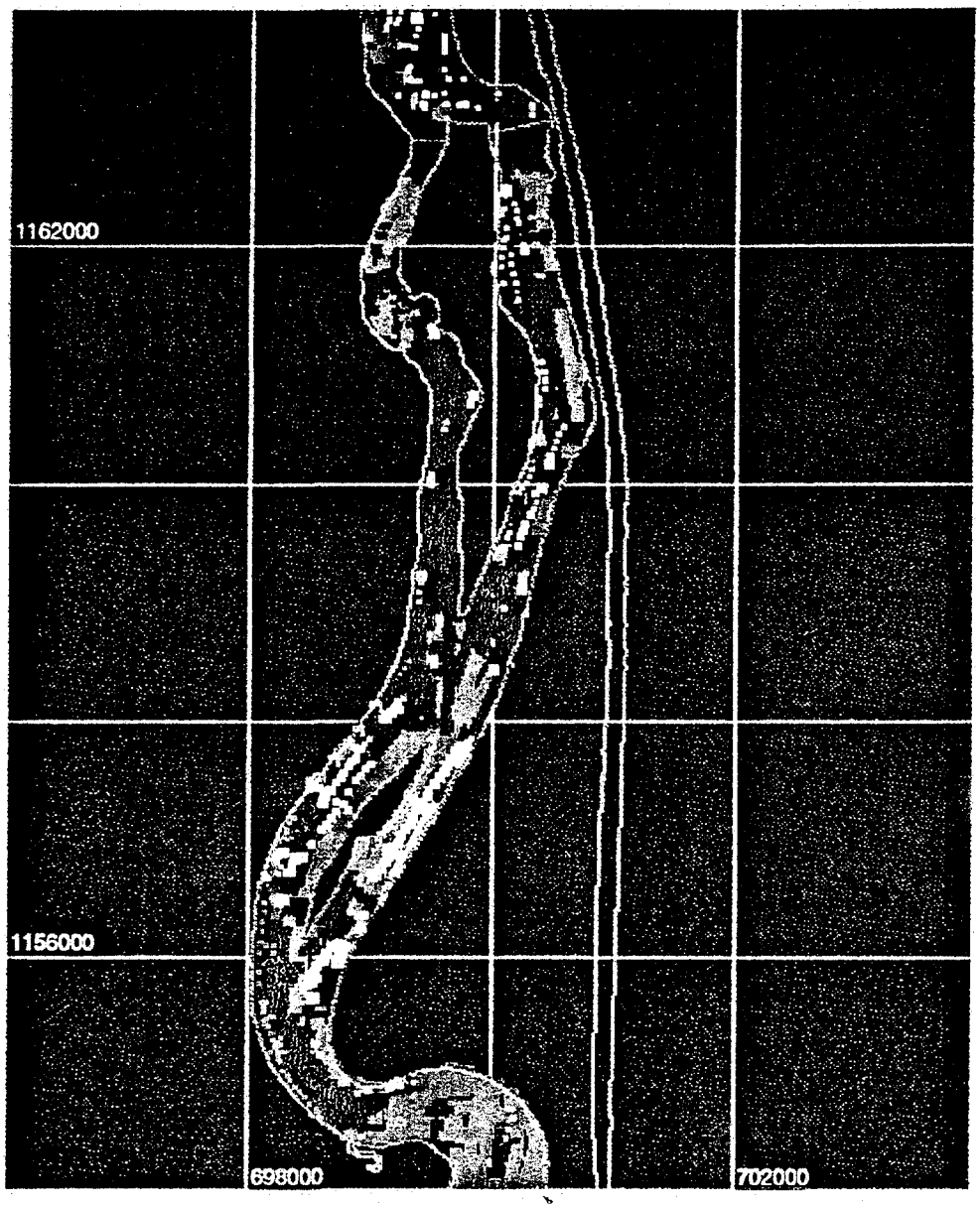

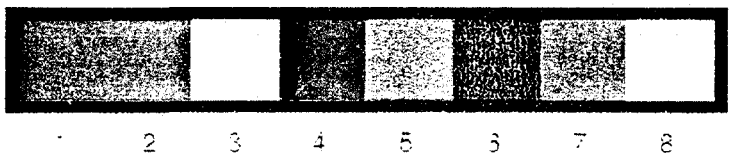

Plate 3. Classification of subbottom profiles in the Hudson River (Map sb-3)

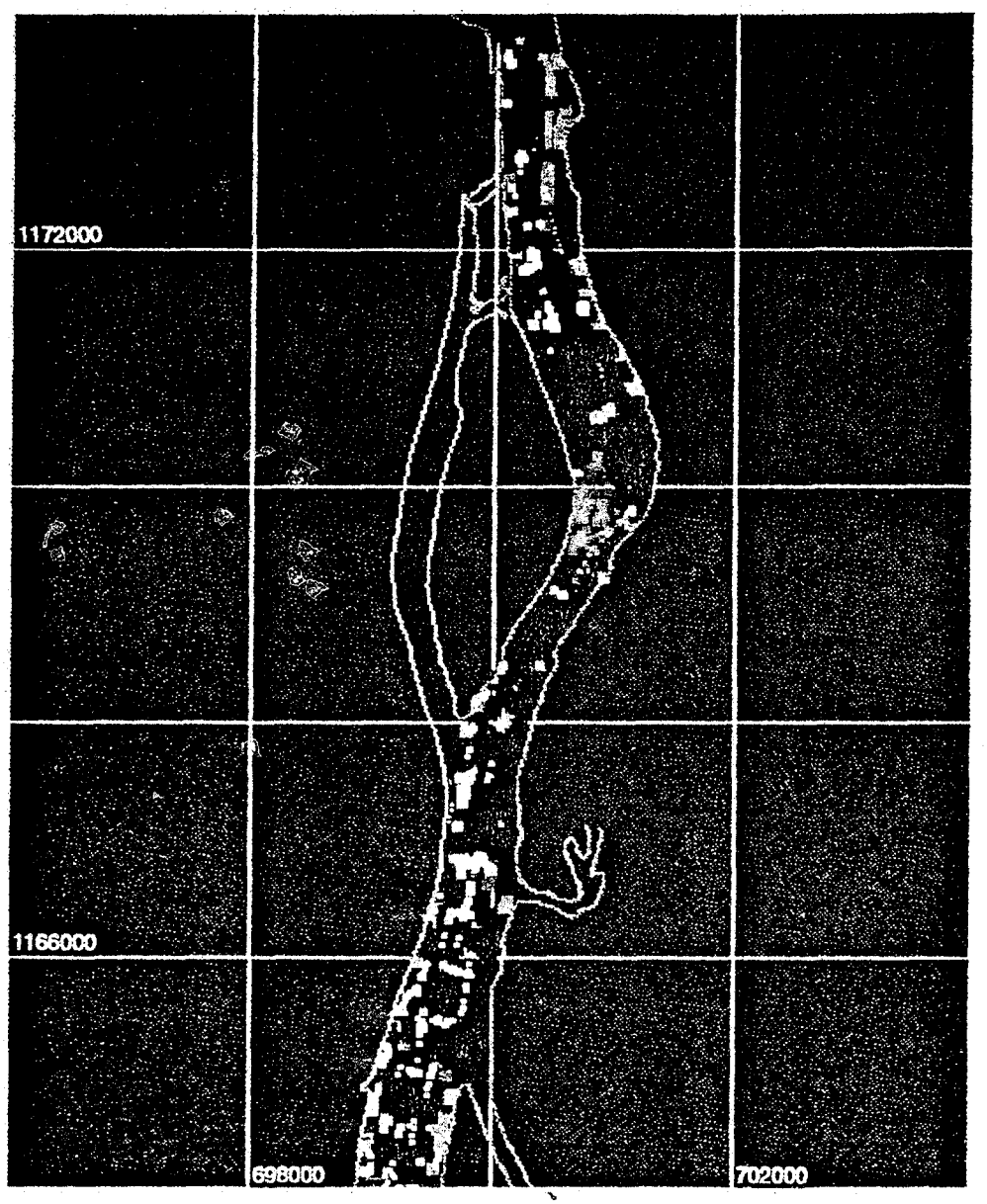

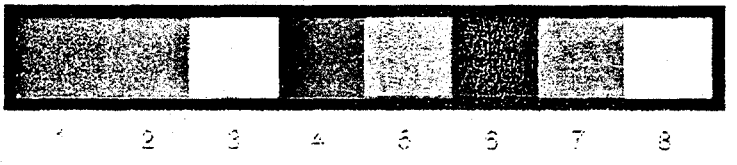

Plate 4. Classification of subbottom profiles in the Hudson River (Map sb-4).

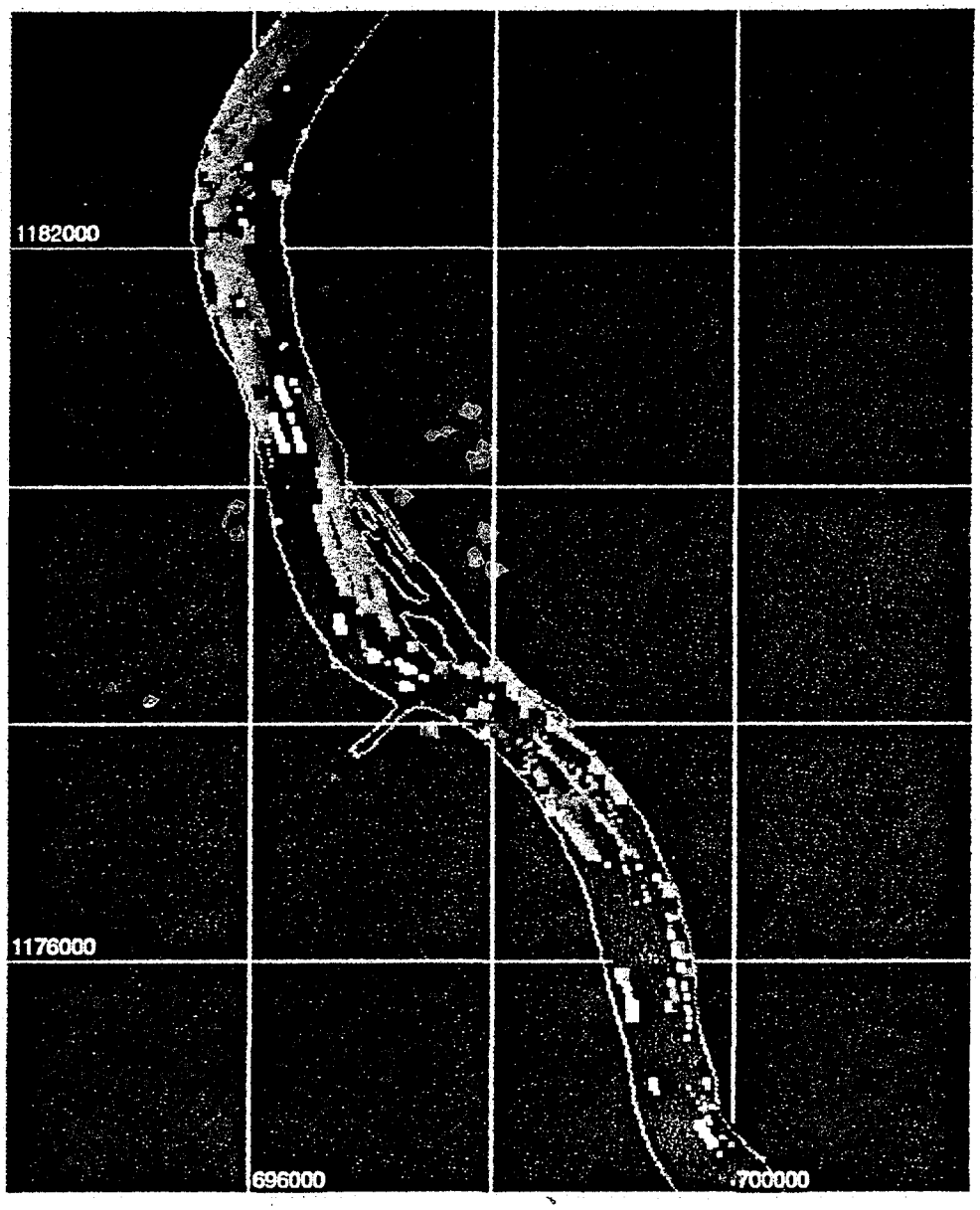

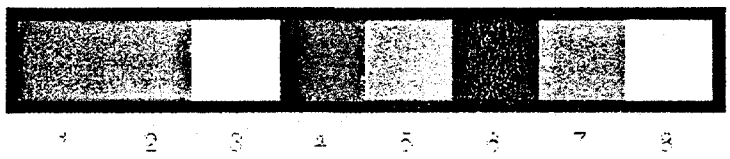

Plate 5. Classification of subbottom profiles in the Hudson River (Map sb-5).

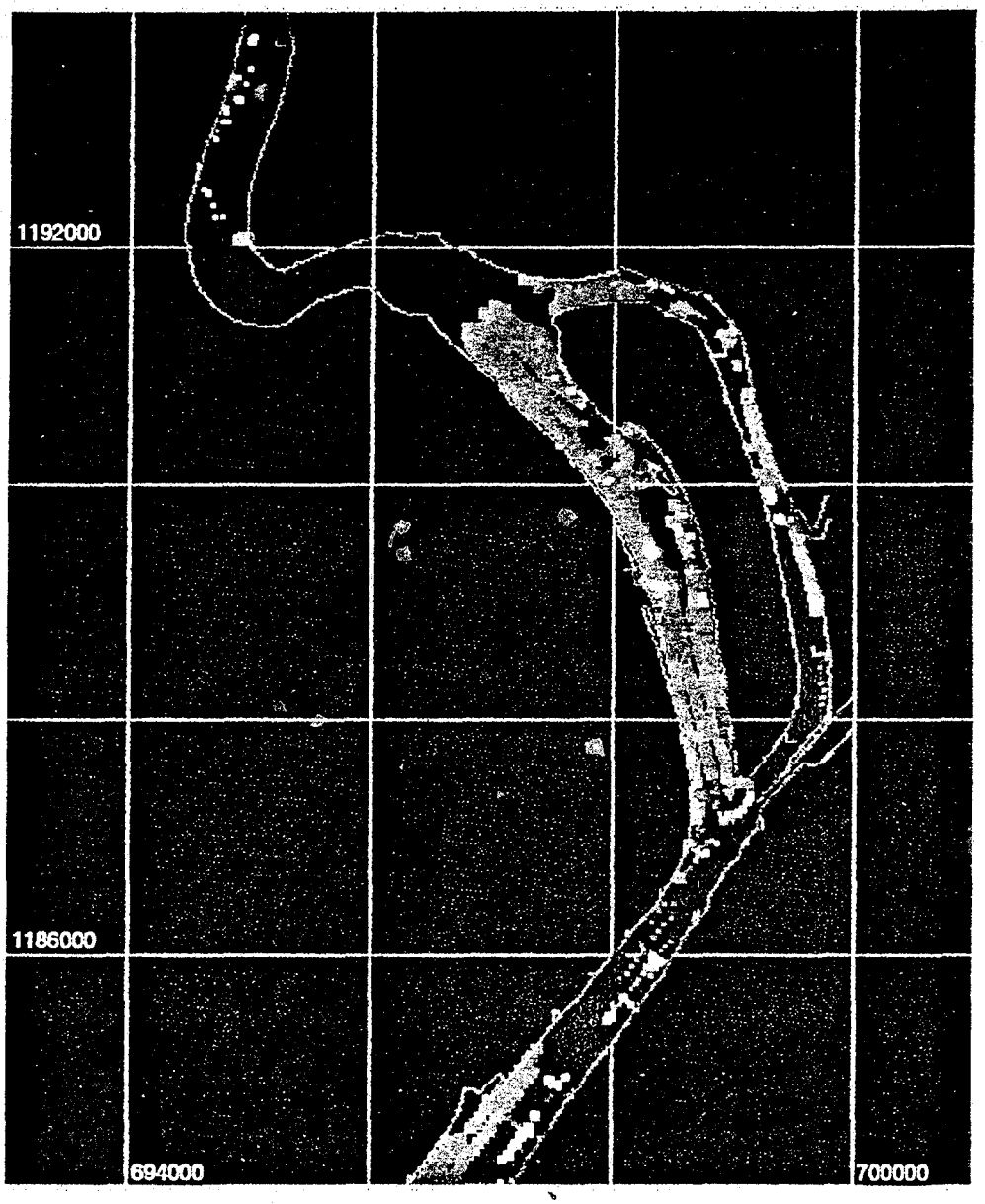

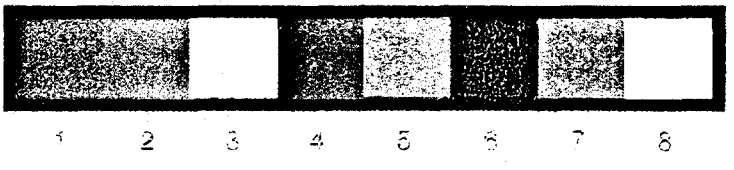

Plate 6. Classification of subbottom profiles in the Hudson River (Map sb-6).

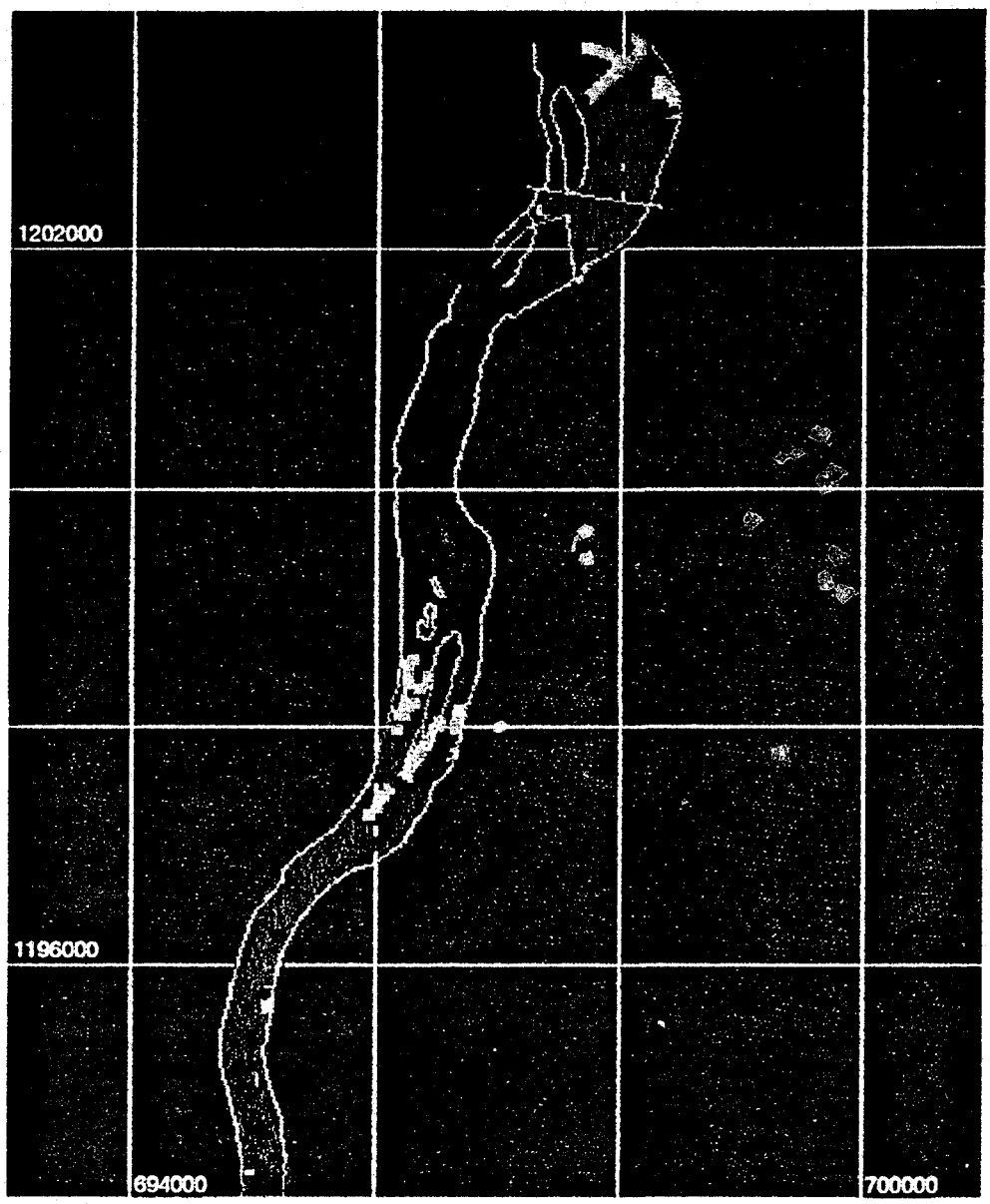

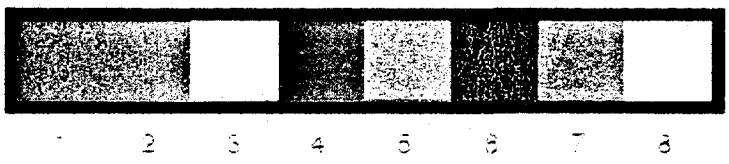

Plate 7. Classification of subbottom profiles in the Hudson River (Map sb-7).

Appendix D

X-Radiographs of Confirmatory Cores

(X-Radiographs will be provided at a later date)

Appendix E

Interpretive Maps based on Sonar Mosaics

(scale 1 inch = 200 feet)

37 map areas (map areas 1-36 and 40)

(previously provided to TAMS Consultants, Inc.)